Sorption of Arsenic Species using Chitosan Based Biopolymer Sorbent Materials

A Thesis Submitted to the College of Graduate Studies and Research in Partial Fulfillment of the Requirements for the Master's Degree in the Department of Chemistry University of Saskatchewan Saskatoon

By

Dawn Yvonne Pratt

Permission to Use

In presenting this thesis in partial fulfillment of the requirements for a Postgraduate degree from the University of Saskatchewan, I agree that the Libraries of this University may make it freely available for inspection. I further agree that permission for copying of this thesis in any manner, in whole or in part, for scholarly purposes may be granted by the professor or professors who supervised my thesis work or, in their absence, by the Head of the Department or the Dean of the College in which my thesis work was done. It is understood that any copying or publication or use of this thesis or part thereof for financial gain shall not be allowed without my written permission. It is also understood that due recognition shall be given to me and to the University of Saskatchewan in any scholarly use which may be made of any material in my thesis.

Requests for permission to copy or to make other use of material in this thesis in whole or part should be addressed to:

Head of Department of Chemistry

University Of Saskatchewan

Saskatoon, SK (S7N 5C9)

Canada

Acknowledgements

I am truly grateful to have been given the opportunity to study at the University of Saskatchewan and pursue my Master's of Science in Chemistry. This opportunity was the work of three people specifically Drs. Lee Wilson, Julita Vassileva and Janusz Kozinski, with their encouragement, guidance and mentorship during my graduate studies they made my dream a reality. I will always speak highly of this profound University and I will always remember the kindness and generosity of everyone I met while in the pursuit of my graduate degree. I wish you all the best in your lives.

I am thankful to Dr. Steve Reid for his guidance on my thesis writing. I am thankful to the Department of Chemistry at the University of Saskatchewan for allowing me the opportunity to perform research and the Science Ambassador Program for giving me the opportunity to promote science and be a role model to many First Nation youth. I hope to have inspired these youth to consider a career in the science or engineering fields at the University of Saskatchewan.

I am grateful to have worked with a terrific team of students and researchers: Mohamed Mohamed, Rai Guo, Abdulla Karoyo, Jae Kwon and Louis Poon, Monique Koskie and Natasha Dreaver who all contributed to my learning in the lab.

I am thankful to my very good friends Yolanda Peigan Terrina Bellegarde, Cindy Sheffield, Melissa Gus and Omeasoo Butt; all have inspired and empowered me as women.

I am forever grateful to my fiancée Owen Kay and to my beautiful daughter Charley Pratt-Kay, both make my life happy and perfect.

Dedication

This thesis is dedicated to my parents; Charles Pratt Sr. and Yvonne Pratt and to my siblings; Angela Pratt (Craig Wesaquate), Charles Pratt Jr. (deceased), Ross Pratt and Keith Pratt. Your love and encouragement has been my strength in the pursuit of my education.

Abstract

The research focuses on the design and characterization of two- (chitosan/glutaraldehyde) and three-component (chitosan/glutaraldehyde/β-cyclodextrin) biopolymer sorbent materials. The chitosan prepolymer investigated had a low molecular weight (~ 50,000-190,000 $gmol^{-1}$) and high molecular weight (~ 150,000-375,000 $gmol^{-1}$) whereas glutaraldehyde was used as the cross linking agent for each biopolymer. Two component chitosan/glutaraldehyde co-monomers were reacted at variable mole ratios (1:15, 1:25 and 1:35). Three-component copolymers containing β-cyclodextrin (β-CD) were obtained by reacting variable mass ratios of β-CD with chitosan (1-3, 1-1 and 1-1/3; chitosan/β-CD (w/w)). The chitosan/glutaraldehyde fraction was held constant at a 1:6 mole ratio comparable to the two-component copolymers. The two- and three-component biopolymer materials were characterized using TGA, FT-IR spectroscopy and elemental analysis (C, H & N). The solid-solution isotherm properties in aqueous solutions for the biopolymers were characterized with two detection methods (UV-Vis and ICAP-OES) with two types of adsorbates, respectively; *p*-nitrophenol (PNP) and arsenate oxoanion ($HAsO_4^{2-}$) at alkaline conditions.

The Langmuir (*i.e.* Sips restricted) and the Sips sorption isotherm models were utilized to obtain sorption parameters at pH 8.5 and 295 K, (*i.e.* surface area estimates, sorption capacities and removal efficiencies) for each biopolymer material. The surface area estimates are as follows for the 1:15, 1:25 and 1:35 chitosan-based two-component biosorbent materials: the Sips restricted values are 46.7, 46.7 and 31.6 m^2g^{-1} and the Sips values are 124, 46.7 and 31.6 m^2g^{-1} for the low molecular weight chitosan material. The Sips restricted are 58.7, 54.2 and 64.7 m^2g^{-1} and for the Sips are 79.8, 64.7 and 96.3 m^2g^{-1} for the high molecular weight chitosan material, respectively. The surface area estimates are as follows for the 1-3, 1-1 and 1-1/3 chitosan and

β-cyclodextrin three-component biopolymer materials: for the Sips restricted are 34.6, 54.2 and 116 m^2g^{-1} and for the Sips are 275, 51.2 and 161 m^2g^{-1}, respectively. Removal efficiencies are dependent upon the pH, temperature, and the relative amount of sorbent and sorbate. The removal efficiencies of *p*-nitrophenol by the biopolymers ranged between 7.1 and 48.9% for low and high molecular weight chitosan biosorbent materials. The removal efficiencies of *p*-nitrophenol by three components, the chitosan, β-cyclodextrin and glutaraldehyde biopolymers ranged between 7.3 and 28.0%. The removal efficiencies of the arsenate oxoanion by the biopolymers ranged between 30.7 and 92.2% for low and high molecular weight chitosan biosorbent materials. The removal efficiencies of arsenate oxoanion by the three-component biopolymers (chitosan, β-cyclodextrin and glutaraldehyde) ranged between 22.8 and 55.4%. The removal efficiencies for the unmodified commercial chitosan (high and low molecular weight) and activated carbon sorbent materials was negligible (~ 0%).

The Langmuir (i.e. Sips restricted) and the Sips sorption isotherms both showed similar "best-fit" results for the sorption in aqueous solution data which resulted in neither isotherm model being favoured over the other.

Table of Contents

List of Schemes

List of Figures

List of Tables

List of Abbreviations

LMWCH	Low Molecular Weight Chitosan
HMWCH	High Molecular Weight Chitosan
CH	Chitosan
As(V)	Arsenate
$HAsO_4^{2-}$	Arsenate oxoanion
PNP	*p*-nitrophenol
CD	Cyclodextrin
βCD	β-Cyclodextrin
Glu	Glutaraldehyde
N	Nitrogen
C	Carbon
H	Hydrogen
EA	Elemental Analysis
ICAP-OES	Inductively Coupled Argon Plasma-Optical Emission Spectroscopy
UV-Vis	Ultraviolet Visible Spectrophotometry
TGA	Thermal Gravimetric Analysis
FT-IR	Fourier Transform Infrared Spectroscopy
ε_R %	Removal Efficiency
DRIFT	Diffuse Reflectance Infrared Fourier Transform
log K_{ow}	n-Octanol/Water partition coefficient
P_v	Vapour pressure
pK_a	Dissociation constant
EXAFS	Extended X-ray Absorption Fine Structure

PXRD	Powder X-Ray Diffraction
XANES	X-ray Absorption Near Edge Structure
XPS	X-ray Photoelectron Spectroscopy
MS	Mass Spectrometry
ITC	Isothermal Calorimeter
HSAB	Hard and Soft Acids and Bases
AC	Activated Carbon
IUPAC	International Union of Pure and Applied Chemistry

1.0 Introduction

1.1 Research Objectives

Many examples of economical and environmentally friendly biomaterials that use chitosan as a framework component in biopolymer sorbents materials are well known and their usage for the sorption of metal contaminants (i.e. lead, copper, arsenic, etc.)[14,21] from aqueous environments. Organic pollutants, such as phenolic derivatives and inorganic pollutants such as arsenic are a cause for concern. These pollutants may potentially build up in aquatic environments through their widespread usage, posing serious concerns for water quality and human health. Arsenic and phenolic derivatives are considered toxic and carcinogenic compounds.

It is known that surface area effects have a profound influence on the sorption properties of polymeric materials. Thus, it is hypothesized that biopolymers based on co-monomer mole ratios of chitosan-glutaraldehyde (with and without β-cyclodextrin) will affect the surface area and the sorption properties of such sorbent materials. Two-component chitosan-based biopolymers have been prepared using a systematic design strategy by varying the relative co-monomer mole ratios (1:15, 1:25 and 1:35) of the cross linker (i.e. glutaraldehyde) to offer novel sorbent materials. The physicochemical properties of these frameworks have been investigated by comparing low and high molecular weight chitosan. Three-component hybrid chitosan-based biopolymers incorporate β-cyclodextrin into a design strategy by varying the mass ratios of chitosan and β-cyclodextrin into a 1:6 chitosan:glutaraldehyde framework of biopolymer material.

The objectives of this research were to synthesize and characterize the physicochemical properties of chitosan-based sorbent biomaterials. As well, the sorption properties of chitosan biopolymers were investigated in aqueous solutions containing arsenate oxoanion (i.e. $HAsO_4^{2-}$) and an organic anion (i.e. phenolate form of PNP) respectively. In addition, the equilibrium sorption properties were evaluated to provide an estimate of the sorbent surface area and the sorption capacity. The Langmuir (*i.e.* Sips restricted) or Sips isotherm models[4] (see eqns. 13 and 14) provide parameter estimates of the monolayer coverage (Q_m) and related thermodynamic sorption parameters of the sorbent biomaterials.

The research was focused on a systematic design approach of chitosan based biopolymer materials by tuning the relative composition of the copolymer. The materials are characterized using thermal gravimetric analysis (TGA), elemental analysis (EA) and FT-IR spectroscopy. The sorption properties were investigated using equilibrium isotherms according to the uptake of arsenic oxoanion and PNP, respectively, at variable concentration conditions. Arsenic sorption was quantified using ICAP-OES and the sorbent accessible surface area was estimated using a dye-based adsorption method with UV-Vis spectroscopy; whereas the sorption results were analyzed using Langmuir (*i.e.* Sips restricted) and Sips isotherm models. The biopolymer sorbents were compared with unmodified commercially available sorbents; high mol. wt. chitosan flakes, low mol. wt. chitosan powder and granular activated carbon.

1.2 *p*-Nitrophenol (PNP)

PNP is a model organic pollutant which possesses toxic and carcinogenic properties and poses potentially serious environmental and human health problems[4]. There is no known natural source of PNP, it is produced as an intermediate during the synthesis of azo dyes, insecticides,

herbicides and pesticides. PNP has also been detected in the exhaust of light-duty gasoline and diesel vehicles. PNP is formed from the photochemical degradation of aromatic compounds such as benzene and toluene while in the presence of nitric oxide or hydroxyl radicals and nitrous dioxide.[72] There are three manufacturers in the USA with estimated production volumes of 45 – 450 kg/year up to 45 000 – 450 000 kg/year, where a total release of PNP into the air is reported at 420 kg; no data available on the release of PNP into aquatic environments. Through wet and dry deposition, airborne nitrophenols can be released into the hydrosphere and geosphere. Nitrophenols in water are estimated to be at least in the order of several thousand tonnes per year on a global basis.[72]

PNP has surface area of 52.5 $Å^2$ in its co-planar orientation and a surface area of 25.0 $Å^2$ in its orthogonal orientation.[22] PNP is soluble in water (12.4 g/L at 293K) with a vapour pressure , $P_v = 3.2x10^{-6}$ kPa at 293 K, $pK_a = 7.08$ at 294.5 K, log $K_{ow} = 1.85 – 2.04$; thus, the environmental fate of PNP favours partitioning into the hydrosphere.[72] There is a clear need to develop novel materials for the remediation of aquatic environments containing PNP.

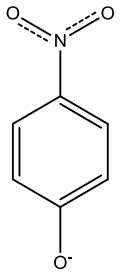

Figure 1.1. The ionized form of PNP at pH (i.e. pH=9) values above the pK_a 7.08[72] of PNP.

1.3 Arsenic Background

Water is an essential requirement for every living organism to grow and to survive on the Earth. Water pollution has become a grave concern for many people living in developing nations of the world that have been affected by natural the occurrence or anthropogenic sources of pollutants; thus, making safe clean drinking water a limited resource. It is projected that by the year 2025, the world population will have grown to ~8.45 billion people, resulting in 60% of the total population (5.1 billion) living in regions of the world that will be faced with moderate to extreme water scarcity and food vulnerability. With increasing industrial growth and climate change,[15] there are several water borne contaminants, chemical and microbial, that need to be addressed through sequestration methods using low cost and innovative materials. Recently, heavy metals have become a cause for concern due to the fact that mining, oil refining and the combustion of fossil fuels release large amounts of heavy metals into the environment. In particular, arsenic is a toxic element that warrants special concern owing to its carcinogenic properties and its high relative abundance alongside mercury, palladium and cadmium.[12] The recent BP oil spill in the Gulf of Mexico on April 20th, 2010 has resulted in a renewed interest in arsenic contamination, "the presence of oil in seawater disrupts the ocean's mechanism to naturally filter out arsenic".[13] Oil spills clog up the ocean floor sediments preventing arsenic to absorb onto mineralized surfaces, resulting in increased arsenic concentrations. The resulting build up results in the transport of contaminants into the food chain, causing birth defects and behavioral changes in marine animals.[13] The oil spill in the Gulf represents potentially significant and detrimental environmental effects and concern for human health in the coming years if no efforts are made to remediate such contaminants.[13]

World-wide, arsenic is widely recognized as a hazardous and toxic contaminant to human health and to the environment. High arsenic concentrations found in shallow zones of ground water have been reported in the USA, China, Bangladesh, Taiwan, Mexico, Argentina, Poland, Canada, Hungary, Japan, Mongolia, Chile, Pakistan, Romania, Vietnam, Nepal, Myanmar, Cambodia and India. Bangladesh and West Bengal have the largest population (~36 - 70 million people) at risk for high arsenic groundwater contamination.[1,2,9-11] Some regions of Bangladesh are reported to have concentrations as high as 1000 μg/L.[11] The surrounding wastewater released from oil production platforms may contain comparable arsenic levels up to 1000 μg/mL.[12] In Canada, a community called George Gordon First Nation located in Saskatchewan, is reported to have unacceptable high levels of arsenic above 70 μg/L in its raw water.[46] Health Canada has established a maximum acceptable arsenic concentration in drinking water of 10μg/L.[49]

1.4 Arsenic Properties

Arsenic was isolated in 1250 A.D. by Albertus Magnus. It is a silver-grey, brittle, crystalline solid, metalloid with an atomic number of 33 and an atomic weight 74.9 amu. It ranks 20th in natural abundance of the known elements, 14th in seawater and 12th in abundance within the human body. Arsenic becomes mobile through natural weathering reactions, biological activity, geochemical reactions, volcanic emissions and other anthropogenic activities. Arsenic concentrations in most minerals range from 0.5 to 2.5mg/Kg. The natural weathering of minerals converts arsenic sulfides to arsenic trioxides and enters the hydrological cycle by dust, dissolution in rain, rivers or groundwater.[9,10] Anthropogenic sources of arsenic include mining, combustion of fossil fuels, use of pesticides, herbicides and crop desiccants. The use of arsenic additives to livestock feed contribute as an additional source of arsenic in the environment.[9,10]

1.5 Acid-Base Dissociation Constants

The acid dissociation constants (K_a) of chitosan, β-cyclodextrin and arsenate are important parameters to consider in this study because pH plays a key role in the speciation and sorption properties of arsenic. Arsenic species exist in three different dissociated forms in aqueous solution, all of which are dependent upon the pH and undergo dissociation. The amine groups of chitosan display a variable ionization state depending on the pH of the solution, as well as the hydroxyl groups of β-CD. Table 1.1 lists various types R-NH_2 groups and their corresponding K_a and K_b values.

Table 1.1. Acid and Base Dissociation Constants with the conjugate acid dissociation constants of various organic amines (adapted from reference 47).

Weak Base	**Ionization Reaction**	***K_b**	****K_a**	**pK_a**
Methylamine (CH_3NH_2)	$CH_3NH_{2(aq)} + H_2O_{(l)} \leftrightarrow CH_3NH_2^+{}_{(aq)} + OH^-_{(aq)}$	4.4×10^{-4}	2.27×10^{-11}	10.6
Ethylamine ($C_2H_5NH_2$)	$C_2H_5NH_{2(aq)} + H_2O_{(l)} \leftrightarrow C_2H_5NH_3^+{}_{(aq)} + OH^-_{(aq)}$	5.6×10^{-4}	1.79×10^{-11}	10.7
Aniline ($C_6H_5NH_2$)	$C_6H_5NH_{2(aq)} + H_2O_{(l)} \leftrightarrow C_6H_5NH_3^+{}_{(aq)} + OH^-_{(aq)}$	3.9×10^{-10}	2.56×10^{-5}	4.59

*Refers to the non-protonated amine base.
**Refers to protonated form of base

1.6 Hard and Soft Acids and Bases (HSAB)

Ralph G. Pearson was the first to introduce the Hard and Soft Acids and Bases (HSAB) theory in 1963[45], where he proposed a simple rule that "hard acids bind strongly to hard bases and soft acids bind strongly to soft bases". The arsenate species is considered a soft acid due to the large polarizability of the molecule and the arsenite species is considered a hard acid due to the limited polarizability of the molecule.[10]

1.7 Arsenic Speciation

Arsenic mobility occurs mostly in aqueous environments, whereby it gains primary access to the human body through contaminated water and food intake laden with this material. Arsenic exists in different oxidation (-3, 0, +3, +5) states.[9,11] Arsenate(V) exists in aqueous solution at ambient conditions and it will hydrolyze depending on the solution pH, hence, affecting the arsenate speciation according to eq. 1-3:[30]

$$H_3AsO_4\,(aq) \leftrightarrow H_2AsO_4^-\,(aq) + H^+\,(aq),\ pK_{a,1} = 2.19 \qquad (1)$$

$$H_2AsO_4^-(aq) \leftrightarrow HAsO_4^{2-}(aq) + H^+\,(aq),\ pK_{a,2} = 6.94 \qquad (2)$$

$$HAsO_4^{2-}(aq) \leftrightarrow AsO_4^{3-}(aq) + H^+\,(aq),\ pK_{a,3} = 11.50 \qquad (3)$$

At pH 8.5 and by Eq. (2), reveals the predominant arsenate species in solution is $H_2AsO_4^-$ and $HAsO_4^{2-}$. The mass action law provides confirmation of the percentage of each form of arsenate at pH 8.5 in aqueous solution:

$$K_{a,2} = \frac{[H^+][HAsO_4^{2-}]}{[H_2AsO_4^-]} \qquad (4)$$

The total arsenic(V) concentration in solution $[As(V)]_T$ is expressed by the following:

$$[As(V)]_T = [H_2AsO_4^-] + [HAsO_4^{2-}] \quad (5)$$

Therefore, the percentage of $H_2AsO_4^-$ and $HAsO_4^{2-}$ species in solution is 2.60% and 97.4%, respectively. This is confirmed by Scheme 1.1.

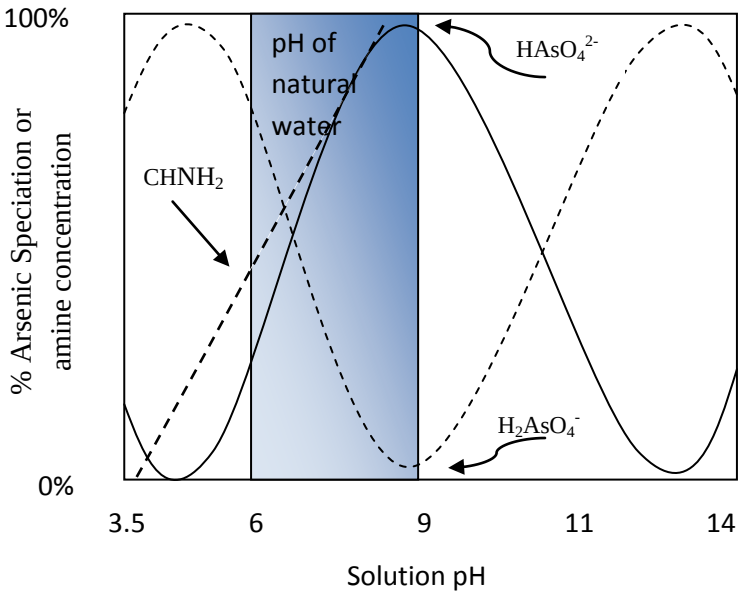

Scheme 1.1. Arsenic speciation in aqueous solution at various pH conditions (adapted from reference 31) where $CHNH_2$ represents the monomer units of chitosan in its neutral form for the chitosan amine group.

The most dominant forms of arsenic is arsenite, As(III), and arsenate, As(V); As(V) is commonly found in uranium mill tailings and As(III) is the most mobile and toxic form of arsenic found in groundwater.[34] Arsenite and arsenate vary in their state of protonation from pH 2-12 in solution, see Scheme 1.2.

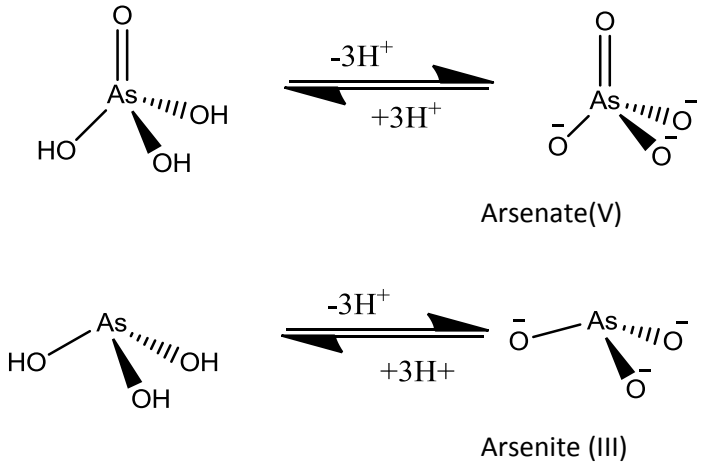

Scheme 1.2. The arsenic species (As(III)/As(V)) capable of variable states of protonation from pH 2-12.

1.8 Arsenate(V) Oxoanion Species Bond Distances, Molecular Volume and Surface Area

The isolated tetrahedral shaped oxoanion arsenate species was built using Spartan 2008 1.2.0 (see Figure 1.2) where the bond lengths, volume and area were calculated using equilibrium geometries in the ground state with Hartree-Fock 3-21G in vacuum. Table 1.2 shows the various bond lengths of each bond in the Arsenic(V) oxoanion species. The bond lengths, volume and surface area are important to compare relative to the cavity dimensions of βCD. From Table 1.2, it is apparent the arsenate(V) oxoanion species can fit comfortably into the βCD cavity because the cavity volume of the βCD exceeds the van der Waals volume the arsenate(V) oxoanion species.

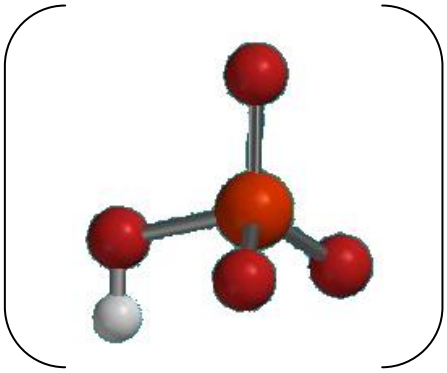

Figure 1.2. The isolated tetrahedral shaped arsenate oxoanion species was built using Spartan 2008 1.2.0, calculated in the absence of any counter ion(s) or solvent.

Table 1.2. The covalent bond distances of the tetrahedral oxoanion arsenate species.

Bond	Bond Lengths/Å
As═O	1.66
As—O$^-$	1.67
As—OH	1.85
O—H	0.973

Note: The van der Waals Volume of $HAsO_4^{2-}$ is 34.3 Å^2 and the Molecular Surface Area is 92.Å^2

1.9 Technologies of Arsenic Remediation from Contaminated Water/Wastewater

There are several potential methods for the removal of arsenic from contaminated waters and they may be classified into two general types, *i*) physicochemical and *ii*) biological[10,11]: The physicochemical techniques include oxidation/precipitation, adsorption, ion exchange, precipitation-coagulation, membrane filtration and permeable reactive methods. The biological techniques include phytoremediation and biological treatment with living microbes/bio-filtration. There are disadvantages and advantages to each technique and choosing the best arsenic

remediation technology depends on various parameters including pH conditions and concentration levels. The economics to operate and maintain the arsenic remediation technology must consider the management of the toxic sludge waste by-products produced in the overall process. Municipal-scale technologies may employ a pretreatment step in combination with any of the approved methods for total arsenic removal: coagulation/filtration, lime softening, activated alumina, ion exchange, reverse osmosis, manganese greensand filtration, electrodialysis and adsorption/filtration. The pretreatment step in combination with an arsenic removal method show removal efficiencies >90% that result in the reduction of total arsenic removal to levels as low as 3-5 μg/L.[50]

1.10 Biosorbents and Heavy Metal Sorption

Adsorption/filtration using various media, such as iron, aluminum and titanium oxide, indicate the great potential for arsenic removal technology strategies.[50] Activated carbon (AC) is a popular sorbent for wastewater treatment and is one of the most widely used materials for sorption-based applications.[14] The relative cost of AC, regeneration costs and its worldwide demand has driven research and development efforts toward alternative biomaterial sorbents with improved sorption properties and lower cost. The development of such biomaterial sorbents will improve the sorption capabilities and widespread usage of various biomaterial sorbents for water treatment and remediation processes. Several low-cost sorbents such as, chitosan, natural zeolites, clays, industrial waste (i.e. waste slurry, lignin, iron (III) hydroxide and red mud), low rank coal (lignite) and agricultural biomass have been studied as sorbent materials.[14] A comparison of the costs and sorption capabilities of AC with other commercially available sorbents for heavy metal cations (Hg^{2+}, Cr^{6+}, Cd^{2+}, Pb^{2+}) indicate that chitosan showed among

the greatest sorption capacity due to its ability to specifically remove various types of heavy metal cations (Hg^{2+}, Cr^{6+}, Cd^{2+}).[14]

1.11 Chelation

Chelation is the formation or presence of coordinate covalent (or other attractive interactions) between two or more separate binding sites within the same ligand and a single central atom.[35] The terms bidentate, tetradentate or hexadentate indicates the number of potential binding sites of the ligand[35]. Sir Gilbert T. Morgan and H.D.K. Drew[36] first applied the term chelate in 1920, "The adjective chelate, derived from the great claw or *chele* (Greek) of the lobster or other crustaceans, was suggested for the caliper-like groups which function as two associating units and fasten to the central atom so as to produce heterocyclic rings." Chitosan and its derivatives possess the unique ability to form complexes by chelating to metal ions.

1.12 Chelation Applications

Common chelators include phosphates and ethylenediaminetetraacetic acid (EDTA). EDTA is a hexadentate (six-toothed) ligand and chelating agent; see Scheme 1.3. EDTA is used for chelation therapy[81], which involves the use of chelating agents for poisonous heavy metal detoxification. There are several applications for chelators such as, chemical analyzers, water softeners, and ingredients in many commercial products such as shampoos and food preservatives and as a soil treatment method to extract heavy metals (Cd, Cu, Pd, Zn).[58]

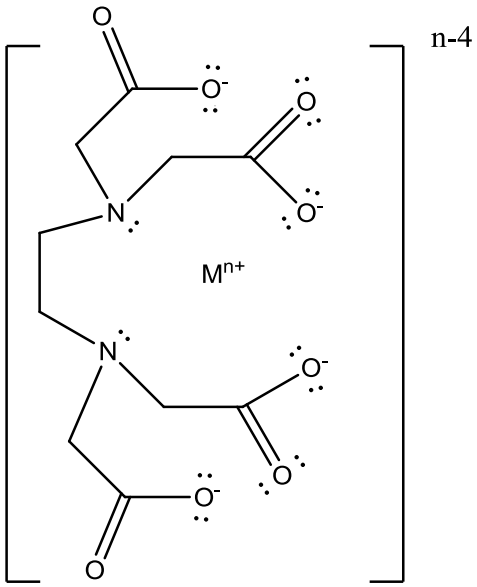

Scheme 1.3. The structure of $EDTA^{4-}$ chelating a metal ion; where n=charge on the metal ion (M^{n+})

1.13 Anion Binding

Designing anion receptors is a challenging task because the sorbent and sorbate both need to behave as team in order to reach the ultimate goal of the sorbent which is attracting anion sorbates in aqueous solution. There are five intrinsic properties[43] that make anion receptor chemistry a challenge: *i*) anions are larger in comparison to cations and the size of the receptor needs to be greater to accommodate the anion (*i.e.* F^- is the smallest anion with an ionic radius of 1.33 Å in comparison to K^+ with an ionic radius of 1.38 Å), *ii*) inorganic anions such as halides (spherical shaped), SCN^- (linear shaped), $PtCl_4^{2-}$ (tetrahedral shaped) and $Fe(CN)_6^{3-}$ (octahedral shaped) occur in various atomic and molecular geometries, *iii*) anions have higher free energies of hydration resulting in receptors competing more with the surrounding solvent to attract the anion (*i.e.* $\Delta G_{hydration}$ (F^-) = -465 $kJmol^{-1}$ and $\Delta G_{hydration}$ (K^+) = -25 $kJmol^{-1}$), *iv*) Depending on the size of the pH window of the anion. For example, the arsenate dissociates initially at pH 2.19,

the second dissociation at 6.94 and the third dissociation at 11.50[31] resulting in a wider pH range; thus an anion receptor has more opportunity to be influenced into a more complimentary cationic behavior. On the other hand, arsenite does not dissociate until pH 9.1[31]; thus having a smaller pH window and requiring more thought as to the design of the anion receptor and *v*) most anions are formerly "coordinately saturated" and interact through hydrogen bonding or van der Waals interactions, thus resulting in relatively weak binding compared with cation binding.

1.14 Receptors/Hosts Frameworks

Supramolecular chemists have focused most of their attention on binding of cationic guests with receptor/hosts. Natural waters are mostly (pH = 6 - 8) neutral to slightly alkaline conditions and previous research efforts have investigated chitin or chitosan in acidic and/or alkaline environments.[51] To the best of my knowledge, there is limited research focused on the use of chitin or chitosan as neutral receptors/hosts with anionic guests. However, there are several other sorbent systems that report arsenate oxoanion sorption under varying pH conditions. See Table 1.3.

Table 1.3. Various receptor/hosts frameworks with their corresponding parameters for arsenate oxoanion sorption.

Sorbent Material	pH	Sorption Mechanism	Receptor /Host Type	Removal	Reference
Surfactant Modified Zeolite	6.5-6.8	Anion exchange	Cation	Q_m^L = 7mmol/Kg	52
Surfactant Modified Kaolinite	7.2-7.5	Anion exchange	Cation	----	52
Carbonate rich soils	8.4	Inner sphere complex via ligand exchange	Neutral		53
Fe^0, citrate and solar light	8.1-8.4	Combing Fe(III) with citrate form Fe-citrate that absorbs solar radiation generating $OH^{\cdot}$, H_2O_2 and $O_2^{\cdot -}$ which are highly oxidizing species favouring the oxidation of Fe^0 to Fe(III) generating Fe(III) for the formation of iron hydroxide which adsorbs arsenic		98.9%***** 1000 – 1200 μgL^{-1} arsenic	54
Fe^0, citrate and solar light	8.2-8.5	Combing Fe(III) with citrate form Fe-citrate that absorbs solar radiation generating $OH^{\cdot}$, H_2O_2 and O_2^{-} which are highly oxidizing species favouring the oxidation of Fe^0 to Fe(III) generating Fe(III) for the formation of iron hydroxide which adsorbs arsenic		99.5%***** 1100 – 1300 μgL^{-1} arsenic	54
Chitosan-montmorillonite	4.5	External surface and interlayer adsorption	Cation	Q_m^L=120m mol/Kg	55

Q_m^L denotes the Langmuir monolayer coverage.

*****Arsenic removal levels were optimized by using 1.3 g of zero-valent iron and 4.5 mg citrate/L natural water followed by 6 hrs of irradiation. After solar irradiation was followed by 18 hrs of equilibration.

1.15 Chitosan

Chitosan is a derivative of chitin which is second to cellulose as the most naturally abundant biopolymer in the world. Chitin originates from the exoskeletons of arthropods, particularly from crab and shrimp shells or the cell walls of fungi and yeast.[20] Chitin exists as three polymorphic forms: the α-, β- and γ-forms; the γ-form may be considered as a pseudo-chitin form much like a distorted version of either α- or β-form of chitin[33]. The α- form of chitin has intramolecular and intermolecular hydrogen bonding with an anti-parallel alignment; thus, exhibiting stronger hydrogen bonding[59]. While the β-chitin form shows only intramolecular hydrogen bonding with parallel alignment[20]; the γ-chitin exists as two chains up (parallel alignment) for every chain down (anti-parallell alignment).

The α-form of chitin is the stronger more abundant in the environment, it is found in arthropod cuticles where extreme hardness is a structural requirement. The β- and γ-forms of chitin are found in squid, *Loligo* where flexibility and structural strength are required.[33] Cellulose and chitin are structurally analagous, they differ at the C-2 position; where the hydroxyl group on cellulose is replaced with an acetamido group on chitin[18] (see Figures 1.3 and 1.4).

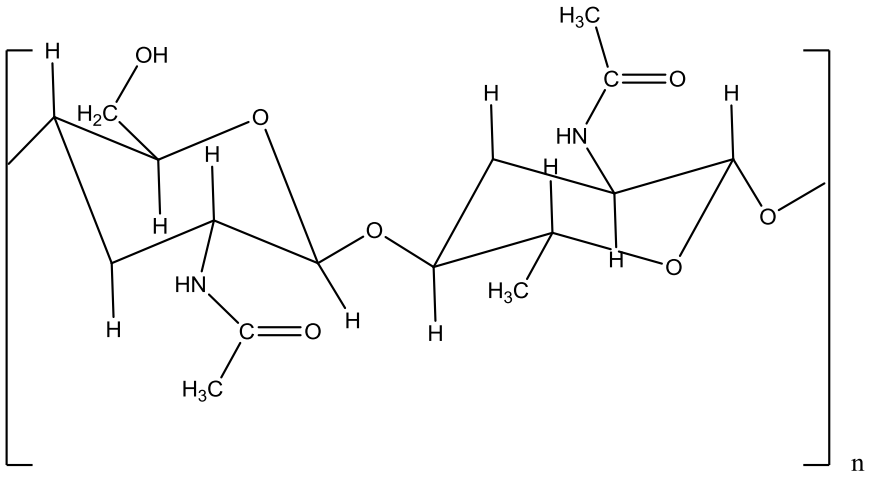

Figure 1.3. The molecular structure of chitin a natural linear polysaccharide polymer consisting of (1, 4) 2-acetamide-2-deoxy-D-glucose units; where n represents the number of monomer units.

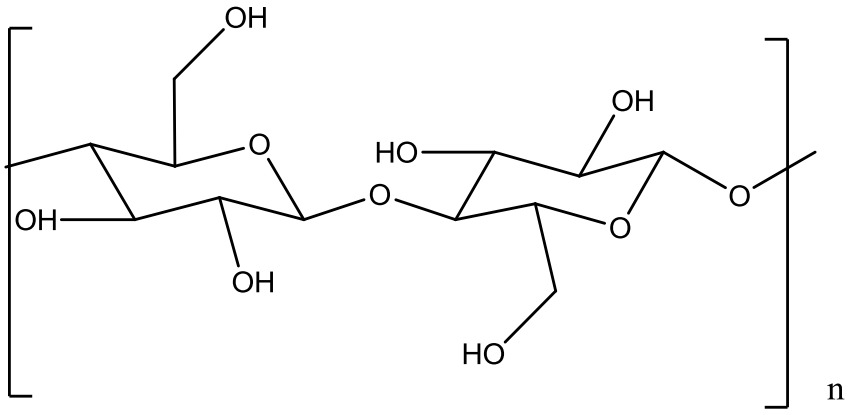

Figure 1.4. The molecular structure of a linear cellulose a polymer consisting β(1→4)-D-glucose units; where n represents the number of monomer units.

The advantage of chitosan, in comparison to cellulose and chitin, is the occurrence and the relative accessibility of the primary amine groups,[17,18,19] shown in Fig. 1.5. The amine groups of chitosan provide an advantage over conventional carbohydrate-based biosorbents studied in terms of their heavy metal adsorption properties[14], because they are relatively efficient

chelators for metal ions. It is important to recognize that the $-NH_2$ group of chitosan may participate in cross linking reactions, in addition to the hydroxyl groups.

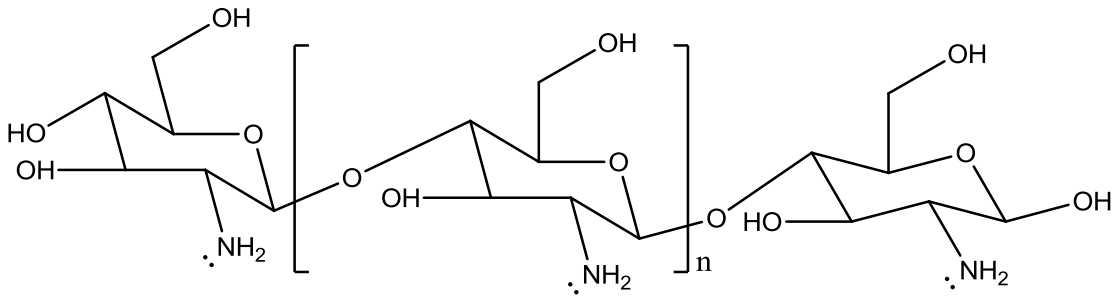

Figure 1.5. The structure of chitosan (adapted from reference 30).

The amine groups of chitosan have a pK_a of 6.5[30] and become neutral amine groups when the pH is above the pK_a of the amine group. The pH effect is an important consideration when designing experimental conditions for studies aimed at investigating of the cation or anion binding sites at the sorbent surface. In this sorption study, a neutral sorbent surface was created at pH 8.5. Chitosan is a readily available biomaterial which can be modified for the sorption of arsenate species by varying the pH conditions. The percentage of neutral amine groups can be determined by the following acid-base equilibria in aqueous solution:[30]

$$CHNH_3^+ \rightleftharpoons CHNH_2 + H^+ \quad (7)$$

$$K_a = \frac{[H^+][CHNH_2]}{[CHNH_3^+]} \quad (8)$$

By the law of mass action:

$$[CHNH_2]_T = [CHNH_3^+] + [CHNH_2] \quad (9)$$

Where the $CHNH_2$ unit represents the neutral amine monomer of chitosan and $CHNH_3^+$ represents the protonated ammonium ion monomer species. The percentage of neutral amine ($CHNH_2$) on the sorbent surface is obtained by using Eqs. (8) and (9):

$$\frac{[CHNH_2]}{[CHNH_2]_T} = \frac{1}{1+\frac{[H^+]}{K_a}} \qquad (10)$$

Therefore, at pH 8.5 the amounts of $CHNH_2$ (99%) and $CHNH_3^+$ (1%) species in solution differ significantly and the predominance of $CHNH_2$ favours neutral adsorbate binding at these conditions for the chitosan based synthetic materials. The percentage of neutral amine is plotted against pH in Scheme 1.1.

The primary amine ($CHNH_2$) groups are important for adsorption because they can chelate many heavy metal cations through the nonbonding electrons of N. The abundance of primary amine groups is affected by the degree of deacetylation; *i.e.* a low degree of deacetylation implies a low percentage of primary amine groups are potentially available for sorption. Crystallanity and molecular weight also affect the sorption properties of chitosan.[16] Chitosan is a biologically safe, non-toxic, biocompatible and biodegradable polymer.[28] These features offer chitosan as a promising sorbent for applications in pharmaceuticals, cosmetics, biomedical, biotechnological, agricultural, food and non-food industries and sorbents for the environmental remediation of contaminated water.[29]

Chitin and chitosan are aminopolysaccharides; the complete N-deacetylation of chitin produces chitosan.[14] The chemical modification of the amino functionality of chitosan can be modified to engineer biopolymers designed for tailored sorption applications. The amino functionalities are applicable to chemical reactions as acetylation, quanternization, reaction with

aldehydes and ketones (yielding Schiff bases), alkylation, grafting and chelation of metals.[20] Commercially available chitosan possesses a range of molecular weights (*i.e.* polydispersity) and degrees of acetylation. The high mol. wt. chitosan is soluble under mild acidic conditions and limits its applications since the N-centre becomes protonated[29] and requires acidic pH conditions to ensure adequate solubility in aqueous solution.

1.16 Chitosan Biopolymers

The hydroxyl groups on chitin are also of importance in various types of chemical modification. Trimukhe and Varma[21] studied the chelation/complexation of heavy metals with cross linked chitin. Chitosan was cross linked using three different cross linkers: diisocyanatohexane (HDI), trimetallic anhydride (TMA) and dibromodecane (DBD) where the hydroxyl groups of chitin were involved in the cross linking (see scheme A). After the cross linking step, deacetylation of the cross linked chitin was performed to expose primary amino groups. This process was repeated to ensure that all of the amine groups were available for heavy metal chelation/complexation. The advantages for cross linking allow tuning of the sorbent SA, pore structure properties and swelling characteristics of the biopolymer. They obtained sorption capacities comparable to unmodified chitosan powder. The advantages of using chitosan based biopolymers are their relatively low cost, capacity for regeneration, enhanced biodegradability and biocompatibility.

To synthesize a chitosan cross linked with Glu biopolymer, the relative amount of chitosan and Glu, acetic acid, pH and temperature of the reaction determines the physiocochemical properties of the biopolymer.[5] Chitosan based biopolymers are used for several applications such as the immobilization of protein[5], metal chelation,[1,5,16,21,24] and as drug

delivery carriers.[28] There are numerous biomedical applications that employ various cross linked forms of chitosan that rely on their unique adsorption/desorption properties.

1.17 Cyclodextrin Properties

The most common Cyclodextrins (CDs) are α-,β- and γ- which are composed of 6-,7- and 8- glucopyranose units attached by α-(1→4) linkages[44]. They have a unique toroidal molecular shape and their inclusion chemistry has been the subject of many studies[4]. Primary hydroxyl groups line the narrow end of the cyclodextrin cavity while secondary hydroxyls group are located at the wider end of the cyclodextrin cavity resulting in a hydrophilic exterior and a lipophilic cavity interior due to the abundance of apolar groups in the CD interior; see Scheme 1.4 and 1.5. The toroidal molecular shape and the well defined cavity of CD's dimensions (diameter of 4.9-7.9 Å with a cavity depth of 7.9Å) allows them to form stable host-guest complexes with various organic compounds and heavy metals.[23,40,44] Table 1.4 gives a list of physical properties with their corresponding parameters with respect to the type of cyclodextrin.

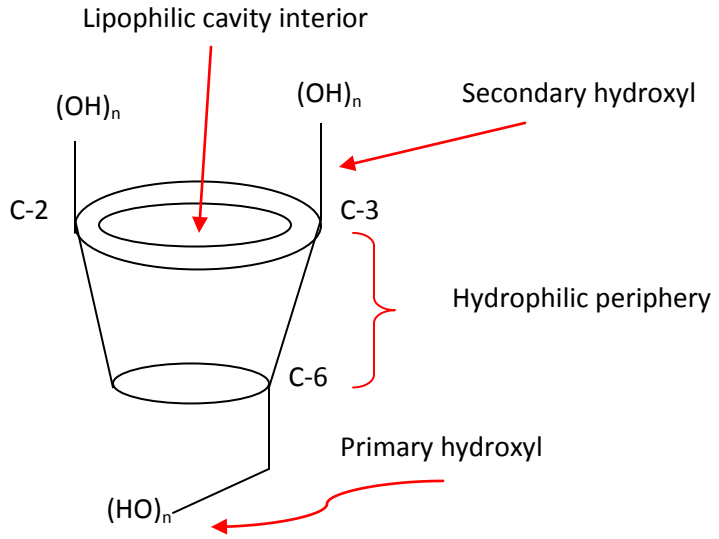

Scheme 1.4. The structure of amphiphilic β-cyclodextrin showing the hydrophilic primary and secondary hydroxyl groups and the lipophilic cavity, where n=7 (adapted from reference 22 and 44).

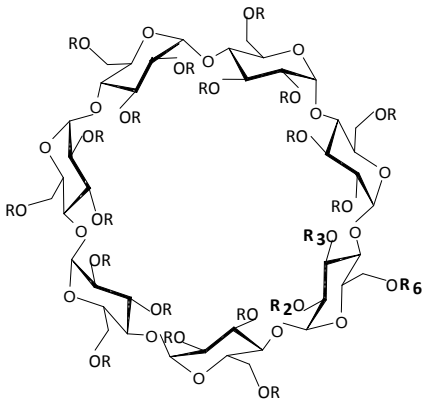

Scheme 1.5. The structure of βCD showing the positions (R_2, R_3, and R_6) of the hydroxyl groups (adapted from reference 56).

Table 1.4. Physical properties and molecular dimensions of α-,β-,γ-cyclodextrins. (Adapted from references 22 and 44)

Properties	α	β	γ
Number of glucopyranose units	6	7	8
Empirical formula (anhydrous)	$C_{36}H_{60}O_{30}$	$C_{42}H_{70}O_{35}$	$C_{48}H_{80}O_{40}$
Relative Molecular Weight (g/mol)	972	1,135	1,297
Water solubility (g/100mL) at 25ºC	14.5	1.85	23.2
Internal average diameter (Å)	4.9	6.2	7.9
External average diameter (Å)	14.6	15.4	17.5
Length of macrocycle (Å)	7.9	7.9	7.9
Cavity volume ($Å^3$)	176	346	510
Average pK_a determined by (potentiometry at 25ºC) where the average value of the primary and secondary OH groups	12.33	12.20	12.08

1.18 Cyclodextrin Biopolymers

CDs are moderately water soluble (see Table 1.4). Their solubility behaviour and physicochemical properties can be modified through copolymer formation. The degree of cross linking in biopolymers containing βCD can be varied by the reaction conditions and the nature of

the cross linkers, such as glutaraldehyde or epichlorohydrin[4]. The synthesis of a water insoluble cyclodextrin polymer can is accomplished by varying the mole ratios of cyclodextrin to the cross linker; thus, modifying the sorption and swellability characteristics of the biopolymer.[4] In this sorption study, two and three-component biopolymers were synthesized using chitosan and β-cyclodextrin as the carbohydrate framework and cross linking with glutaraldehyde to form an extensive co-polymer framework. To synthesize a chitosan/β-cyclodextrin/glutaraldehyde (three-component) biopolymer, the amount of chitosan, β-cyclodextrin and glutaraldehyde, pH conditions and temperature of the synthetic conditions determine the physical and chemical properties.[5] The host-guest properties of such cyclodextrin biopolymers have been used in in the production of industrial chemicals, biochemical products and chemical separations[60], optimizing drug formulations[61], analytical methods for chromatography[62], food processing[63] and for food production (*i.e.* flavour stabilization, improving shelf life, flavour carriers, cholesterol sequestrant, taste modifiers and as debittering agents[64]).

1.19 Glutaraldehyde

Glutaraldehyde (Glu; glutaric acid dialdehyde, glutaric aldehyde, 1,5-pentanedial) is a multifunctional cross linker with two aldehyde groups each positioned at the 1,5 terminal sites of a pentyl chain. Glutaraldehyde (see Figure 1.6) is among many cross linkers, such as epichlorohydrin[4], that is used as a versatile cross linker for designing polymeric frameworks.

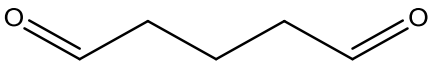

Figure 1.6. The molecular structure of glutaraldehyde, a bi-functional cross linker unit.

1.20 Interactions of Chitosan & β-Cyclodextrin Biopolymers with Metal Species

Roberts[33] reports that chitosan is a metal chelating polymer; however, it must have two or more ligands to bind to a metal ion if it is a chelator. Therefore, either the OH/O^- or NH/NH^- groups on the D-glucosamine monomers of chitosan may act as ligands from two or more chitosan chains to bind a metal ion. By employing X-ray photoelectron spectroscopy (XPS), Dambies[41] studied the sorption interactions between three metal ions (Cu(II), Mo(VI) and Cr(VI)) with chitosan flakes, chitosan beads and glutaraldehyde cross linked chitosan beads, respectively. XPS was used to study the oxidation state of metal ions sorbed onto the surface of the chitosan. It was found that the amine functional groups are the main sorption sites for the metal cations. It was also found that chitosan in the form of flakes, beads and cross linked beads "reduce the oxidation state of the sorbed metal ion". Dambies concluded that the reducing activity depends on two main criteria: i) the oxidation potential of the metal (correlated to the normal redox potential scale) and ii) the "framework" of the biopolymer; where the glutaraldehyde cross linked chitosan significantly increased the reducing effect. This could explain possible interactions occurring in this study between the oxoanion arsenate species and the amine anionic sites located on the surface of the chitosan glutaraldehyde cross linked biopolymer. There are many possible interactions occurring between the chitosan, β-cyclodextrin biopolymers and the arsenic species in solution at pH 8.5. As mentioned, the biopolymers could chelate metal ions requiring two or more binding sites of the biopolymer (referred to as a ligand or host). However, several other interactions are possible such as electrostatic (non-directional) interactions, hydrogen bonding, ion-ion interactions and Lewis acid-Lewis base interactions.

1.21 Summary of Introduction

Arsenic contamination is a growing concern throughout the world especially in countries such as Bangladesh and West Bengal where arsenic is a major health and environmental concern. There are conventional treatments for arsenic removal such as coagulation/filtration, lime softening, activated alumina, ion exchange, reverse osmosis, manganese greensand filtration and electrodialysis; each treatment has advantages and limitations. There has been a lot of research using conventional sorbents for adsorption using various receptor/host frameworks. The Langmuir (*i.e.* Sips restricted) and Sips isotherms provide insight about the sorption mechanism; at varying experimental conditions such as the type of receptor/host framework, pH, ionic strength, temperature, concentration of sorbate and the amount of sorbent. However, there needs to be further research on different types of novel biomaterial sorbents to understand the relationship between structure and function of sorbents (*i.e.* receptor/host frameworks as described in this research).

The overall objective of this research is to design two- and three-component chitosan based biopolymers which will be characterized and tested for arsenate oxoanion sorption in aqueous solution. The thermodynamic sorption properties will be modeled through two types of sorption isotherms (*i.e*. Sips and Langmuir models).

Chapter 2 Materials and Methods

2.0 Materials

High molecular weight chitosan (HMWCH) (from crab shells practical grade 150,000-375,000 $gmol^{-1}$ ≥75% deacetylation), low molecular weight chitosan (LMWCH) (50,000-190,000 $gmol^{-1}$, 75-85% deacetylation) and Glutaraldehyde (Glu) were all Aldrich products and used as received without further purification. β-CD hydrate was obtained as an Alfa Aesar product and used as received without further purification.

2.1 Biomaterials Preparation

2.1.1 Chitosan Calculation: to determine the amount of Glutaraldehyde for biopolymer synthesis

Firstly, the mean molar mass (M.M.M.) of a monomer of chitosan ($C_6H_{11}NO_4$) with respect to (w.r.t) nitrogen (N) was calculated from the % of N determined by an elemental analysis (EA):

Sample Calculation[5]:

$$M.M.M = \frac{(molar\_mass\_of\_N)\times(N\_atoms\_in\_Chitosan)}{(\%\_of\_N)}$$

The calculated M.M.M. of HMWchitosan w.r.t. N worked out to be 189.3 g mol^{-1}.

The calculated M.M.M. of LMWchitosan w.r.t. N worked out to be 196.7 g mol^{-1}.

Therefore, I could now calculate the amount of Glu required for each mole ratio 1:15, 1:25 and 1:35.

A sample calculation for amounts of chitosan and Glu required for a 1:15 co-monomer mole ratio:

$$1\_mole\_of\_HMWchitosan \times \frac{189.3\_g}{1\_mole\_of\_HMWchitosan} = 189.3\_g\_HMWchitosan$$

$$15\_moles\_of\_Glu \times \frac{100.1\_g\_Glu}{1\_mole\_Glu} = 1501.8\_g\_Glu$$

1 mole of chitosan monomer:1 mole of Glu ≈ 189.3 g chitosan:1501.8 g Glu

∴ 1 g of chitosan:7.933 g Glu

$$7.933\_g\_\ Glu \times \frac{1\_mL}{1.106\_g\_Glu} = 7.173\_mL\_Glu$$

∴ 7.173 mL of Glu is needed for a 1:15 co-monomer mole ratio of CH:Glu

2.2 Biopolymer Synthesis

2.2.1 Low Molecular Weight Chitosan (50,000-190,000 gmol^{-1})/Glutaraldehyde

Approximately 0.40 g of chitosan was placed in a 100 mL round bottom flask and was stirred to complete dissolution overnight with 60 mL of 5.0 x 10^{-2} M acetic acid. To the dissolved chitosan, a desired (1:15 , 1:25, 1:35 mole ratios of chitosan:glutaraldehyde) amount of a 50% (w/v) Glu aqueous solution was added rapidly to the chitosan/acetic acid aqueous solution. Rapid addition of Glu was required due to the onset of rapid gelation (~3 minutes). The clear solution turned to a dark orange-yellow color over the course of one hour. The mixture

was allowed to stir until complete gelation then allowed to sit for 1 hour before neutralizing with a 0.2 M NaOH solution to pH 6-7. The orange-yellow gellated product was washed several times with cold millipore water and cold HPLC grade acetone. The orange-yellow spongy material was then dried in a vacuum oven at 56ºC at reduced pressure (0.94 atm Hg) overnight. The oven dried products were crushed and ground into a fine powder form before drying in a pistol dryer under vacuum with P_2O_5 at 50°C overnight. The products were ground in a mortar and pestle and passed through a 40 mesh sieve. The products were then washed in soxhlet extractor with HPLC grade methanol for 24 hours then repeated for a second washing cycle with HPLC grade diethyl ether for 24 hours.

2.2.2 High Molecular Weight Chitosan (150,000-375,000 $gmol^{-1}$)/Glutaraldehyde

The synthesis procedure is the same as above except that chitosan with a greater molecular weight (150,000-375,000 $gmol^{-1}$), was used in a place of the LMWCH. (The photograph of synthesized chitosan/glutaraldehyde biopolymer material is shown in Figure 2.1.)

Figure 2.1. The photograph of crude product chitosan/glutaraldehyde biopolymer material.

2.2.3 High Molecular Weight Chitosan -β-Cyclodextrin:Glutaraldehyde

These three-component polymeric materials were designed to cover a range of mass ratios (1-1, 1-3 and 1-1/3) of HMWCH to β-CD; where the amount of Glu added was kept constant for each material in a 1:6 mole ratio (1 mole of HMWCH to 6 moles of Glu). The amount of Glu added was kept constant and based on a total mass of 1.0 g of HMWCH (150,000-375,000 $gmol^{-1}$); the mass ratio (w-w) amounts of HMWCH to βCD was varied from 1-1 to 1-3 to 1-1/3.

2.2.3.1 1:6 High Molecular Weight Chitosan-β-Cyclodextrin (1-1): Glutaraldehyde

0.50 g of HMWCH and 0.50 g of β-CD hydrate were placed in a 100 mL round bottom flask and stirred in ~20 mL of 1 M HCl until complete dissolution overnight; an additional 1 mL of 1 M HCl was added to ensure adequate solvent while the stir bar maintained stirring. After the reaction was place in an 80 ºC oil bath and the mixture turned from a cloudy solution to a clear solution indicating the CH was dissolved. After stabilization at 80 ºC, a desired 1:6 mole ratio of (chitosan:glutaraldehyde) was obtained by addition of a 50% (w/v) glutaraldehyde aqueous solution while stirring rapidly. Rapid addition of glutaraldehyde was required because gelation occurs within 3 minutes of mixing at these conditions. The reaction mixture was promptly removed upon gelation from the 80 ºC oil bath and allowed to cool to room temperature for 1 hour before neutralizing with a drop-wise addition of 2 M NaOH solution to a pH 7-8. The clear solution turned to a dark orange-yellow color over the course of an hour. The neutralized reaction mixture was allowed to stir for an additional 30 minutes and cooled in a ice bath before washing. The orange/yellow coloured gel was washed several times with 75 mL millipore water and 50 mL HPLC grade acetone. The product was then dried in a vacuum oven

at reduced pressure (0.94 atm Hg) overnight. The oven dried products were crushed and ground to a powder before drying in a pistol dryer under vacuum conditions with P_2O_5 at 50°C overnight. The products were ground in a mortar and pestle and passed through a 40 mesh sieve. The material was then washed in soxhlet extractor with HPLC grade methanol for 24 hours then HPLC grade diethyl ether for 24 hours and subsequently dried under vacuum conditions with P_2O_5 at 50 °C overnight.

2.2.3.2 1:6 High Molecular Weight Chitosan-β-Cyclodextrin (1-3): Glutaraldehyde

0.25 g of HMWCH (150,000-375,000), and 0.75 g of β-CD hydrate were used for this synthesis and the procedure is the same as described above in the previous section.

2.2.3.3 1:6 High Molecular Weight Chitosan-β-Cyclodextrin (1-1/3): Glutaraldehyde

0.75 g of HMWCH (150,000-375,000) and 0.25 g of β-CD hydrate was used for this synthesis and the procedure is the same as described above.

2.3 Biomaterials Characterization

The biopolymers were characterized using TGA to investigate their thermal stability and relative co-monomer composition, FT-IR spectroscopy to show specific functional groups and vibrational bonds that are key signatures to the characterization of products. CH&N elemental analysis (EA) determines the relative composition (wt %) of carbon, hydrogen and nitrogen. ICAP-OES[22] and Varian Cary 100 Scan UV-Vis spectrophotometry were used to measure arsenate (λ_{em}=189 nm) and PNP (λ_{max}=400 nm) in aqueous solution at pH 8.5

2.3.1 Biomaterials Characterization Instrumentation

2.3.1.1 Inductively Coupled Argon Plasma-Optical Emission Spectroscopy

Liquid samples are pumped through a nebulizer to produce a fine misty spray; large droplets are removed by the spray chamber where the fine droplets pass through to the plasma source. The small droplets (residual sample) are decomposed to atoms and ions that become electronically excited and emit a characteristic emitted light for a given wavelength. This characteristic light (emission) is measured and provides a measurement of the concentration of each element in the sample. Arsenate equilibrium sorption experiments were measured with a Thermoscientific ICAP-OES. The arsenic concentration was obtained using emission spectroscopy at λ_{em} = 189 nm. The analysis protocol of each sample was measured in triplicate with a 30 second sample flush time with millipore water between each sample. The sample introduction was a nebulizer with an axial plasma view. The calibration mode was set to concentration. The flush pump rate was 100 rpm and the analysis pump rate was 40 rpm with a pump stabilization of 5 seconds. RF power was 1150 W with an auxiliary gas flow of 0.5 $Lmin^{-1}$ and nebulizer gas flow of 0.30 $Lmin^{-1}$.

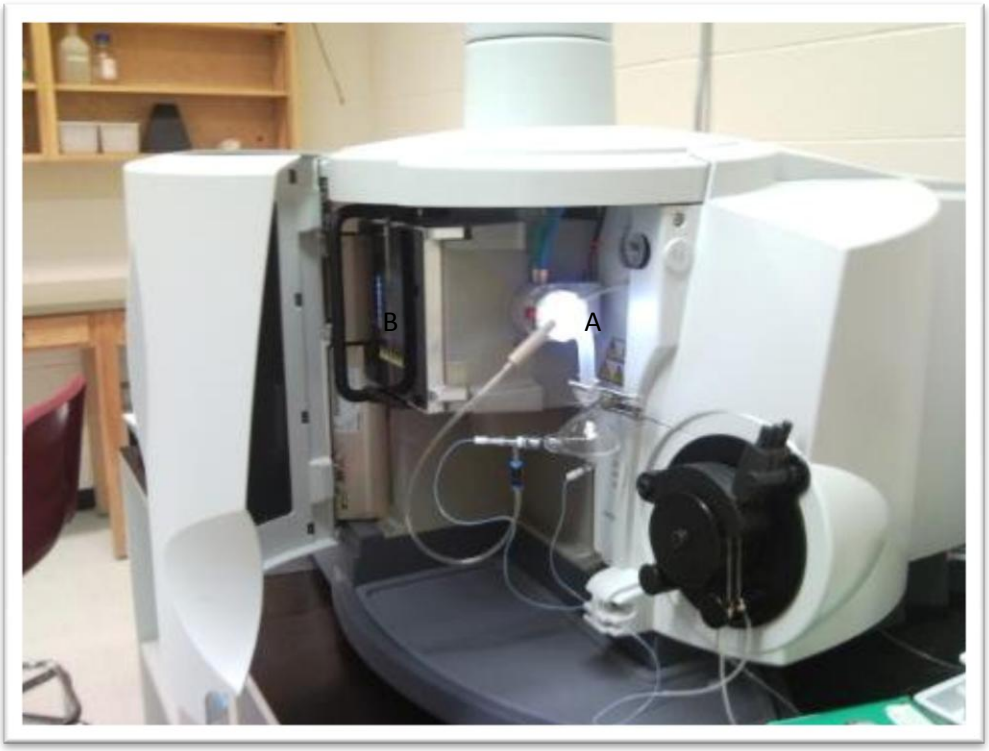

Figure 2.2. The photograph of the ICAP-OES A) Nebulizer B) Plasma Source.

2.3.1.2 Fourier Transform-Infrared Spectroscopy

The IR spectra were obtained with a BIO-RAD FTS-40 spectrophotometer and powdered samples were analyzed in reflectance mode. Biopolymers were prepared by mixing ~45 mg of biopolymer sample with pure spectroscopic grade KBr (~120 mg) by grinding in a small mortar and pestle. DRIFT spectra were recorded at room temperature with a resolution of 4 cm^{-1} over the range of 400-4000 cm^{-1}. Two hundred and fifty six scans were recorded and corrected against a background spectrum of pure KBr. The DRIFT spectra were obtained in reflectance mode and the results are reported as arbitrary units.[22]

2.3.1.3 Ultraviolet-Visible Spectroscopy

The sorption isotherm for biopolymers with PNP were obtained using a Cary 100 Scan UV-Vis spectrophotometer at pH 8.5 and room temperature (295 K). Absorbance values of PNP were recorded at λ=400 nm to calculate residual equilibrium dye concentration (C_e).

2.3.1.4 Thermal Gravimetric Analysis

Thermal events were measured on a TGA Q50 Series with a standard furnace. Biopolymers were equilibrated at 30ºC, heated with a ramp profile of 5ºC per minute for 500ºC under N_2 as the carrier gas and air as the coolant gas (flow rate = 50 ml min^{-1}).

2.3.1.5 Carbon, Hydrogen and Nitrogen Elemental Analysis

The content (w/w%) of carbon (C), Hydrogen (H) and Nitrogen (N) were measured by Perkin Elmer 2400 CHN Elemental Analyzer with a detection limit of ±0.3%.[22]

2.4 Equilibrium Sorption Experiments

The $HAsO_4^{2-}$ and PNP sorption study of chitosan based copolymers was adapted from a published literature method.

2.4.1 Arsenate(V) Equilibrium Sorption Experiments

Fixed amounts (~20 mg) of the sieved biopolymers in powder form were mixed with 10 mL of adsorbate ($Na_2HAsO_4.7H_2O$) solution at pH 8.52 in 6 dram vials at variable concentrations (45-120 ppm) of adsorbate and equilibrated at room temperature on a horizontal shaker table for 24 hours. After shaking, the supernatants solutions were filtered through 0.45 μm nylon syringe filters and then analyzed by Thermoscientific ICAP-OES 6000 series. The initial concentration (C_o) was determined before sorption and after sorption (C_e) with biopolymers at 22°C at pH 8.5.

Uptake of the adsorbate was determined from the difference between the initial and final residual arsenate ion concentration in aqueous solution with eq. (1).

2.4.2 *p*-Nitrophenol Equilibrium Sorption Experiments

Fixed amounts (~20 mg) of the sieved biopolymers in a powder form were mixed with 10 mL of aqueous adsorbate (PNP dissolved in a 10 mM potassium phosphate monobasic buffer solution) in 6 dram vials at variable concentration (0.2 – 10 mM) and equilibrated at room temperature on a horizontal shaker table for 24 hours. The initial concentration (C_o) was determined before sorption and after sorption (C_e) with biopolymers at 22°C at pH 8.5. Uptake of the adsorbate was determined from the difference between the initial and final PNP ion concentration in the aqueous phase with eq. (1).

2.5 Arsenate(V) Solution Preparation

Arsenate solution was prepared by dissolving ACS grade $Na_2HAsO_4.7H_2O$ (Alfa Aesar), into millipore water at pH 8.5. The arsenic solutions used in the sorption study were prepared by fresh appropriate dilution of this stock solution.[2]

2.6 *p*-Nitrophenol Solution Preparation

A PNP dye concentration (0.4 – 10 mM) was prepared by dissolving PNP into a 10 mM potassium phosphate monobasic buffer solution; the phosphate buffer was prepared at pH 8.5 by adjusting the pH with 2 M NaOH. The molar absorptivity (ε) value for PNP was estimated as ε = 18,478 $Lmol^{-1}cm^{-1}$ (pH 8.5; λ_{max} = 400 nm) using the Beer Lambert Law.

2.7 Equilibrium Sorption Study

The equilibrium sorption study was carried out with chitosan - based biomaterials using two types of adsorbates: PNP and $HAsO_4^{2-}$, respectively. The Langmuir (*i.e.* Sips restricted) and Sips isotherm models, eqns. 2 and 3, were applied to both sets of sorption results; however the isotherm parameters for PNP provide an independent estimate of the sorbent surface area, (SA; $m^2\ g^{-1}$: see eq. (11)).

2.7.1 Surface Area

The Langmuir[25,26] and Sips[24] isotherm models provide surface area (SA) estimates of the monolayer coverage (Q_m) of the sorbent material, where PNP is the adsorbate species.

$$SA = \frac{A_m Q_m L}{N} \qquad (11)$$

Where A_m represents the cross-sectional area occupied by PNP (A_m for "planar" orientation is 5.25 $x10^{-19}$ m^2/mol; whereas, an "end-on" orientation is 2.5 $x10^{-19}$ m^2/mol), L is Avogadro's number (mol^{-1}) and N is the coverage factor which equals unity for PNP at these conditions.

2.7.2. Equilibrium Concentration of Adsorbate Species

The sorption isotherms are plots of equilibrium concentration of adsorbate species adsorbed from solution per mass of adsorbate (Q_e) versus the equilibrium concentration of unbound adsorbate species in aqueous solution (C_e). The Q_e value is defined below where C_o is the initial adsorbate concentration, V is the volume of solution and m is the mass of sorbent, as outlined previously.[4,22]

$$Q_e = \frac{(C_o - C_e) \times V}{m} \qquad (12)$$

2.7.3. Langmuir Isotherm

The Langmuir (*i.e.* Sips restricted) isotherm model[25,26]

$$Q_e = \frac{K_L Q_m C_e}{1 + K_L C_e} \qquad (13)$$

Where K_L is the Langmuir constant[2] and is related to the sorption capacity and energy, respectively.

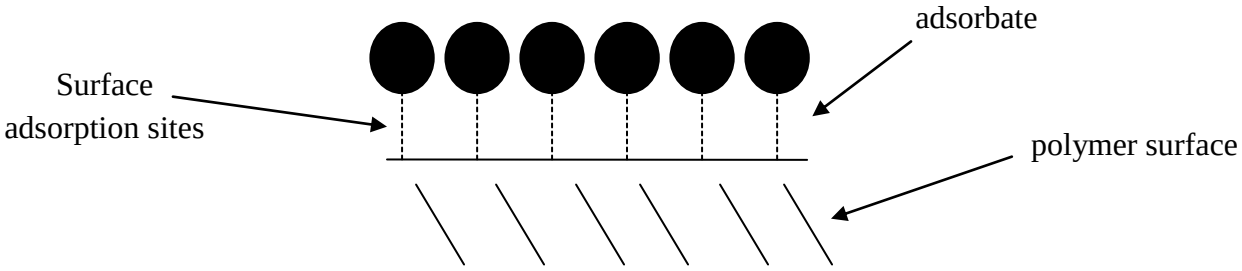

Scheme 2.1. The monolayer coverage representation according to the Langmuir isotherm.

2.7.4. Sips Isotherm

The Sips isotherm represents a generalized model which can be expressed as a monolayer or multilayer equilibrium process with respect to the adjustable fit parameter (n_s; *cf.* eq.(14)):

$$Q_e = Q_m \frac{(K_s C_e)^{n_s}}{1 + (K_s C_e)^{n_s}} \qquad (14)$$

Where K_s is the adsorption constant, n_s represents the degree of heterogeneity of the sorbent surface, C_e is the residual equilibrium concentration of sorbate in aqueous solution and Q_m represents the monolayer coverage of the sorbate as defined in eq. (11). The Langmuir (*i.e.* Sips

restricted) isotherm (eqn. 13) assumes equivalent adsorption sites; whereas, the Sips isotherm (eqn. 3) accounts for multiple adsorption energies.

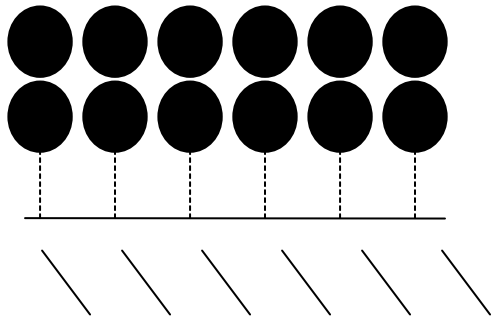

Scheme 2.2. The sorbate coverage representation according to the Sips isotherm.

The Langmuir (*i.e.* Sips restricted) isotherm model describes monolayer surface coverage and assumes independent homogenous sorption sites. The Sips isotherm model provides an assessment of the heterogeneity of the sorption process according to the value of the exponent parameter (n_s)[40]. The Langmuir or the Sips isotherm models can be used to estimate the surface area according to the estimated sorption parameters (Q_m) parameters using eqns.11 and 12, respectively.

2.7.5. Criterion of the Best-Fit

The criterion of the best-fit of the experimental data with the isotherm models (eqn. 13 and 14) is determined by the correlation coefficient (R^2) and the sum of the square of the errors (SSE), see eqn. 15

$$SSE = \sum \sqrt{\frac{(Q_{e,i} - Q_{f,i})^2}{N}} \qquad (15)$$

Where $Q_{e,i}$ is the experimental value, $Q_{f,i}$ is the simulated value according to the chosen isotherm model and N is the number of experimental data points.

2.7.6. Error Analysis

The error analysis was adapted from Kwon[22], using equation (1) above to calculate the Q_e values and the error contributions (ΔQ_e and Q_e) which are related to uncertainties in the mass of sorbent (m) and the initial concentration (C_o) and the equilibrium concentration (C_e). To differentiate Q_e with respect to each quantity, the following contributions are obtained, as shown in equations (16-18).

$$\Delta Q_e = 2\left|\frac{(C_o - C_e)\times V}{m^2}\times \Delta m\right| \quad (16)$$

$$\Delta Q_e = 2\left|\frac{V}{m}\times \Delta C_o\right| \quad (17)$$

$$\Delta Q_e = 2\left|\frac{V}{m}\times \Delta C_e\right| \quad (18)$$

Where ΔC_e, ΔC_o and Δm are the standard errors associated with each measurement. The total error in Q_e is obtained from the sum of each of the individual quantities represented by equations (16–18) for each data point. It is noted that there is both a positive and negative error associated with each data point as reflected by a factor of 2 and the absolute value for each quantity given in the equations (16-18). The uncertainties in absorbance gives rise to standard errors in C_e and C_o which can be calculated from the straight line regression parameters of the Beer-Lambert coefficients. An uncertainty in the consecutive weightings on an electronic balance (*i.e.* $1x10^{-5}$ g per weight measurement) gives rise to the variable uncertainty in mass. For example, to obtain a

mass of sorbent, three weightings are needed; thus, the standard error is ~$3x10^{-5}$ g for a digital balance with a weighing precision of ± 0.01 mg.

2.8. Removal Efficiency

The removal efficiencies of PNP and $HAsO_4^{2-}$ from aqueous solution were calculated using equation (19)[4]:

$$\varepsilon_R\% = \left(\frac{C_o - C_e}{C_o} \right) \times 100\% \qquad (19)$$

Where C_o and C_e are defined as above. The pH, temperature, adsorbate concentration and both the relative amount and nature of biopolymer material all contribute to the magnitude of the removal efficiencies.

Chapter 3 Results and Discussion for Materials Characterization

3.0 Materials Characterization

Chitosan cross linked with glutaraldehyde has been previously studied for its sorption properties towards inorganic and organic compounds. However, characterization of the biomaterial warrants more research in order to understand the sorption mechanism in aqueous solution. In this thesis, the materials characterization has been briefly examined in order to provide a better understanding of the relationship between the structure of the sorbents and the sorption phenomena of chitosan modified materials. Several materials characterization techniques employed in this research include FT-IR spectroscopy, TGA, EA and synthetic yield of products. These techniques provide support for the product identity and provide a platform upon which to carry out future studies.

3.1 Synthetic Yields

Product yields may give insight to the factors affecting the efficiency of the cross linking reaction such as viscosity, mass transfer effects, reactant ratios of precursors and the nature of the cross linker. It is apparent that the two-component 1:15 biopolymers, for both the high and low molecular weight chitosan had the greatest yields (cf. Table 3.1). The product yields for chitosan copolymers with glutaraldehyde were observed to decrease in proportion to the cross linking density of the biopolymer.[4] The mass transfer efficiency between chitosan and glutaraldehyde is hypothesized to decrease with increasing viscosity of the reaction mixture as the polymerization reaction proceeds through solution, gelation and solid polymer phases.

Table 3.1. The product experimental yield (%)* of each CH-Glu (two-component) based biopolymer.

Sorbent Biomaterial	1:15	1:25	1:35
LMWCH:Glu	24.4%	22.0%	16.3%
HMWCH:Glu	29.3%	14.8%	11.6%

*% yield is based on the reaction mechanism 1 where both aldehyde groups of Glu react with two glucose units of chitosan; cross linked product not shown.

There are several approaches outlined for a hypothesized reaction mechanism and all would be valid; however, there are several products predicted for this type of synthesis. Three generalized reaction schemes (Schemes 3.1 to 3.3) have been proposed based on a previous study by Knaul et. al[65] according to evidence based on FT-IR and ^{13}C NMR data. Mechanism 1 (Scheme 3.1) occurs through a Schiff base reaction at the amine functional group:

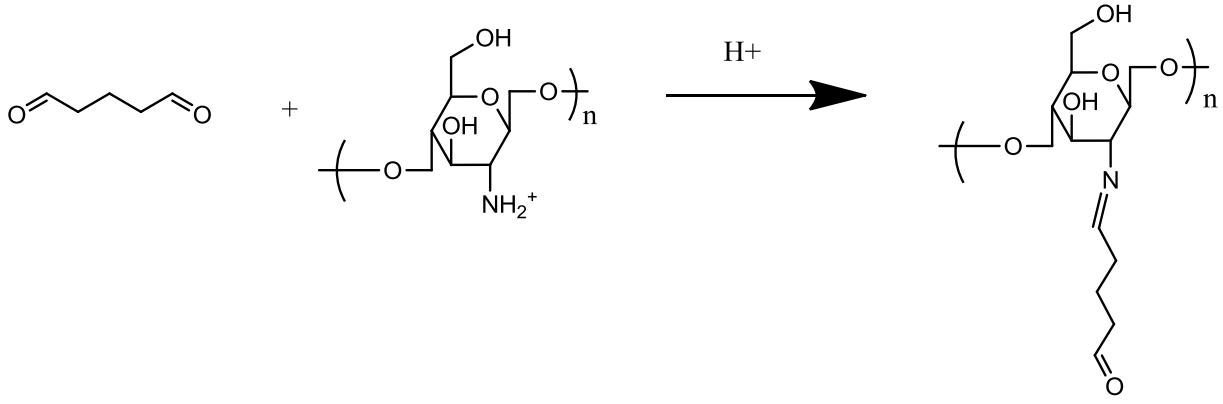

Scheme 3.1. Glu is reacted with dissolved chitosan in mild acetic acidic conditions at 295 K to produce a glutaraldehyde linked product reaction of the amine groups of chitosan. Note that the cross linked copolymer is not shown for the sake of brevity.

Mechanism 2 (Scheme 3.2) involves reaction of the hydroxyl groups of chitosan and is based on the same conditions outlined in mechanism 1:

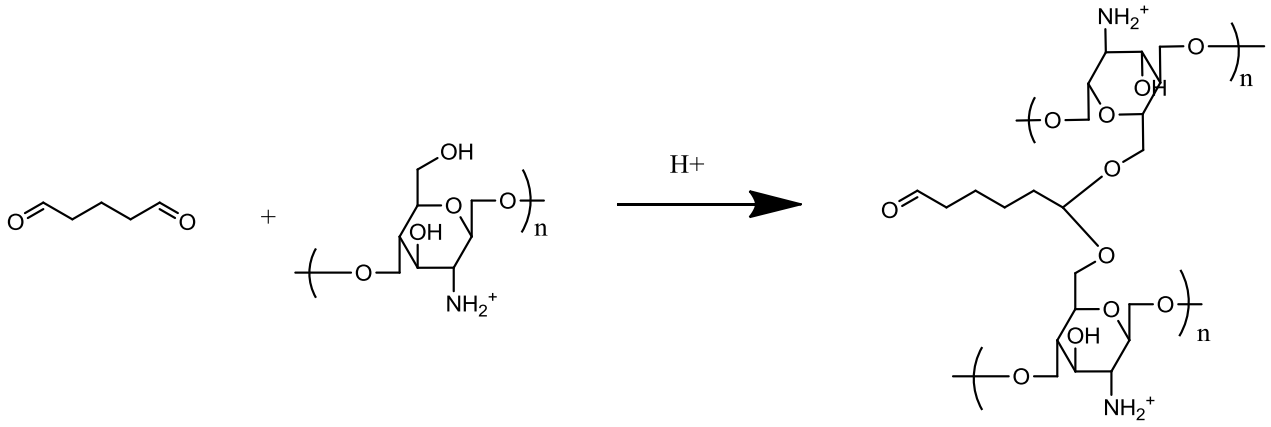

Scheme 3.2. Glu is reacted with dissolved chitosan in mild acetic acidic conditions at 295 K to produce a cross linked product via reaction of the hydroxyl groups of chitosan.

Reaction mechanism 3 (Scheme 3.3) is based upon the ^{13}C NMR spectrum of a 25% Glu solution in water and assumes that Glu is unstable in water because it may adopt a similar structure to glyoxal which is also unstable in water. This fact is the basis of mechanism 3 because the structure of Glu in water gives rise to a "pyran isomer, or its dimer, trimer, or a crown ether, depending on the molecular weight"[65]; thus, mechanism 3 proposes that the molecular structure of Glu in water is that of a hemi-acetal which cross links with the amine groups of chitosan:

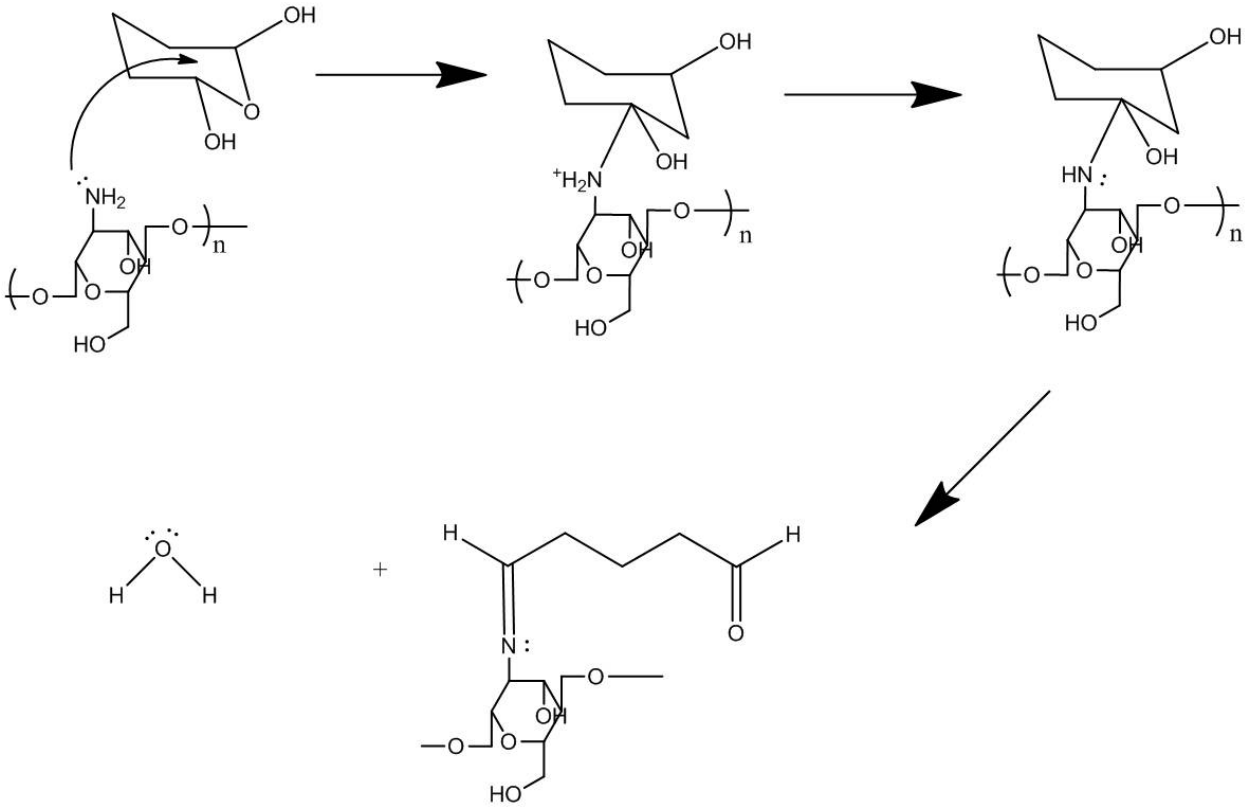

Scheme 3.3. Glu is reacted with dissolved chitosan in mild acetic acidic conditions at 295 K to produce a cross linked product via mechanism 3.

A Schiff base is expected to occur between the amino group on an adjacent chitosan polymer and the remaining aldehyde group; the FT-IR spectra indicates the presence of a C=N bond occurring between Glu and chitosan.[65]

The generalized reaction scheme for a two-component copolymer is as follows, where A is chitosan and B is Glu:

$$A + B_{(solution)} \longrightarrow A/B_{(gel\ phase)} \longrightarrow (A\text{-}B)_{n\ (solid\ product)} + (A_n\text{-}B_n)_{n\ (solid\ product)}$$

A previous independent study on the modification of chitosan films with Glu to regulate solubility and swellability showed that the viscosity increases as the amount of chitosan is increased.[57] This is consistent with the rheological behavior of polymer in solution.

The product experimental yields obtained for the three-component biopolymers composed of HMWCH, βCD and Glu (cf. Table 3.2) shows that as the mass ratio of chitosan to βCD (1-1/3 to 1-3) changes the viscosity of the solution changes. When there are equivalent mass amounts of CH and βCD for the polymerization reaction, the highest yield is obtained among amount the three ratios of reagents. When the mass ratio is 1-1/3, the amount of βCD is 1/3 the amount of CH and the percent yield decreases. As the mass ratio changes to a 1-3 mixture, the relative amount of chitosan is 1/3 the amount of βCD and the lowest percent yield was obtained. The relative amounts of CH and β-CD play a huge role in the cross linking and is evident in the product yields. The mass transfer effects (*i.e.* stirring effects) is vital and plays an important role in the connectivity of the framework.

Table 3.2. The product experimental yields of each CH-βCD-Glu (three-component) based hybrid biopolymer.

Mass ratio of chitosan to βCD	**1-3**	**1-1**	**1-1/3**
1:15 HMWCH-βCD:Glu	11.4%	34.1%	31.7%

Note: Chitosan and Glu content were fixed whereas the βCD content was varied.

3.2 Elemental Analysis

Elemental Analysis (EA) is a common technique used for biopolymer samples to determine the relative amount of carbon, hydrogen and nitrogen (C, H and N) composition through combustion analysis. In cases where the polymer contains impurities such as unreacted starting materials, occluded solvents and moisture, the results from this technique may be semi-quantitative.[57] EA is useful when the theoretical composition can be calculated and compared to the experimental values. In order to calculate a theoretical yield, the weight of the products from a polymerization reaction, an understanding of the reaction mechanism is necessary. Several reaction mechanism have been proposed involving chitosan/Glu (two-component) and for chitosan/βCD:Glu (three-component) for polymerization reactions. The cross linking reaction mechanism of CH with Glu involves four types of potential products, as discussed by Oyrton et al.[5] Four types of products or a combination of any four types leads to ambiguous theoretical estimates for the weight percentages of carbon, hydrogen and nitrogen.

In general, the content of C increases as expected for Table 3.3; however, the content of N decreases and H does not scale quantitatively as expected. The cross linking of glutaraldehyde with LMWCH depressed the amount of N available in the biopolymer framework. As noted previously, an understanding of the reaction mechanism is of paramount importance for the development of a systematic design approach of these types of biopolymers. For Table 3.4, the content of C, H & N does not scale quantitatively as expected. The 1:25 has the highest content of C and the lowest content of H and N.

It is noted that as the content of C increases as the content of N decreases for each LMWCH and HMWCH incorporated into the respective frameworks; however, there is no clear correlation for the content of H available within each biopolymer framework. The percentage

weights are uncorrected for residual solvents that may have remained adsorbed within the biopolymer frameworks during the cross linking stage. Theoretical estimates cannot be calculated based solely on the proposed mole ratios because the basis of this calculation relies on a knowledge of the reaction mechanism and the site of cross linking occurs. i.e. amine groups versus hydroxyl groups or both.

Table 3.3. The CHN Elemental Analysis and Theoretical Estimates of LMWCH:Glu biopolymers.

Sorbent Biomaterial	**Experimental**			**Theoretical***		
	%C	%H	%N	%C	%H	%N
1:15	54.0	7.37	2.65	84.5	8.77	1.22
1:25	55.7	7.50	2.18	59.8	7.96	0.53
1:35	57.0	7.38	2.16	87.9	8.94	0.57

*Assumes reaction of Glu with amine groups of chitosan

Table 3.4. The CHN Elemental Analysis and Theoretical Estimates of HMWCH:Glu biopolymers.

Sorbent Biomaterial	**Experimental**			**Theoretical***		
	%C	%H	%N	%C	%H	%N
1:15	51.8	7.55	3.21	84.5	8.77	1.22
1:25	53.2	7.20	2.61	59.8	7.96	0.53
1:35	51.87	7.23	2.69	87.9	8.94	0.57

*Assumes reaction of Glu with amine groups of chitosan.

Table 3.5. The CHN Elemental Analysis of HMWCH-βCD:Glu biopolymers.

Sorbent Biomaterial	%C	%H	%N
1:15 CH-βCD (1-3):Glu	48.1	7.28	3.22
1:15 CH-βCD (1-1):Glu	44.5	6.71	2.53
1:15 CH-βCD (1-1/3):Glu	49.4	7.23	2.80

In Table 3.5, when there is an equivalent amount of chitosan and β-CD in the framework, the lowest percentage of C, H & N was obtained. However, when we change the relative ratios of CH and β-CD there are observable differences among each biopolymer framework. Although the 1-1/3 has 1/3 the amount of β-CD incorporated into the framework it results in the second highest amount N content. The 1-3 has three times the amount of β-CD incorporated into the framework and the highest amount of N content is obtained. This is a direct contradiction of what is expected for this type of product assuming that chitosan and βCD react similarly toward Glu. Mass transfer plays a role in the product yields and is obviously reflected in the EA data. CH is the sole bearer of N whereas β-CD and Glu do not contain N. This type of inconsistency would come from a more detailed understanding of the reaction pathway in conjunction with analysis from other characterization techniques. The composition of the products and the presence of characteristic functional groups from this cross linking reaction may be obtained from TGA and FT-IR spectroscopy.

3.3 Thermal Gravimetric Analysis

Thermal Gravimetric Analysis (TGA) is a technique where a sample is heated and the weight loss is monitored with increasing of temperature. TGA shows thermal losses of a sample using a first derivative plot of the weight (weight loss %/°C) versus temperature (°C). Second derivative plots illustrate regions where the weight loss is most significant over a given temperature range.[57] The LMWCH and HMWCH, see Fig. (3.4) have a peak centered ~300°C. In general, each chitosan:Glu biopolymer (*cf.* Figure 3.1 and 3.2) exhibits thermal events near ~215°C and ~420°C. It is noted that the peaks corresponding to cross linked chitosan are shifted to higher temperatures. These thermal events represent mass losses from the biopolymer as follows: *i*) mass losses due to loss of Glu ~215°C and *ii*) weight losses due to CH ~420°C. In Figure 3.1, the thermal event occurring around ~185°C is related to the Glu monomer content of chitosan and this peak area increases as the glutaraldehyde content of the biopolymer increases. Thermal transitions occurring below 100°C are attributed to desorption of water and/or residual solvents. Figure 3.3, has thermal events centered on ~250°C and ~420°C; the biopolymer is composed of three components and represents a more complex product due to the peak area between 390°C to 475°C.

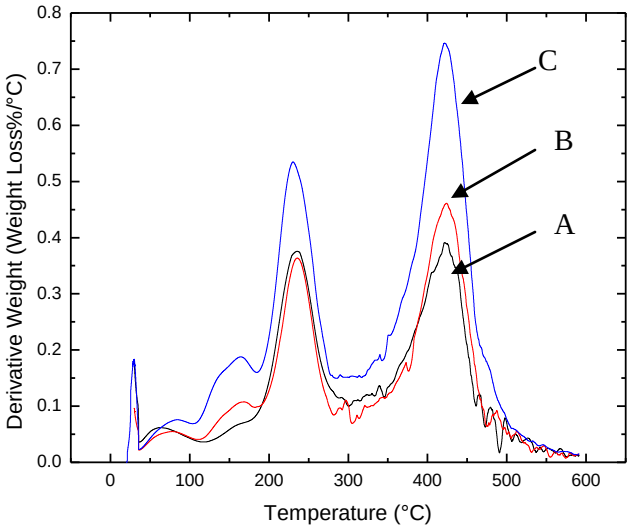

Figure 3.1. The first derivative TGA plot of LMWCH:Glu where A) 1:15 B) 1:25 and C) 1:35 two-component biopolymers.

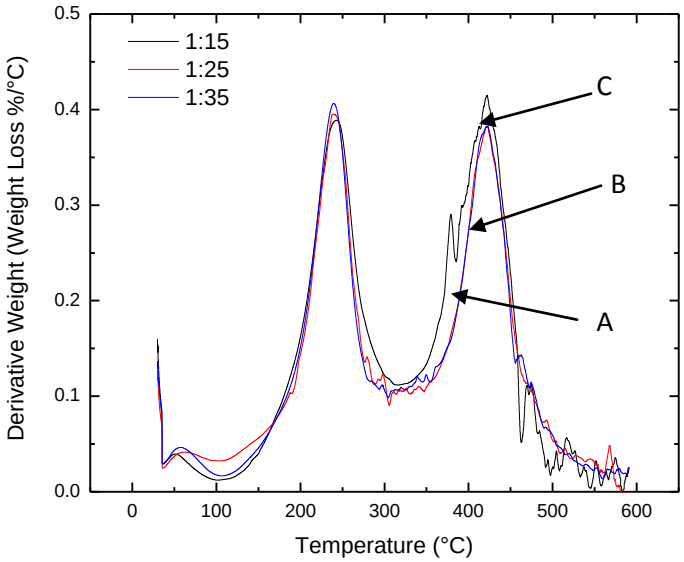

Figure 3.2. The first derivative TGA plot of HMWCH:Glu where A) 1:15 B) 1:25 and C) 1:35 of two-component biopolymers.

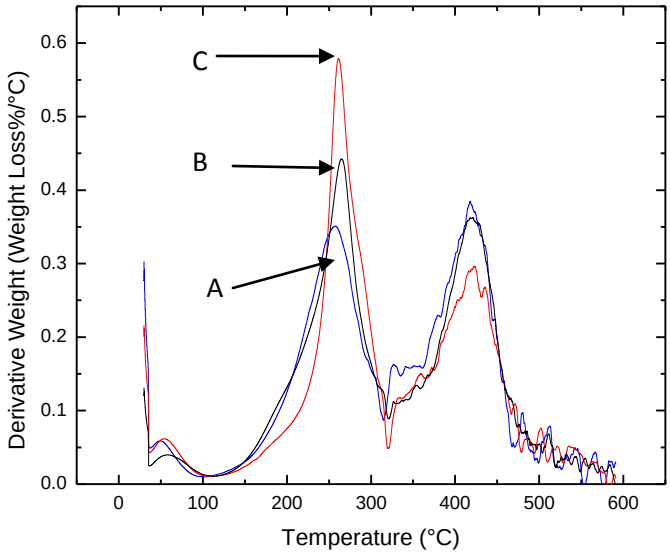

Figure 3.3. The first derivative TGA plot of 1:15 HMWCH-βCD:Glu where A) 1-3 B) 1-1 and C) 1-1/3 three-component biopolymers.

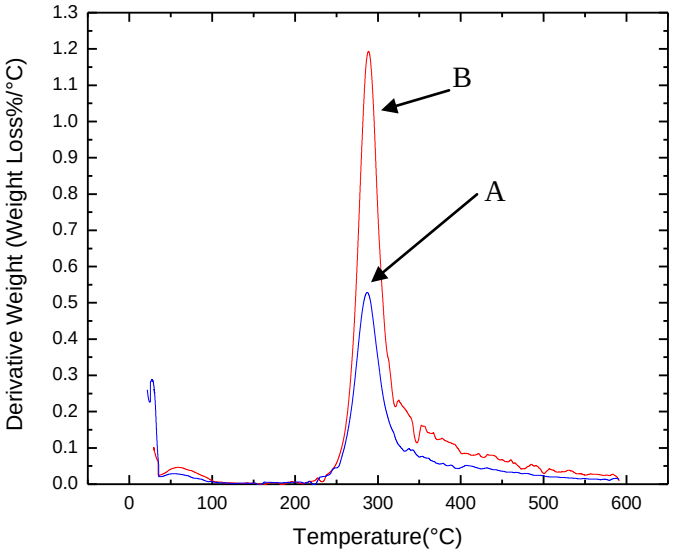

Figure 3.4. The first derivative (weight loss %/°C) TGA plot of A) LMWCH and B) HMWCH.

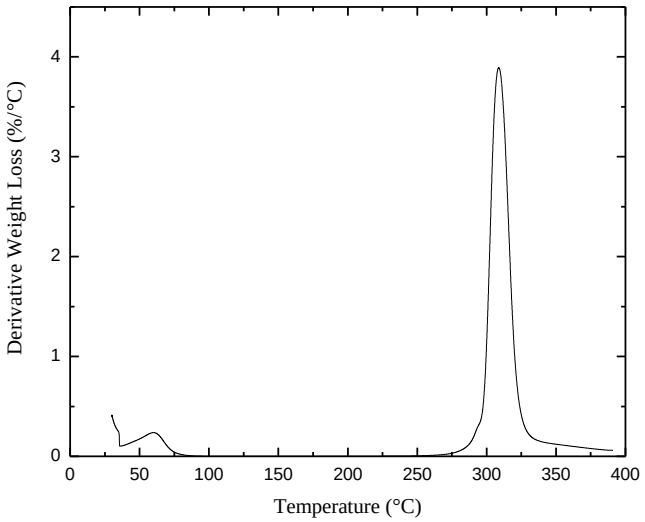

Figure 3.5. The first derivative TGA plot of βCD hydrate prepolymer.

3.4 Fourier Transform-Infrared Spectroscopy

Fourier Transform-Infrared **(**FT-IR) spectroscopy is the most commonly used spectroscopic method of characterization for these biopolymers.[5] The FT-IR spectrum for the LMWCH:Glu (*cf*. Figure 3.7) and HMWCH:Glu (*cf*. Figure 3.8) biopolymers and LMWCH and HMWCH prepolymers are shown (*cf*. Figure 3.6). The O-H stretching region ~3400cm^{-1}, C-H stretching region ~2900cm^{-1}, C-C stretching region ~1600cm^{-1} are similar amongst the biopolymers.[5] Two new bands appear at ~1560cm^{-1} (C=C) and ~1655cm-1 (C=N); the appearance of these bands indicate cross linking has occurred between the amine groups on CH and the aldehyde groups of Glu.

The IR spectra for the CH-βCD:Glu (*cf.* Figure 3.9) biopolymers have similar IR and display characteristic peaks at ~1560cm^{-1} (C=C) and ~1655cm^{-1} (C=N). The appearance of these bands indicate that the cross linking between the amine groups on chitosan and the aldehyde groups of glutaraldehyde. The relative similarly of the vibrational bonds amongst the chitosan, βCD and the glutaraldehyde cross linked biopolymers observed in this study is consistent with other reports.[5,8]

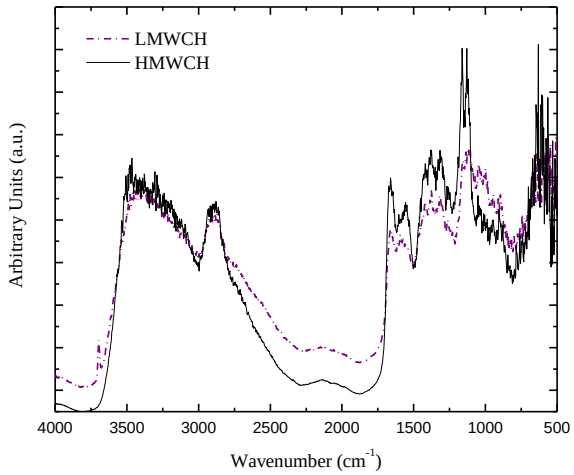

Figure 3.6. The FT-IR spectra of LMWCH in powder form and HMWCH and flake form.

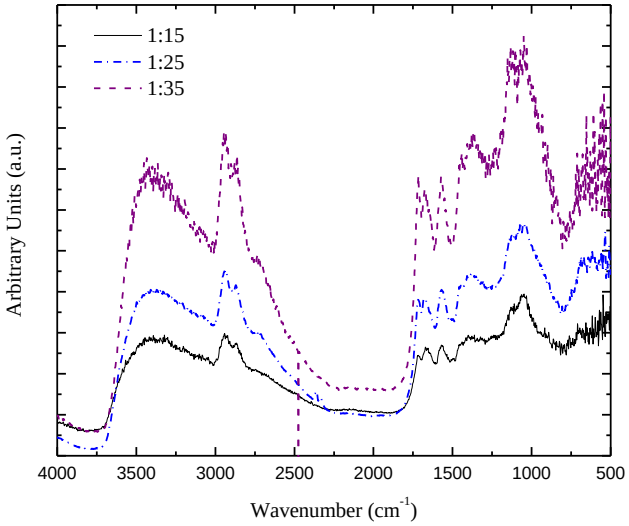

Figure 3.7. The FT-IR spectrum of LMWCH:Glu biopolymers in their powder form.

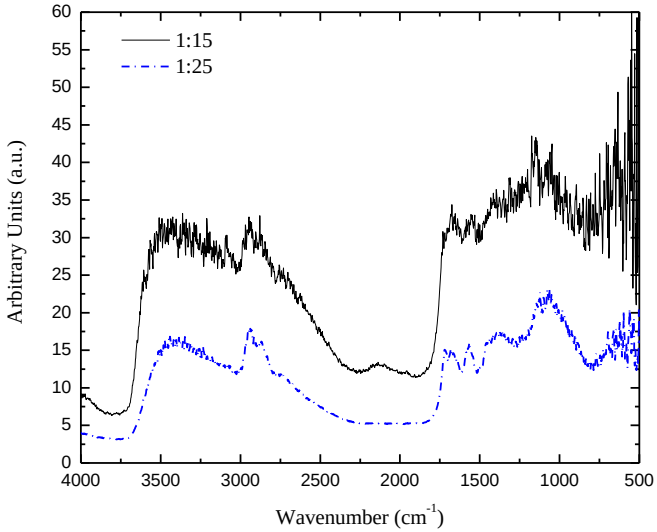

Figure 3.8. The FT-IR spectrum of HMWCH:Glu biopolymers in their powder form.

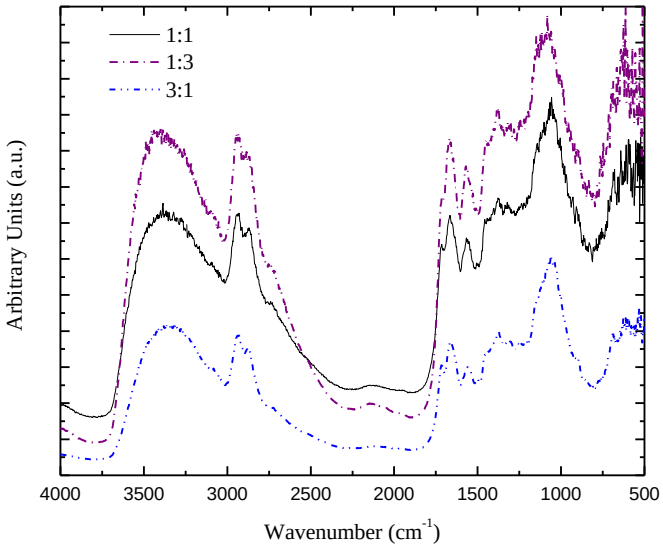

Figure 3.9. The FT-IR spectra of the1:15 HMWCH:βCD:Glu (3 component) biopolymers in their powder form.

Knaul et al., studied the cross linking of chitosan with dialdehydes and proposed a reaction mechanism, as discussed previously.[65] The ν(C=N) absorbance is shifted much more than the expected absorbance (1620-1660 cm^{-1}) which may be due to an acetal type bonding as shown by mechanism 2. The broad ν(O-H) indicates strong intermolecular and intramolecular hydrogen bonding.[66]

Table 3.6. The FT-IR band assignments for each biopolymer.

Biopolymer	ν(C=N) (cm^{-1})	ν(C=O) (cm^{-1})	ν(C=C) (cm^{-1})	ν(C-H) (cm^{-1})	ν(O-H) (cm^{-1})
LMWCH:Glu	1664	1716	1574	2872, 2933	3447
HMWCH:Glu	1683	1721	1570	2872, 2952	3433
1:15 HMWCH:βCD:Glu	1669	1711	1565	2867, 2938	3357
LMWCH	NR	NR	NR	2850	3400
HMWCH	NR	NR	NR	2850	3400

NR – not reported because of the absence of the vibrational bond.

Chapter 4 Results and Discussion for Equilibrium Sorption Experiments

The Langmuir model (*i.e.* Sips restricted) is a well-established model used in the analysis of adsorption behaviour. However, recent research in our laboratory indicates that the Sips model is more general and versatile since it can describe Langmuir and Freundlich behaviour for certain limiting conditions. Therefore, the Langmuir (herein referred to as the Sips restricted where n_s=1) and Sips isotherms were investigated in this research in order to obtain a greater understanding of "Langmuir" type behaviour and test the utility of the Sips isotherm which describes a wider range of adsorption behaviours.

4.0 *p*-Nitrophenol Equilibrium Sorption Results

An aqueous solution containing PNP and fixed amounts (~20 mg) of chitosan based biopolymers were shaken and equilibrated for 24 hours in aqueous solution where PNP was used as the adsorbate species. Each set of solid-solution equilibrium experiments were carried out similarly, the following co-monomer mole ratio (1:15, 1:25 and 1:35) was varied and compared. A comparison was made between the sorption capacities obtained using the Sips and the Sips restricted isotherm models of the LMWCH:Glu and HMWCH:Glu where PNP was the adsorbate species.

4.0.1 Two-Component Low Molecular Weight Chitosan Cross Linked Biopolymer

Figures 4.1-4.2 illustrate the PNP sorption isotherms obtained for each biopolymer with variable co-monomer mole ratios where PNP is the adsorbate species, in aqueous solution at pH 8.5 and 295 K. The sorption properties of the LMWCH:Glu biopolymer materials were analyzed using various isotherm models, as shown by the fitted lines. At these conditions, PNP exists as an organic anion and previous work with CD:EP copolymers[4] indicated that PNP was a suitable adsorbate that could be quantitatively monitored using UV-Vis spectroscopy. PNP provides

estimates of Q_m and estimates of the sorbent SA. The pH dependent ionization behaviour of PNP allows it to be used as a probe for anion binding in a similar manner to that of arsenic oxoanion species. The equilibrium sorption properties of two- and three-component chitosan based biopolymers were investigated using a similar strategy. The concentration dependence of Q_e is well-described with the Sips restricted and Sips isotherm models. In general, the quantity of PNP adsorbed increases monotonically as C_e increases for each co-monomer mole ratio of LMWCH based biopolymers. The magnitude of Q_e shows a stronger increase with increasing C_e for biopolymers with lower Glu co-monomer mole ratios.

The sorption results in Table 4.2, show that the 1:25 biopolymer had the highest ε_R% (48%) for the LMWCH:Glu biopolymer with PNP over the entire range of adsorbate concentration (C_e; 1-9 mM). This concentration range was examined because it corresponds to conditions used in a previous study.[4] At pH 8.5, PNP exists in its anionic form and was used as the adsorbate dye with a copolymer sorbent (βCD:EP).; see Table 4.1 for isotherm parameters. It was beneficial to mirror the conditions of the PNP sorption study[4] herein and to compare and contrast the present study with chitosan biopolymers (*cf.* Table 4.1). In comparing the two sets of sorption it gave us insight into the performance of chitosan based biopolymers with a related series of βCD copolymers. The performance was demonstrated through removal efficiencies, sorbent SAs and sorption capacities. Tables 4.4 to 4.5 show the parameters obtained from each isotherm model.

Overall, the co-monomer ratios for LMWCH:Glu exhibit a non-uniform increase in Q_e indicating a low affinity towards PNP. The Langmuir and Sips isotherms for the 1:15 copolymer had the "best-fit" and the highest Q_m value (0.307 and 0.822 $mmolg^{-1}$, respectively) The sorption curves show regions (< 2.5 mM) with little concentration dependence of Q_e for all three

co-monomer sorbent materials. From the Sips restricted isotherm, it could be interpreted that the homogenous monolayer coverage is attained ~2.5 mM PNP and beyond this concentration the results indicate weak binding because all potential binding sites are occupied and this is observed in each of the three LMWCH biopolymer materials. The LMWCH prepolymer has a lower degree of polymerization then the HMWCH. The results indicate that the sorption of fewer PNP anions occurs because all of the sorption sites are assumed to be equivalent and homogenous according to the Sips restricted isotherm model. The varying sorption capacity could be related to the variable SA, (*cf.* Table 4.3) of the biopolymer materials. It is interesting to note that both isotherm models (Sips restricted and Sips) for the 1:15 biopolymers have drastically different SA estimates which range from 46.7 to 123.7 m^2/g. The 1:25 and 1:35 SA estimates, obtained from each isotherm model provide support for the reliability of the sorption capacity parameter (Q_m) since each isotherm model yielded comparable SA estimates for each co-monomer mole ratio obtained.

At low values of C_e (<2.5 mM PNP) the sorption values show similarity and differences above 2.5 mM PNP amongst the three biopolymers. The variation in data points indicates weak binding of PNP, which may be due to a lack of available inclusion sites within the biopolymer or that the surface of the biopolymer is homogenous in nature and the monolayer coverage is completely established ~2.5 mM. A case can be made for either of the above hypotheses. Hydration effects may play a major role in PNP sorption because the LMWCH:Glu biopolymers may not swell to the extent as the HMWCH:Glu biopolymers[57]. These types of chitosan based biopolymers have the unique ability to swell while in aqueous solutions depending on the level of their cross link density and molecular weight.[57] A comparison between LMWCH and HMWCH in this study indicates that hydration may play a major role in the sorption capacity.

The lipophilic nature of the LMWCH:Glu is attenuated in comparison to the HMWCH:Glu biopolymers. It is apparent that the lipophilicity is less pronounced as the co-monomer ratio increases, therefore, hydrophobic interactions may be more evident for PNP and the LMCH:Glu based biopolymers.

Previous studies indicated that the Langmuir (*i.e.* Sips restricted) isotherm model was well suited for chitosan based sorbent materials. In this study, the Sips restricted and the Sips models may provide more evidence for homogeneity *vs.* heterogeneity of the sorbent surface. Since the Sips model can account for Langmuir behaviour when $n_s=1$, a stronger case can be made for homogeneity. If $n_s \neq 1$ then we can conclude that the sorption sites are heterogeneous. The comparable goodness of fit for the Sips restricted and Sips model does not allow for a clear choice of isotherm model; and this may be related to the scatter of the results relative to the concentration dependence of Q_e.

At 295 K and pH 8.5, the Sips restricted provides estimates of Q_m for the three chitosan based biopolymers: 1:15 ≈ 1:25 > 1:35 and the Sips estimates of Q_m values 1:15 >> 1:25 > 1:35. The magnitude of Q_m for the 1:25 and 1:35 are similar for each model; whereas, the difference of the 1:15 biopolymer amongst the two isotherm models is significant. This significance may be explained by the fact that the Sips has three adjustable parameters, whereas the Sips restricted has only two parameters. The Q_m for the βCD:EP copolymers were previously studied at two pH conditions (pH 4.6 and 10.3) and three different temperatures (295 K, 308 K, 318 K). It is evident that the 1:35 βCD:EP consistently had the highest Q_m value (Q_m = 0.389 mmol PNP/g sorbent) amongst the three copolymers for all temperatures and pH conditions investigated. However, the conditions that most resemble this study are those at 295 K and pH 10.3 because PNP exists as an organic anion species above pH 7. The LMWCH:Glu biopolymers have lower

Q_m values than the βCD:EP copolymers; 0.21 – 0.31 mmol PNP/g sorbent). The Sips restricted estimate for Q_m for all three co-monomer mole ratios, are equal to or less than 0.31 mmol PNP/g sorbent. The sorption results in Fig. 4.1 and 4.2 indicate that the sorption sites are ~86% saturated since the corresponding values are less than ~0.31 mmol PNP/g sorbent.

Both isotherms have very low SSE values (< 2.25×10^{-3}) and poor $R^2 \sim 0.0813 – 0.699$. Since good fits should have $R^2 > 0.9$, there is no cause for concern since the "best-fit" line resides within the allowable error estimates. In addition to the "best-fit" criteria, analysis of the isotherm parameters needs to be evaluated as part of the isotherm model analysis. The parameter $n_s \approx 0.870 – 1.210$ is close to unity indicating that the 1:25 and 1:35 biopolymers favour the Sips restricted isotherm and show Langmuir type behaviour. Thus, homogeneity is favoured and monolayer coverage seems plausible; the 1:15 biopolymer $n_s \neq 1$ indicating heterogeneous sorption sites.

Table 4.1. Best-fit parameter[a,b] estimates (Q_m, K_{BET}) using the BET non-linear isotherm model at various temperatures and pH conditions for the sorption of PNP with βCD:EP copolymers (adapted from reference 4).

Conditions	1:15	1:25	1:35
295 K pH=4.6	0.387[a], 56.6[b]	0.345[a], 57.5[b]	0.599[a], 12.4[b]
308 K pH=4.6	0.420[a], 74.0[b]	0.381[a], 39.8[b]	0.620[a], 26.7[b]
318 K pH=4.6	0.119[a], 184[b]	0.784[a], 11.4[b]	0.810[a], 20.0[b]
295 K pH=10.3	0.294[a], 72.4[b]	0.269[a], 38.0[b]	0.389[a], 42.7[b]

[a] Q_m (mmol/g)
[b] K_{BET} ($Lmmolg^{-2}$)

Table 4.2. Removal efficiencies for PNP in aqueous solution for two-component biopolymers of LMWCH:Glu at 295 K and pH 8.5.

Biopolymer Sorbent Material	ε_R %
1:15	8.8-40
1:25	8.7-48
1:35	7.1-39

[a] The calculated range of ε_R% values correspond to a range of PNP concentrations ($[PNP]_o$ = 1 – 9 mM) with a fixed mass (~20 mg) of biopolymer sorbent material.

Table 4.3. Dye based surface area estimates for two-component biopolymers of LMWCH:Glu using PNP in aqueous solution at 295 K and pH 8.5

Biopolymer Sorbent Material	Surface Area Estimate ($m^2 g^{-1}$)[a]	
	Sips restricted[b]	Sips
1:15	46.7	124
1:25	46.7	46.7
1:35	31.6	31.6

[a] Dye-based method surface area estimates obtained from eq.(11) using a value for A_m for the planar orientation of PNP and a Q_m value estimated from eq. (13 and 14).
[b]Sips restricted is defined when n_s=1.

Table 4.4. Sorption parameters for PNP in aqueous solution for two-component biopolymers of LMWCH:Glu at 295 K and pH 8.5 (unbuffered)* obtained from the "best-fit" using the Sips restricted isotherm model when n_s=1.

Sorbent	Q_m (mmol g^{-1})	K_S (L $mmol^{-1}$)	SSE $x10^{-3}$	R^2
1:15	0.307	2.05	1.27	0.626
1:25	0.309	4.18	1.15	0.478
1:35	0.212	8.67	1.76	0.0813

*Solutions were unbuffered and pH did not require adjustment.

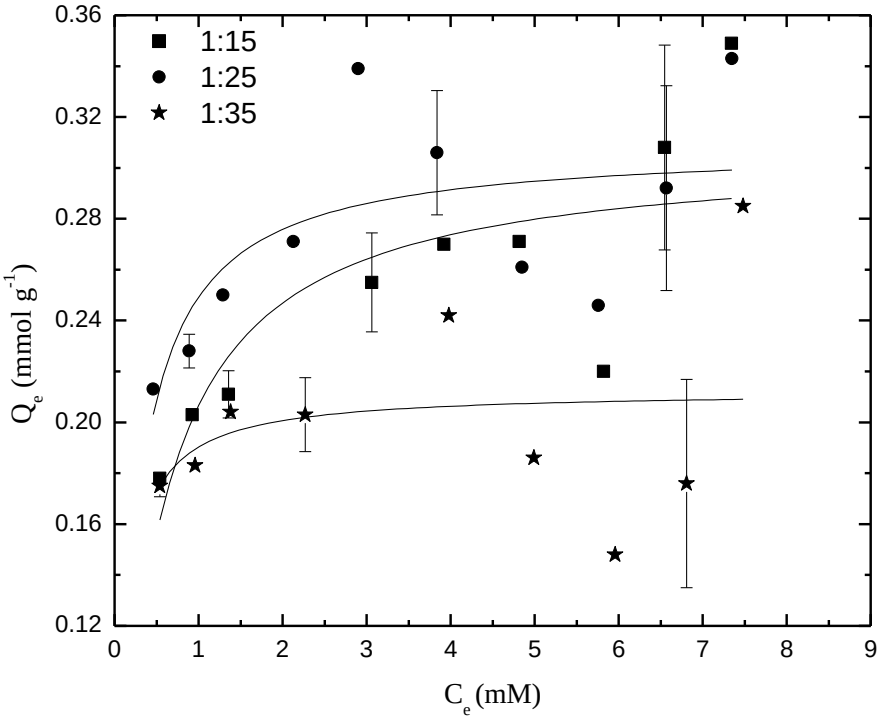

Figure 4.1. The sorption isotherm of fixed amounts (~20 mg) of two-component biopolymers of LMWCH:Glu with PNP at various concentrations at pH 8.5 and 295 K. The solid line represents the best-fit according to the Sips restricted isotherm when n_s=1.

Table 4.5. Sorption parameters for PNP in aqueous solution with two-component biopolymers of LMWCH:Glu at 295 K and pH 8.5 (unbuffered)* obtained from the "best-fit" using the Sips isotherm model.

Sorbent	Q_m (mmol g^{-1})	K_s (L $mmol^{-1)}$	n_s	SSEx10^{-3}	R^2
1:15	0.822	0.0226	0.296	1.19	0.699
1:25	0.309	4.51	0.870	1.32	0.480
1:35	0.212	6.75	1.21	2.05	0.0815

*Solutions were unbuffered and pH did not require adjustment.

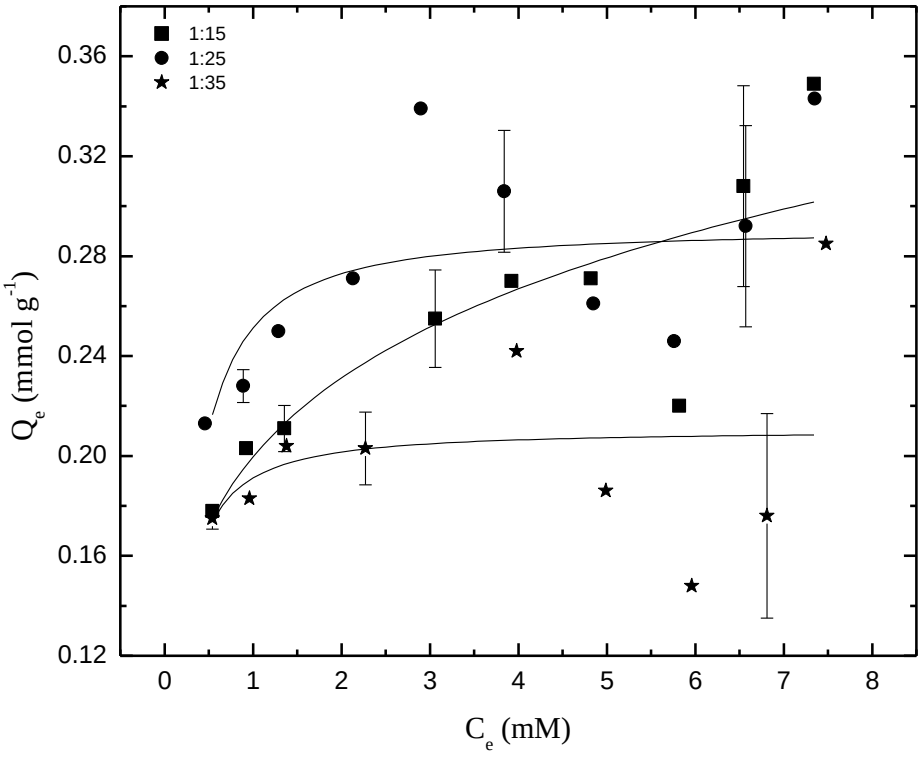

Figure 4.2. The sorption isotherm of fixed amounts (~20 mg) with two-component biopolymers of LMWCH:Glu with PNP at various concentrations at pH 8.5 and 295 K. The solid line represents the best-fit according to the Sips isotherm.

4.0.2 Two-Component High Molecular Weight Chitosan Cross Linked Biopolymer

Figures 4.4 and 4.5 summarize the results obtained from the PNP sorption isotherms at equilibrium obtained at each co-monomer mole ratio. The sorption properties in aqueous solution at pH 8.5 and 295K for the HMWCH:Glu biopolymer materials were quantitatively evaluated, as shown by the fitted lines. The sorption properties of chitosan based biopolymers were investigated using a similar strategy. The concentration dependence of Q_e is well-described by using the Sips restricted and Sips sorption isotherm models. In general, the sorption capacity of PNP increases monotonically as C_e increases for each co-monomer mole ratio for the HMWCH based biopolymers. The magnitude of Q_e shows a greater increase as C_e increases for biopolymers with an increasing co-monomer ratio. The HMWCH:Glu biopolymers were synthesized similar to the LMWCH:Glu biopolymers, however, the sorption capacities followed a reversed ordering. As the co-monomer mole ratio was increased, the sorption capacity increased. For a given co-monomer mole ratio (*i.e.*1:15), the HMWCH:Glu may have more Glu crosslinks than LMWCH:Glu for a given chitosan monomer and/or there are more monomer sites to accommodate the Glu crosslinks. (*cf.* Scheme 4.1).

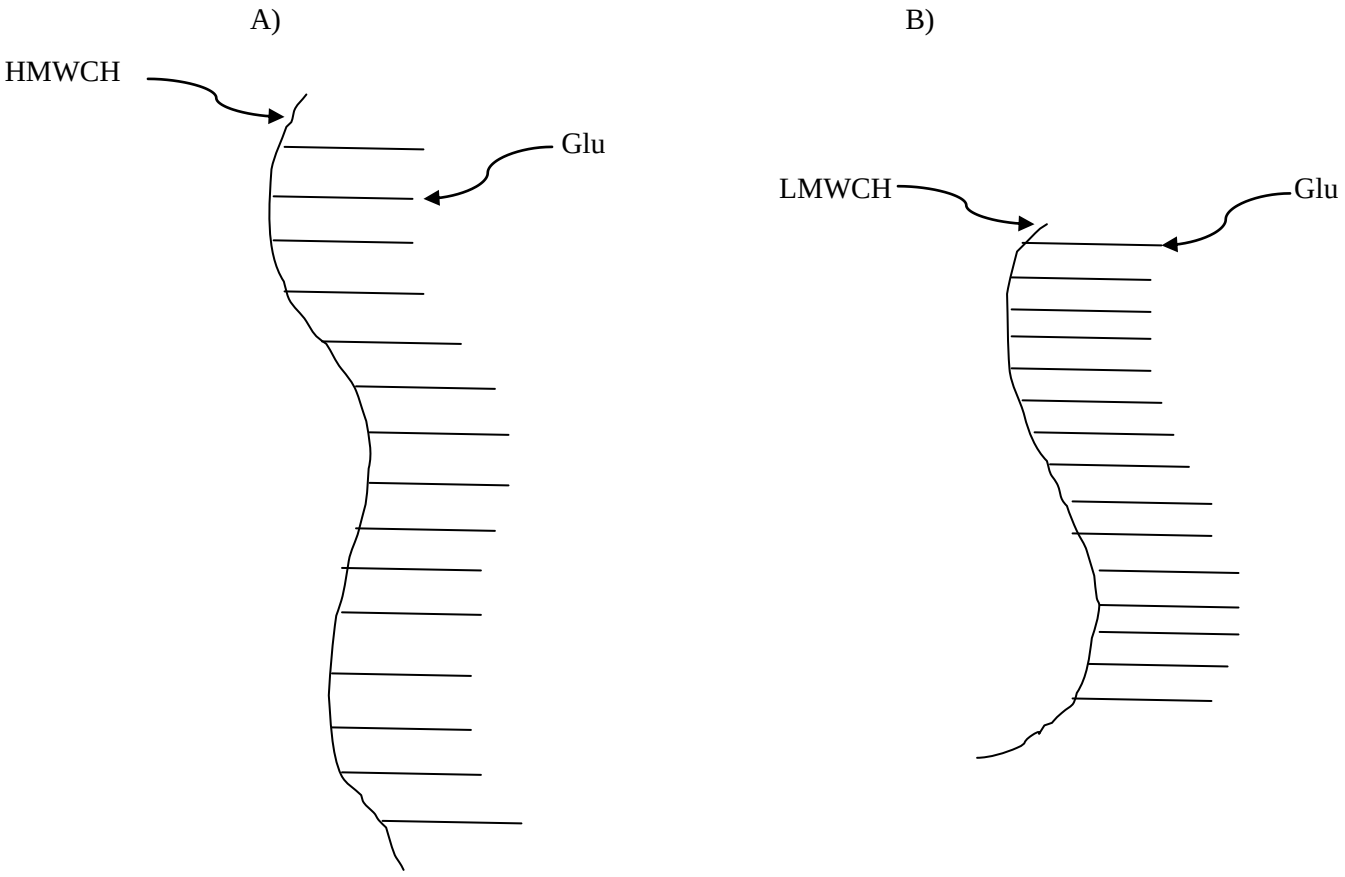

Scheme 4.1. Generalized structures of two-component biopolymers A) 1:15 HMWCH:Glu and B) 1:15 LMWCH:Glu biopolymers showing Glu crosslinks for a given chitosan prepolymer chain length.

In Table 4.6, the sorption results showed that the 1:35 HMWCH:Glu biopolymer material had the highest ε_R% (48.9%) of PNP throughout the range of adsorbate concentration from 0.4 to 3 mM. This concentration range was examined because the LMWCH:Glu biopolymers displayed saturation of their sorption sites ~2.5 mM PNP and showed greater dissimilarities thereafter. Therefore, it was beneficial to lower the PNP concentration of interest because the concentration region where the uniformity existed (0.4 to 3 mM PNP) showed good agreement amongst the isotherm models. Tables 4.8 to 4.9 show the parameters obtained from each isotherm model.

Overall, each co-monomer mole ratio for the HMWCH:Glu sorbents exhibited a uniform increase in Q_e indicating a high affinity towards PNP. The Sips restricted and Sips isotherms for all co-monomer mole ratios displayed a reasonable "best-fit" suggesting that the models provide a good description of the data. As well, the sorption sites are either homogenous or heterogeneous surfaces with a distribution of adsorption energies. The HMWCH has a higher degree of polymerization and larger SA estimates than the LMWCH:Glu biopolymers. More PNP anion species are adsorbed which is obvious by the greater Q_m values, in comparison to the LMWCH:Glu. The variation in the sorption properties could be related to the variable SA (see Table 4.7) and molecular weight of the biopolymer materials. The Sips restricted (SA = 58 - 64.7 m^2/g) gives consistently lower SA estimates, for all co-monomer mole ratios, in comparison to the Sips (SA = 79 – 96.3 m^2/g). Also, the HMWCH:Glu biopolymers may be more porous in nature resulting in a sorbent framework with more accessible pores and decreased steric hindrance[73] of the co-monomer (Glu) or the degree of polymerization. Hydration may contribute to the SA and PNP sorption because the HMWCH:Glu biopolymers may swell to a greater extent than the LMWCH:Glu. Swelling lowers the steric hindrance because it is well known that these types of chitosan based biopolymers are known to swell in aqueous solutions,[57] as outlined above. The isotherm results and Q_m values support the occurrence of swelling. A comparison between LMWCH and HMWCH in this study suggests that hydration plays the major role in the sorption capacity. The lipophilic nature of the HMWCH:Glu is increased in comparison to the LMWCH:Glu biopolymers. The lipophilicity increases as the cross linking density increases; thus, promoting favourable hydrophobic interactions between PNP and the HMWCH:Glu based biopolymers (see Scheme 4.1).

At 295 K and pH 8.5, the Q_m values for the three HMWCH based biopolymers: 1:15 < 1:25 < 1:35; agree for both isotherm models. Sorption of PNP by HMWCH copolymers was carried out similarly as described above for the LMWCH biopolymers. The HMWCH:Glu biopolymers have higher Q_m values than the βCD:EP copolymers; (Sips restricted: 0.39 – 0.43 mmol PNP/g sorbent and Sips: 0.43 – 0.64 mmol PNP/g sorbent).

Both isotherms have very low SSE values (< 7.30×10^{-4}) and $R^2 > 0.771$. The goodness of fit and error estimates were both discussed in the previous section (§4.0.1). The Sips parameter $n_s \approx 0.8$ - 0.9 is close to unity, for all co-monomer mole ratios, indicating good agreement with the Sips restricted model which describes Langmuir type behaviour. Thus homogeneity is favoured and monolayer coverage seems plausible.

This conclusion is further supported by referring to the comparison of the isotherm shapes to the known IUPAC categories, see § 4.0.3 for the types of sorption isotherms.

Table 4.6. Removal efficiencies for PNP in aqueous solution for two-component biopolymers of HMWCH:Glu at 295 K and pH 8.5.

Biopolymer Sorbent Material	ε_R %
1:15	14.3-37.4
1:25	17.3-45.3
1:35	19.7-48.9

[a] The calculated range of values for ε% correspond to a range of PNP concentrations ($[PNP]_o = 0.4 – 3$ mM) with a fixed mass (~20 mg) of biopolymer sorbent material.

Table 4.7. The surface area estimates for two-component biopolymers HMWCH:Glu using PNP in aqueous solution at 295 K and pH 8.5.

Biopolymer Sorbent Material	Surface Area Estimate ($m^2 g^{-1}$)[a]	
	Sips restricted[b]	Sips
1:15	58.7	79.8
1:25	54.2	64.7
1:35	64.7	96.3

[a]Dye-based method surface area estimates obtained from eq.(11) using a value for A_m for the planar orientation of PNP and a Q_m value estimated from eq. (13 and 14).
[b]Sips restricted is defined when n_s=1.

Table 4.8. Sorption parameters for PNP in aqueous solution for two-component biopolymers HMWCH:Glu at 295 K and pH 8.5 (unbuffered)* obtained from the "best-fit" using the Sips restricted isotherm model when n_s=1.

Sorbent	Q_m (mmol g^{-1})	K_L (L $mmol^{-1}$)	SSEx10^{-4}	R^2
1:15	0.386	0.477	6.40	0.823
1:25	0.356	0.992	6.20	0.858
1:35	0.432	0.912	6.40	0.892

*Solutions were unbuffered and pH did not require adjustment.

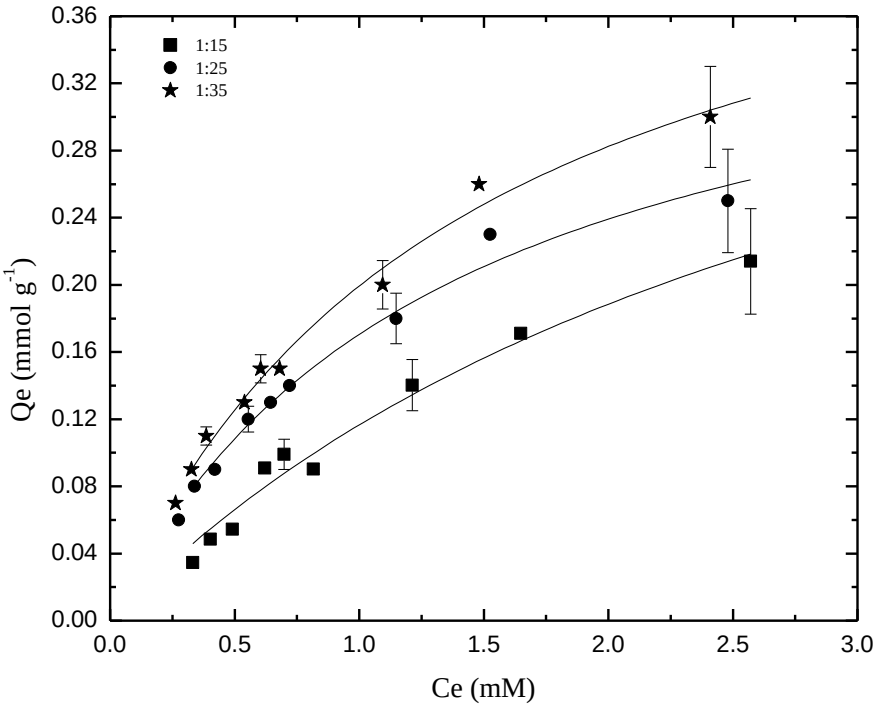

Figure 4.3. The sorption isotherm of fixed amounts (~20 mg) of two-component biopolymers HMWCH:Glu biopolymers with PNP at various concentrations at pH 8.5 and 295 K. The solid line represents the best-fit according to the Sips restricted isotherm when n_s=1.

Table 4.9. Sorption parameters for PNP in aqueous solution for two-component biopolymers HMWCH:Glu at 295 K and pH 8.52 (unbuffered)* obtained from the "best-fit" using the Sips isotherm model.

Sorbent	Q_m (mmol g^{-1})	K_S (L $mmol^{-1}$)	n_s	SSEx10^{-4}	R^2
1:15	0.534	0.245	0.862	7.30	0.824
1:25	0.427	0.661	0.876	7.10	0.863
1:35	0.640	0.358	0.775	6.90	0.899

*Solutions were unbuffered and pH did not require adjustment.

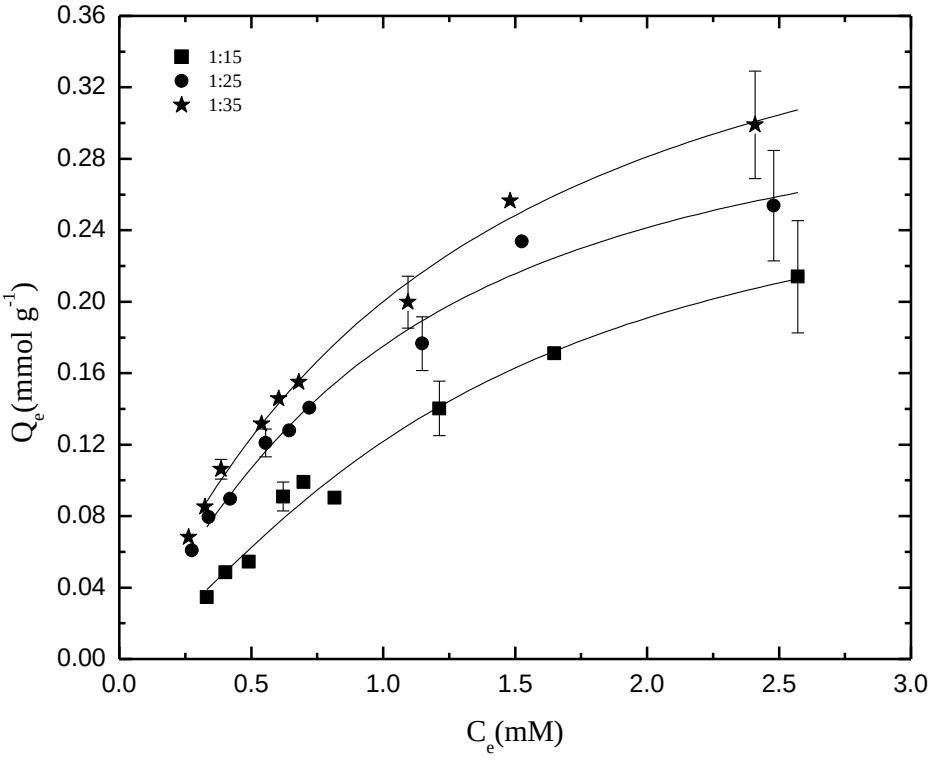

Figure 4.4. The sorption isotherm of fixed amounts (~20 mg) of two-component biopolyers HMWCH:Glu with PNP at various concentrations at pH 8.5 and 295 K. The line through the data represents the best fit according to the Sips isotherm model.

4.0.3 The Various Types of Sorption Isotherms[22]

Brunauer, Deming, and Teller (BDT) classified sorption isotherms as six different categories (Type I, II, III, IV, V, and VI). Those isotherms are shown in Figure 1.9.[77]

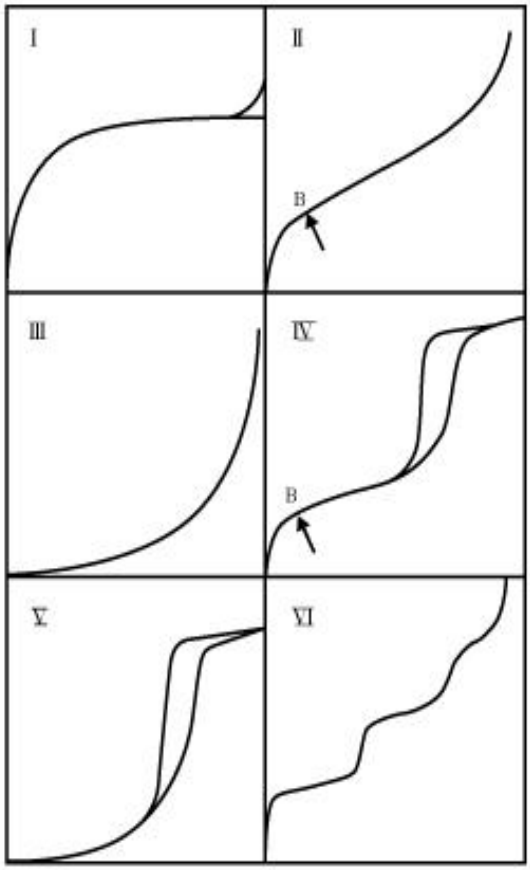

Figure 4.5. The six types of adsorption isotherms (adapted from reference 77).

Type I Isotherm

These isotherms are used to characterize the sorption caused by predominantly microporous structure because most micropore filling occurs at relatively low pressure (< 0.1) and the adsorption process is usually completed at about half relative pressure ($P/P_o \approx 0.5$). Typical adsorptions of this group are the adsorption of molecular nitrogen onto AC at 77 K and ammonia on activated carbon (AC) at 273K.

Type II Isotherm

These isotherms involve physical adsorption of gases by non-porous solids. Point B is the end of monolayer surface coverage and multilayer coverage begins at higher relative pressures after the point B. ACs with mixed micro- and meso-porosity show Type II isotherms.

Type III Isotherm

These isotherms are favored by weak interactions between adsorbate-adsorbent systems such as non-porous and microporous adsorbents. The weak interactions between the adsorbate and the adsorbent result in low loadings at low relative pressures. However, beyond the first sorption point, much stronger sorption can occur and result in maximum loadings at higher relative pressures. The adsorption of water molecules on AC where the primary adsorption sites are oxygen fall into this category.

Type IV Isotherm

These isotherms show a hysteresis loop attributed to capillary condensation, which is commonly shown in the presence of mesoporosity. Point B is the end of monolayer surface coverage and multilayer coverage starts right after the point B. These sorption isotherms exhibit a limited loading at high relative pressures.

Type V Isotherm

These isotherms are achieved with microporous or mesoporous adsorbents and are convex at the high relative pressure. The driving force for adsorbate uptake is the same as Type III isotherms. An example is water adsorption on AC at 100 °C.[78]

Type VI Isotherm

These isotherms are associated with extremely homogeneous, non-porous surfaces. The complete formation of a monolayer which corresponds to the step height is fulfilled before progression to a subsequent layer. An example is the adsorption of krypton on carbon black at 90 K which was previously graphitized at 3000 K.[79]

4.1 Arsenate(V) Oxoanion Equilibrium Sorption Results

An aqueous solution containing arsenate oxoanion ($HAsO_4^{2-}$) and fixed amounts (~20 mg) of chitosan based biopolymers were shaken and equilibrated for 24 hours in aqueous solution where arsenate oxoanion was used as the adsorbate species. Each set of solid-solution equilibrium experiments were carried out similarly for the two component (CH/Glu) biopolymers with varying co-monomer mole ratio (1:15, 1:25 and 1:35). A comparison between the sorption capacities using the Sips isotherm and the Sips restricted isotherm models of the HMWCH:Glu where $HAsO_4^{2-}$ was the adsorbate species.

4.1.1 Two-Component Low Molecular Weight Chitosan Cross Linked Biopolymer

Figures 4.6 and 4.7 summarize the sorption isotherms obtained for each biopolymer at variable co-monomer mole ratio with $HAsO_4^{2-}$. The sorption properties of the LMWCH:Glu biopolymer materials were quantitatively analyzed, as shown by the fitted lines, for the respective model in aqueous solution at pH 8.5 and 295 K. At these conditions, $HAsO_4^{2-}$ exists as an inorganic anion and the concentration dependence of Q_e is well described by using the Sips restricted and Sips sorption isotherm models. In general, for each cross linked LMWCH based biopolymer, the quantity of $HAsO_4^{2-}$ adsorbed increases monotonically as C_e increases. The magnitude of Q_e shows a greater increase as C_e increases for biopolymers with lower co-monomer mole ratios.

The sorption results in Table 4.10 show that 1:15 biopolymer had the highest ε_R%, (92.2%) for the LMWCH:Glu cross linked biopolymer of $HAsO_4^{2-}$ over the entire range of concentration (C_e) for $HAsO_4^{2-}$ from 47-121 ppm. This concentration range was examined because the sorption capacity was attained near saturation ~125 ppm. Therefore, it was

beneficial to investigate a range of adsorbate concentrations < 125 ppm of $HAsO_4^{2-}$. Tables 4.11 to 4.12 show the parameters obtained from each isotherm model.

Overall, both isotherm models yielded "best-fit" for all of the co-monomer ratios. The LMWCH:Glu sorbent exhibits a uniform increase in Q_e indicating a relatively high affinity towards $HAsO_4^{2-}$. The Sips restricted and Sips isotherms for all co-monomer mole ratios had the "best-fit" giving no clear indication that sorption sites are either a homogenous monolayer or heterogeneous surface with a distribution of adsorption energies. The isotherm curves show regions (C_e > 40 ppm) with little variation for all three sorbents. This could be interpreted as the surface coverage is saturated by ~40 ppm. Beyond 40 ppm. the concentration dependence of the isotherm curves plateau because all of the binding sites are occupied. This effect is clearly observed for the 1:25 and 1:35 co-monomer mole ratio sorbents.

At 295 K and pH 8.5, the Sips restricted estimates for Q_m for the three types of LMWCH based biopolymers are as follows: 1:15 > 1:25 > 1:35 and the Sips estimates of Q_m follow a similar trend. Each isotherm model for the 1:35 biopolymer yields similar Q_m values. Both isotherms have high SSE values (> 0.955) and R^2 > 0.771 for all sorbent biopolymers.

In the case of LMWCH:Glu biopolymers sorbents where $HAsO_4^{2-}$ is the adsorbate, it is difficult to clearly discriminate between the two isotherm models because they have similar SSE and R^2 values. However, the SSE is lower for the Sips and $n_s \neq 1$ indicating evidence of the heterogeneity of the sorption sites.

Table 4.10. Removal efficiencies[a] for $HAsO_4^{2-}$ in aqueous solution with two-component biopolymers of LMWCH:Glu at 295 K and pH 8.5.

Biopolymer Sorbent Material	ε_R %
1:15	71.4-92.2
1:25	59.6-85.8
1:35	50.3-82.3

[a] The calculated range of ε_R% values correspond to a range of $HAsO_4^{2-}$ concentrations ($[HAsO_4^{2-}]_o$ = 47-121 ppm) with a fixed mass (~20 mg) of biopolymer sorbent material.

Table 4.11. Sorption parameters for ($HAsO_4^{2-}$) in aqueous solution with two-component biopolymers LMWCH:Glu at 295 K and pH 8.5 (unbuffered)*obtained from the "best-fit" using the Sips restricted isotherm model when n_s=1.

Sorbent	Q_m (mg g^{-1})	K_L (mL μg^{-1})	SSE	R^2
1:15	50.0	0.166	3.37	0.955
1:25	44.5	0.112	2.04	0.955
1:35	36.0	0.113	0.874	0.963

*Solutions were unbuffered and pH did not need require adjustment.

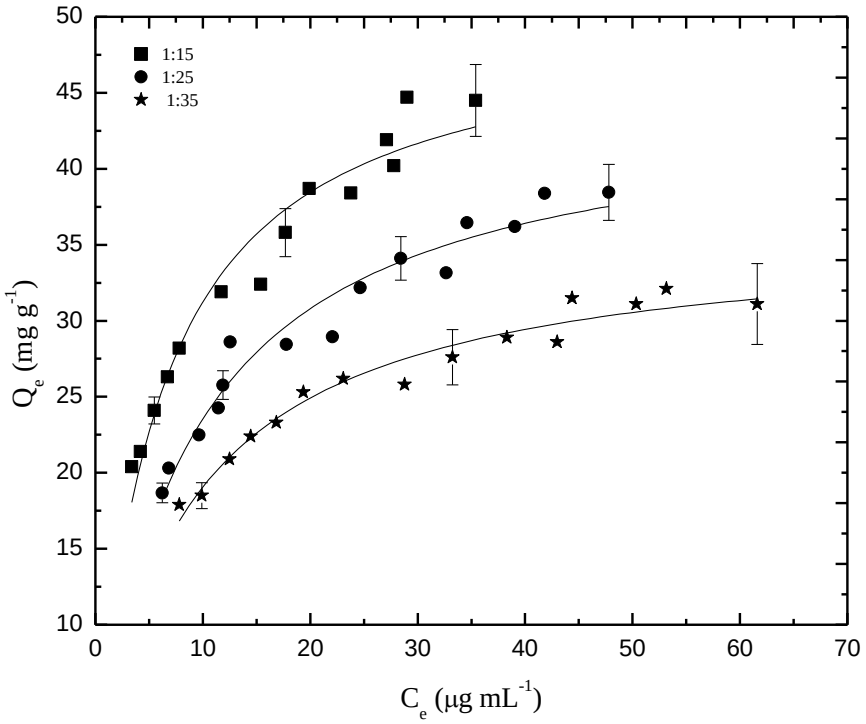

Figure 4.6. The sorption isotherm of fixed amounts (~20 mg) of two-component biopolymers LMWCH:Glu with $HAsO_4^{2-}$ at various concentrations at pH 8.5 and 295 K. The solid line represents the best-fit according to the Sips restricted isotherm when n_s=1

Table 4.12. Sorption parameters for ($HAsO_4^{2-}$) in aqueous solution with two-component biopolymers LMWCH:Glu at 295 K and pH 8.5 (unbuffered)* obtained from the "best-fit" using the Sips isotherm model.

Sorbent	Q_m (mg g^{-1})	K_S (mL μg^{-1})	n_s	SSE	R^2
1:15	228	0.000780	0.391	1.60	0.981
1:25	70.5	0.0295	0.567	1.93	0.958
1:35	39.6	0.0945	0.778	0.782	0.968

*Solutions were unbuffered and pH did not require adjustment.

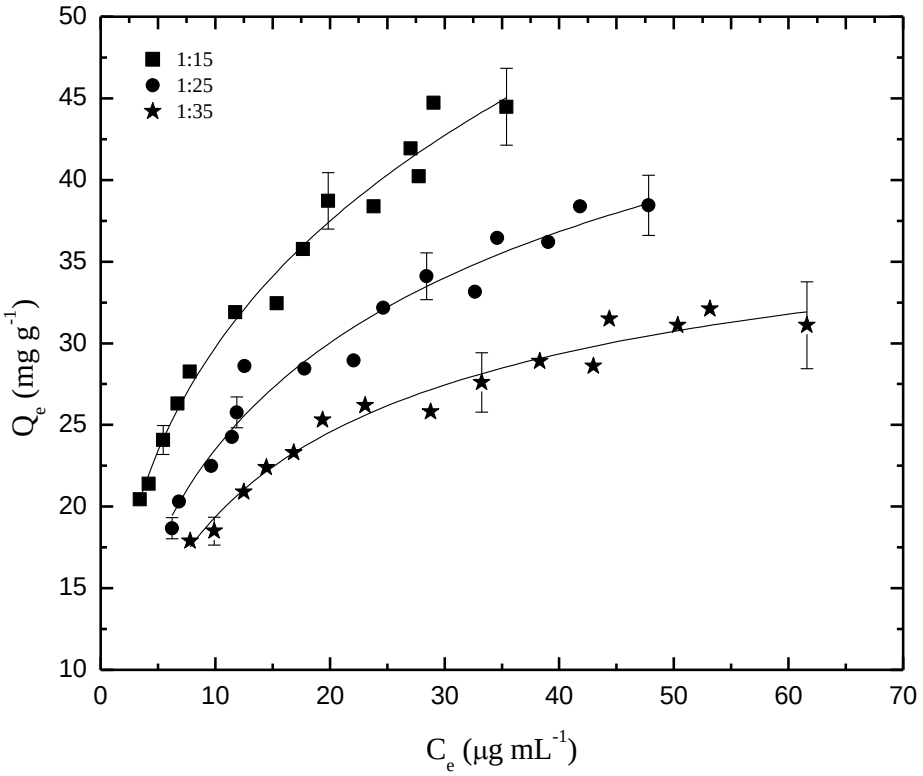

Figure 4.7. The sorption isotherm of fixed amounts (~20 mg) of two-component biopolymers LMWCH:Glu biopolymers with $HAsO_4^{2-}$ at various concentrations at pH 8.5 and 295 K. The solid line represents the best-fit according to the Sips isotherm.

4.1.2 Two-Component High Molecular Weight Chitosan Cross Linked Biopolymer

In general, for each cross linked HMWCH based biopolymer, the sorption quantity of $HAsO_4^{2-}$ increases monotonically as C_e increases. The magnitude of Q_e shows an increase as C_e increases for biopolymers with increasing Glu content and reaches a maximum for the 1:25 co-monomer mole ratio. The sorption capacity increases as the Glu content increases (1:15 < 1:25 ≈ 1:35).

The sorption results show that the 1:35 biopolymer had the highest ε_R% (87.2%) see Table 4.1.3. The ε_R% for the HMWCH:Glu copolymers ranged from 31 – 87% for $HAsO_4^{2-}$ throughout the entire range of equilibrium concentration (C_e) for 47-121 ppm. Tables 4.1.4 to 4.1.5 show the parameters obtained from each isotherm model.

Overall, both isotherm models yielded good "best-fit" results based on the SSE and R^2 values. The 1:25 and 1:35 co-monomer mole ratios for HMWCH:Glu exhibit a uniform increase in Q_e which indicates a relatively high affinity towards $HAsO_4^{2-}$. The sorption affinity of the 1:15 biopolymer is relatively low and the isotherm data illustrates a very limited concentration dependence for Q_e. While the sorption capacity of the 1:25 and 1:35 biopolymers are similar, the Q_m value for 1:15 copolymer is lower. The apparent scatter in the data for 1:15 is a consequence of the low binding affinity toward $HAsO_4^{2}$. The 1:15 isotherm curve does show a region of C_e (> 50 ppm) with little concentration dependence of Q_e. This could be interpretated that the coverage is completely established at ~50 ppm for this biopolymer. The Langmuir Q_m value is 22.2 mg $HAsO_4^{2-}$/g sorbent and the Sips Q_m value for the 1:15 biopolymer is 26.6 mg $HAsO_4^{2-}$/g sorbent and the sorption results in Fig. 4.8 and 4.9 indicate that the sorption sites are ~ 81% and ~68% while the corresponding Q_e values are ~18 mg $HAsO_4^{2-}$/g sorbent. The Langmuir Q_m values for $HAsO_4^{2-}$ are 39.3 and 37.8 mg $HAsO_4^{2-}$/g sorbent for the 1:25 and 1:35 copolymers

respectively. The sorption results in Fig. 4.8 indicate that the sorption sites are 87 - 90% saturated since the corresponding Q_e value is ~34 mg $HAsO_4^{2-}$/g sorbent, respectively. The Sips Q_m values for 1:25 and 1:35 are 44.0 and 56.6 mg $HAsO_4^{2-}$/g sorbent, respectively. The sorption results in Fig. 4.9 indicate that the sorption sites are 60 - 77% saturated since the corresponding Q_e value for $HAsO_4^{2-}$ is ~34 mg /g sorbent.

At 295 K and pH 8.5, the various two-component biopolymers of HMWCH based biopolymers have the following Sips restricted Q_m values: 1:15 < 1:35 ~ 1:25. In contrast the Sips Q_m estimates are as follows: 1:15 < 1:25 < 1:35. The Sips restricted and Sips isotherms displayed equally good "best-fit" results for these two-component biopolymers.

Both isotherms have similar SSE values (> 0.958) and R^2 (> 0.771) coefficients for all sorbent biopolymers. The SSE for the Sips restricted isotherm is less than the Sips isotherm which indicates the former isotherm displays a suitable "best-fit" for the 1:15 biopolymer. Thus homogeneous sorption sites are concluded for the 1:15 biopolymer; whereas, the 1:25 and 1:35 biopolymers are described by the Sips restricted isotherm indicating the occurrence of heterogeneous sorption sites. However, $n_s \neq 1$, for all three co-monomer mole ratios.

Table 4.13. Removal efficiencies[a] for $HAsO_4^{2-}$ in aqueous solution with two-component biopolymers HMWCH:Glu at 295 K and pH 8.5.

Biopolymer Sorbent Material	ε_R%
1:15	30.7-56.0
1:25	56.5-85.8
1:35	57.2-87.2

[a] The calculated range of ε_R% values correspond to a range of $HAsO_4^{2-}$ concentrations ($[HAsO_4^{2-}]_o$ = 47-121 ppm) with a fixed mass (~20 mg) of biopolymer sorbent material.

Table 4.14. Sorption parameters for $HAsO_4^{2-}$ in aqueous solution with two-component biopolymers HMWCH:Glu at 295 K and pH 8.5 (unbuffered)* obtained from the "best-fit" using the Sips restricted isotherm model when n_s=1.

Sorbent	Q_m (mg g^{-1})	K_L (mL μg^{-1})	SSE	R^2
1:15	22.2	0.0708	1.18	0.771
1:25	39.3	0.154	1.37	0.954
1:35	37.8	0.170	1.30	0.950

*Solutions were unbuffered and pH did not require adjustment.

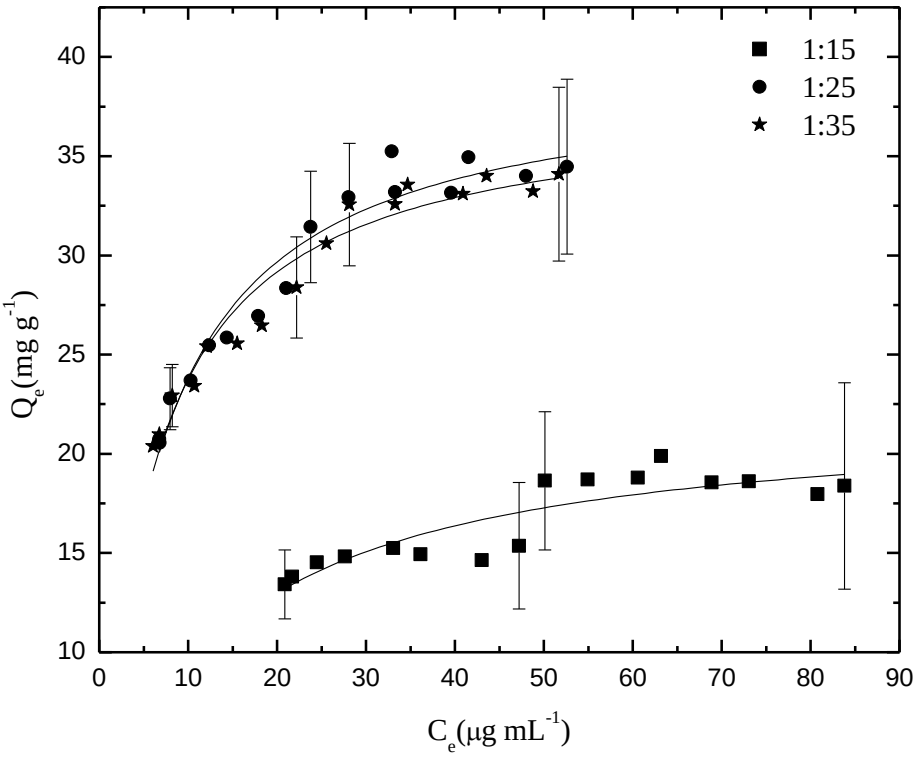

Figure 4.8. The sorption isotherm of fixed amounts (~20 mg) of two-component biopolymers HMWCH:Glu with $HAsO_4^{2-}$ at various concentrations at pH 8.5 and 295 K. The solid represents the best-fit according to the Sips restricted isotherm when n_s=1.

Table 4.15. Sorption parameters for $HAsO_4^{2-}$ in aqueous solution with HMWCH:Glu at 295 K and pH 8.5 (unbuffered)* obtained from the "best-fit" using the Sips isotherm model.

Sorbent	Q_m (mg g^{-1})	K_S (mL μg^{-1})	n_S	SSE	R^2
1:15	26.6	0.0486	0.672	1.25	0.779
1:25	44.0	0.124	0.762	1.34	0.958
1:35	50.6	0.0786	0.557	0.958	0.966

*Solutions were unbuffered and pH did not require adjustment.

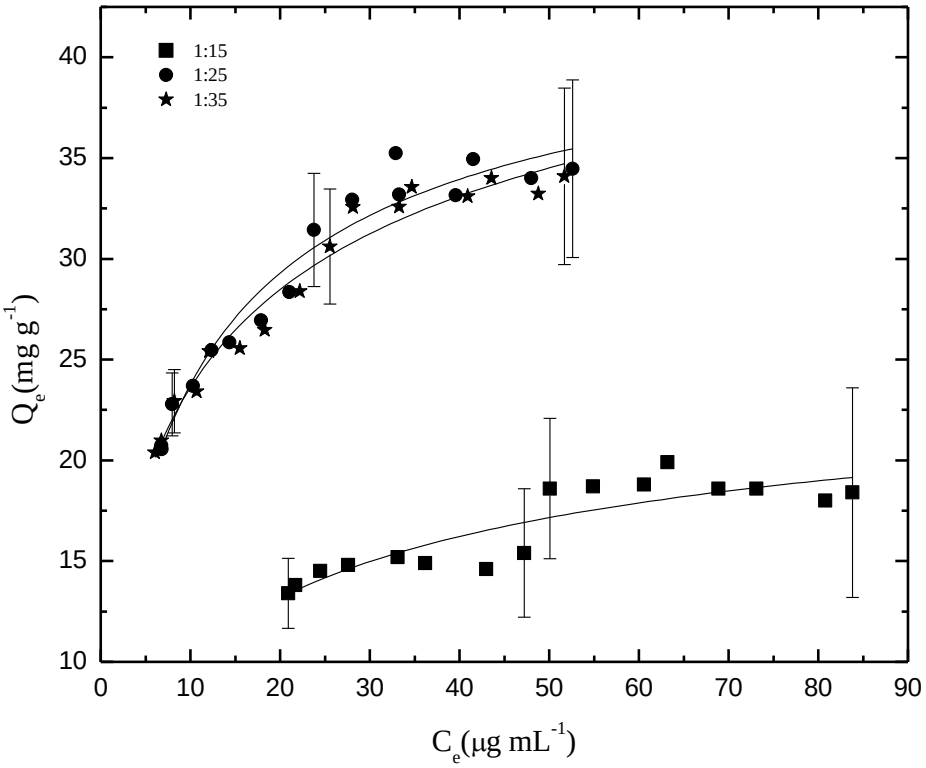

Figure 4.9. The sorption isotherm of fixed amounts (~20 mg) of two-component biopolymers HMWCH:Glu with $HAsO_4^{2-}$ at various concentrations at pH 8.5 and 295 K. The solid line represents the best-fit according to the Sips isotherm.

4.2 Three-Component High Molecular Weight Chitosan-β-Cyclodextrin Cross Linked Biopolymer

An aqueous solution containing PNP and fixed amounts (~20 mg) of HMWCH based biopolymers, with βCD incorporated into the framework were shaken and equilibrated for 24 hours in aqueous solution made up of either sorbate species: PNP and $HAsO_4^{2-}$. Each set of sorption equilibrium isotherm were carried out the similarly to the two-component biopolymers. The βCD content (1-1, 1-3 and 1-1/3) of the three-component biopolymers were varied and compared. The Glu content was held constant at a 1:6 mole ratio (chitosan:Glu) whereas the βCD content was varied relative to HMWCH (chitosan-βCD**;**1-1, 1-3, 1-1/3 (w/w)).

4.2.1 *p*-Nitrophenol Equilibrium Sorption

Figures 4.10 and 4.11 summarizes the PNP equilibrium sorption isotherms for each HMWCH and βCD mass ratio, the sorption properties of the HMWCH-βCD:Glu biopolymer materials were quantitatively analyzed, as shown by the fitted lines, in aqueous solution at pH 8.5 and 295 K.

The concentration dependence of Q_e is well-described using the Langmuir and Sips sorption isotherm models. In general, for each HMWCH-βCD mole ratio biopolymer, the quantity of PNP adsorbed increases monotonically as C_e increases. The magnitude of Q_e increases as C_e increases for biopolymers with greater HMWCH content.

From the viewpoint of available inclusion or adsorption sites, HMWCH is a linear macromolecule whereas βCD is a pre-organized macrocycle with inclusion sorption sites. Three component biopolymers may have less efficient packing of the crosslinked chitosan chains

because of the size of the βCD macrocycle as compared with Glu or chiotsan may which adopt a linear conformation; see Schemes 4.2 and 4.3:

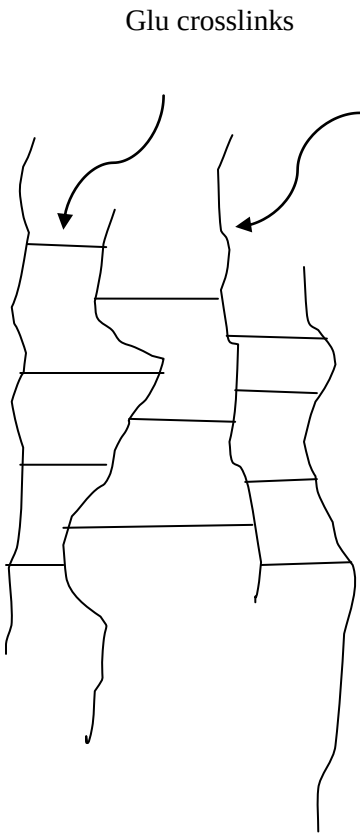

Scheme 4.2. Chitosan cross linked with Glu showing a microporous biopolymer.

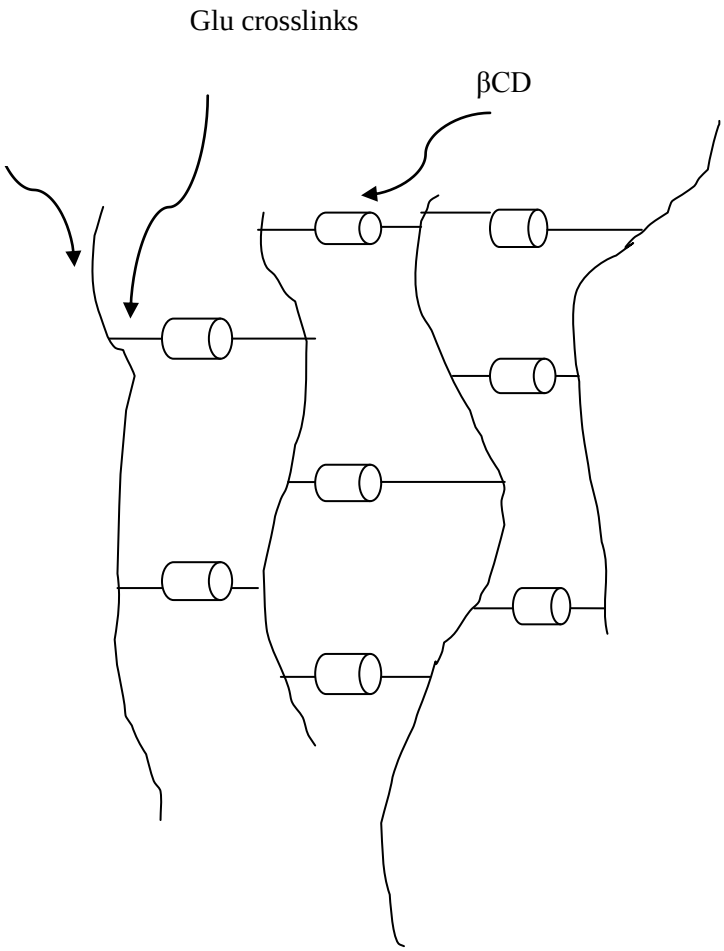

Scheme 4.3. Chitosan and βCD cross linked with Glu showing a variable porosity biopolymer; toroids represent βCD.

The degree of sorption could be related to the variable SA (*cf.* Table 4.17) of the three-component biopolymer materials. It is interesting to note that both isotherm models for the 1-3 give drastically different SA estimates; a range of 34.6 – 275 m^2/g. The 1-1 and 1-1/3 sorbents have similar SA estimates despite the use of different isotherm models. SA estimate

comparisons, obtained from the Langmuir model, for the three component biopolymers when compared to the two component (HMWCH:Glu) biopolymers show that the 1:25 HMWCH:Glu SA estimates are similar to the 1-1 HMWCH:βCD SA estimates (SA = 54.2 m^2/g). The 1-3 biopolymer has the lowest SA estimate and the 1-1/3 has the highest SA estimate. The SA estimates of each biopolymer of HMWCH:Glu are within ±10 m^2/g while the HMWCH-βCD content has a wide range (~81 m^2/g) of SA estimatesm as evidenced from the Langmuir Q_m parameters.

The possibility of steric hinderance occurring in the 1-3 framework is apparent by its sorption capacity. Equal amounts of HMWCH and βCD (1-1) show that an increase of the chitosan content increases the sorption of more PNP from aqueous solution. As the amount of βCD in the framework increases from a 1-1 to the 1-3 biopolymer, it is evident that steric hinderance[73] plays a role in the 1-3 material. The sorption capacity increased from the 1-3 to the 1-1. The sorption capacity of the 1-1/3 frameworks increased and steric hinderance plays a role in the framework. Thus, the framework with the greatest content of chitosan attains the highest sorption capacity amongst the three-component biopolymer materials. Thus, the sorption capacity increased as the chitosan content increased (chitosan-βCD) 1-3 < 1-1 < 1-1/3. Based on the structure of each co-monomer, chitosan is made of a linear polymer chain of glucose substituted amine molecules; whereas βCD is made of cyclic oligomers which form a well-defined inclusion sites in the framework; (*cf.* Scheme 1.4 and 1.5). βCD may contribute to the sorption capacity, in part, due to its inclusion sites.

The foregoing sorption results showed that the 1-1/3 biopolymer had the highest ε_R% (28.0%), see Table 4.17, for the HMWCH-βCD:Glu co-monomer biopolymer over the entire

range of concentrations from 0.4 – 3 mM PNP. This concentration range was examined because the HMWCH-βCD:Glu biopolymers displayed saturation of their sorption sites ~2.5 mM for PNP and showed variability thereafter. Tables 4.1.8 to 4.1.9 show the parameters obtained from each isotherm model.

Overall, both isotherm models give reasonable fits and the 1-1, 1-1/3 and 1-3 mole ratios for three-component biopolymers HMWCH-βCD:Glu exhibit a uniform increase in Q_e indicating a high affinity towards PNP relative to copolymers without βCD. The sorption affinity of the 1-3 biopolymers is relatively low and the isotherm data illustrates a very limited concentration dependence of Q_e. While the sorption capacity of 1-1/3 and 1-3 are relatively similar, the value of Q_m for 1-1 is lower. The isotherm curves for the 1-1 biopolymer show a region (C_e ~2.50 mM; PNP) with little concentration dependence. This could be interpretated that the surface coverage is completely established ~2.5 mM and beyond this concentration, the binding sites are fully occupied.

The Sips restricted Q_m values for 1-1, 1-3 and 1-1/3 are 0.357, 0.232 and 0.769 PNP mmol/g sorbent, respectively. The sorption results in Fig. 4.10 indicate that the sorption sites are 32 - 49% saturated. The corresponding Q_e value is ~ 0.175, 0.075 and 0.275 mmol PNP/g sorbent, respectively. The Sips Q_m values for 1-1, 1-3 and 1-1/3 are 0.340, 1.83 and 1.07 mmol PNP/g sorbent, respectively. The sorption results in Fig. 4.11 indicate that the sorption sites are ~4-50% saturated since the corresponding Q_e value ~ 0.175, 0.075 and 0.275 mmol PNP/g sorbent, respectively.

At 295 K and pH 8.52, the Langmuir Q_m values for the three-component biopolymers are as follows: 1-3 < 1-1 < 1-1/3. The Sips Q_m values follow a similar trend. The n_s values are close to

unity for 1-1 and 3-1 biopolymers; whereas, $n_s = 0.73$ for 1-3 copolymer. The sorption sites are consistent with homogenous monolayer coverage for the 1-1 and 1-1/3 copolymers. When $n_s = 1$, the Sips model is equivalent to the Langmuir. Both isotherms have very low SSE values and $R^2 > 0.950$ for all sorbents. Therefore, an analysis of the magnitude of the isotherm parameters should be considered when determining the "best-fit" criteria.

Both isotherms have similarly low SSE values ($< 5.00 \times 10^{-5}$) and $R^2 > 0.957$ for all HMWCH-βCD biopolymers. The SSE, for the Sips restricted isotherm is less than the Sips isotherm showing evidence of homogeneity of the surface sorption sites for the 1-1 biopolymer. For the 1-3 and 1-1/3 sorbents, the SSE is similar for both isotherms; the n_s value for the 1-3 biopolymer yielded variable Sips restricted parameter estimates. The $n_s \approx 1$ for the 1-1 and 3-1 biopolymer indicates Langmuir-type behaviour. For HMWCH-βCD:Glu biopolymers, the 1-1 and 1-1/3 biopolymers are well-described by the Sips restricted isotherm and the 1-3 biopolymer is well-described ($n_s \neq 1$) by the Sips isotherm model.

Table 4.16. Removal efficiencies for PNP in aqueous solution with three-component biopolymers HMWCH-βCD:Glu at 295 K and pH 8.5.

Biopolymer Sorbent Material	ε_R%
1-3	7.30-10.8
1-1	14.3-25.7
1-1/3	21.1-28.0

[a] The calculated range of ε_R% values correspond to a range of PNP concentrations ($[PNP]_o = 0.39 – 2.9$ mM) with a fixed mass (~20 mg) of biopolymer sorbent material.

Table 4.17. The surface area estimates for three-component biopolymers HMWCH-βCD:Glu using PNP in aqueous solution at 295 K and pH 8.5.

Biopolymer Sorbent Material	Surface Area Estimate ($m^2 g^{-1}$)[a]	
	Sips restricted[b]	Sips
1-3	34.6	275
1-1	54.2	51.2
1-1/3	116	161

[a]Dye-based method surface area estimates obtained from eq.(11) using a value for A_m for the planar orientation of PNP and a Q_m value estimated from eq. (13 and 14)
[b]Sips restricted when n_s=1.

Table 4.18. Sorption parameters for PNP in aqueous solution with three-component biopolymers HMWCH-βCD:Glu at 295 K and pH 8.5 (unbuffered)* obtained from the "best-fit" using the Sips restricted isotherm model when n_s=1.

Sorbent	Q_m (mmol g^{-1})	K_L(L $mmol^{-1}$)	SSEx10^{-5}	R^2
1-3	0.232	0.300	3.00	0.957
1-1	0.357	0.597	4.00	0.987
1-1/3	0.769	0.285	5.00	0.993

*Solutions were unbuffered and pH did not require adjustment.

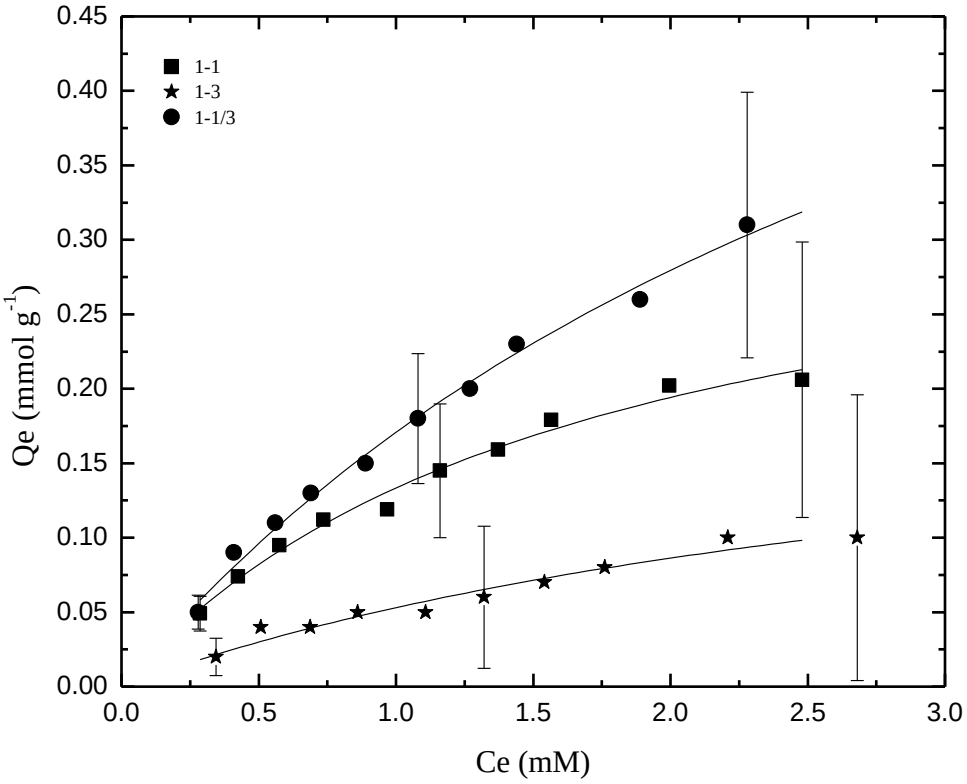

Figure 4.10. The sorption isotherm of fixed amounts (~20 mg) of three-component biopolymers HMWCH-βCD:Glu with PNP at various concentration at pH 8.5 and 295 K. The solid line represents the best-fit according to the Sips restricted isotherm when n_s=1.

Table 4.19. Sorption parameters for PNP in aqueous solution with three-component biopolymers HMWCH-βCD:Glu at 295 K and pH 8.5 (unbuffered)* obtained from the "best-fit" using the Sips isotherm model.

Sorbent	Q_m (mmolg^{-1})	K_S (Lmmol^{-1})	n_s	SSEx10^{-5}	R^2
1-3	1.83	0.00804	0.730	3.00	0.961
1-1	0.340	0.657	1.04	5.00	0.987
1-1/3	1.07	0.159	0.910	5.00	0.994

*Solutions were unbuffered and pH did not require adjustment.

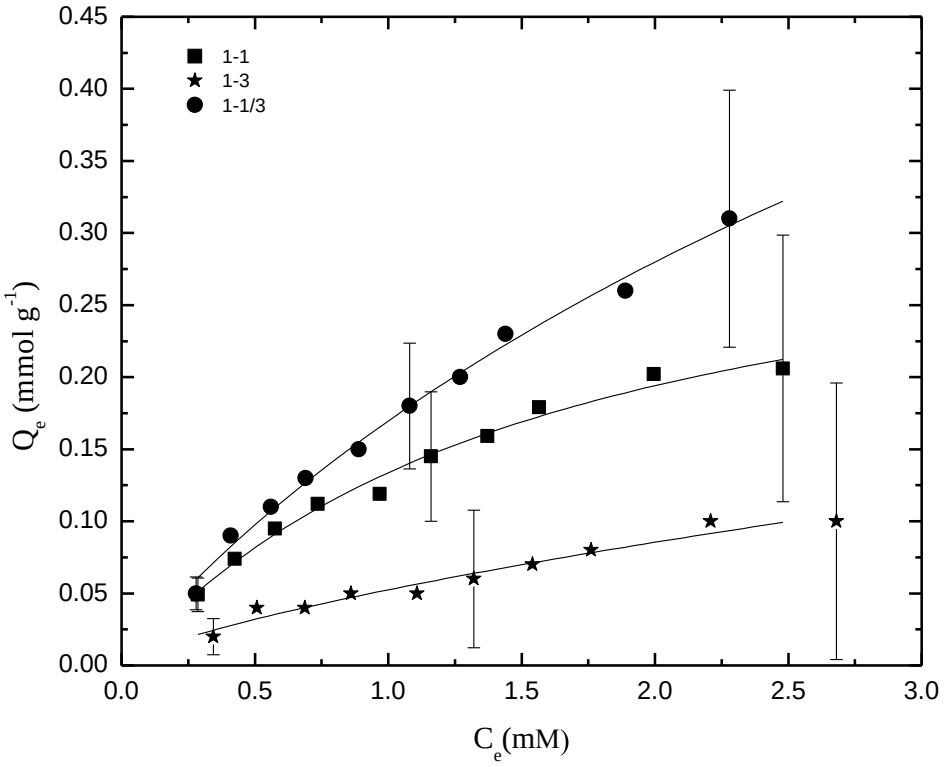

Figure 4.11. The sorption isotherm of fixed amounts (~20 mg) of three-component biopolymers HMWCH-βCD:Glu biopolymers with PNP at various concentrations at pH 8.5 and 295 K. The solid line represents the best-fit according to the Sips isotherm.

4.2.2 Arsenate(V) Oxoanion Equilibrium Sorption

Figures 4.12 and 4.13 summarize sorption isotherms for $HAsO_4^{2-}$ in aqueous solution at equilibrium for each type three-component biopolymer. The sorption properties of the HMWCH-βCD:Glu biopolymer materials in aqueous solution at pH 8.5 and 295 K were quantitatively analyzed, as shown by the fitted lines. For each HMWCH-βCD mole ratio, the adsorbed amount of $HAsO_4^{2-}$ increases monotonically as C_e increases. The magnitude of Q_e shows a gradual increase as C_e increases for biopolymers with increasing βCD content.

The sorption results show that the 1-3 sorbent containing HMWCH had the highest ε_R% (55.4%) (*cf.* Table 4.20) for the three-component biopolymers throughout the entire range of equilibrium concentration of $HAsO_4^{2-}$ from 44 - 118 ppm. This concentration range was examined because the sorption isotherm was near saturation ~ 125 ppm for C_e. Tables 4.21 to 4.22 show the parameters obtained for each isotherm model.

Overall, both isotherm models provided a satisfactory "best-fit". The 1-1, 1-1/3 and 1-3 mass ratios for HMWCH-βCD:Glu exhibit a non-uniform increase in Q_e indicating a low affinity towards $HAsO_4^{2-}$. The sorption affinity of the 1-1 biopolymer is relatively low and the isotherm data indicates a very limited concentration dependence of Q_e. While the sorption capacity of 1-1/3 and 1-3 are relatively similar, the reported value of Q_m for 1-1 is attenuated. The apparent scatter in the experimental data is a consequence of the reduced concentration dependence of Q_e due to the low binding affinity toward $HAsO_4^{2}$.

The isotherm for each copolymer mole ratio where C_e values > 50 ppm display little variation. This could be interpretated that full surface coverage is achieved ~ 50 ppm. Beyond this concentration 50 ppm, the isotherm levels off because the potential binding sites are

occupied. The Langmuir Q_m parameter for the 1-1, 1-1/3 and 1-3 biopolymers are 18.2, 23.7 and 22.0 mg $HAsO_4^{2-}$/g sorbent, respectively. The sorption results in Fig. 4.12 indicate that the sorption sites are 69-86% saturated since the corresponding Q_e value is ~12.5, 16.5 and 19.0 mg $HAsO_4^{2-}$/g sorbent, respectively. The Sips Q_m values for 1-1, 1-1/3 and 1-3 are 41.3, 45.4 and 23.0 mg $HAsO_4^{2-}$/g sorbent, respectively. The sorption results in Fig. 4.13 indicate that the sorption sites are 30-82% saturated.

At 295 K and pH 8.5, the Sips restricted and Sips Q_m values for the three-component biopolymers: 1-1 < 1-1/3 < 1-3. The Sips restricted and Sips isotherms for the three-component biopolymer provided the "best-fit". When $n_s = 1$, the resulting isotherms are equal ($K_L = K_s$) reflecting the behavior of the Langmuir. When the $n_s \approx 1$ for the 1-3 biopolymer it is evident that the sorption sites show homogeneity. Both isotherms have very low SSE values (< 1.29) and $R^2 > 0.716$ for all sorbent biopolymers. Therefore, an assessment of the magnitude of the isotherm parameters is required to verify the goodness of "best-fit" by the isotherm models. The 1-1 and 1-1/3 biopolymers are poorly described by the Sips restricted because $n_s \neq 1$; however, they are well-described by the Sips isotherm model.

Both isotherms have similar SSE values (< 1.29) and $R^2 > 0.716$ for all three-component biopolymers of HMWCH-βCD biopolymers. The SSE for the 1-3 and 1-1 are similar for both isotherms. The $n_s \approx 1$ for the 1-3 biopolymer displays Langmuir type behaviour. For HMWCH-βCD:Glu biopolymers, the 1-1 and 1-1/3 biopolymers are well-described by the Sips isotherm and the 1-3 biopolymer is well-described ($n_s = 1$) by the Sips restricted isotherm model.

Table 4.20. Removal efficiencies for $HAsO_4^{2-}$ in aqueous solution with three-component biopolymers of HMWCH-βCD:Glu at 295 K and pH 8.5.

Biopolymer Sorbent Material[b]	ε_R %
1-3	35.3-55.4
1-1	22.8-35.1
1-1/3	29.5-47.8

[a] The calculated range of ε_R% values correspond to a range of $HAsO_4^{2-}$ concentrations ($[HAsO_4^{2-}]_o$ = 44 -118 ppm) with a fixed mass (~20 mg) of biopolymer sorbent material.
[b] Refers to βCD-chitosan mole ratio.

Table 4.21. Sorption parameters for $HAsO_4^{2-}$ in aqueous solution with three-component biopolymers of HMWCH-βCD:Glu at 295 K and pH 8.5 (unbuffered)* obtained from the "best-fit" using the Sips restricted isotherm model when n_s=1.

Sorbent	Q_m(mg g^{-1})	K_L (mL μg^{-1})	SSE	R^2
1-3	23.7	0.0643	1.14	0.811
1-1	18.2	0.0278	0.714	0.789
1-1/3	22.0	0.0417	1.29	0.765

*Solutions were unbuffered and pH did not require adjustment.

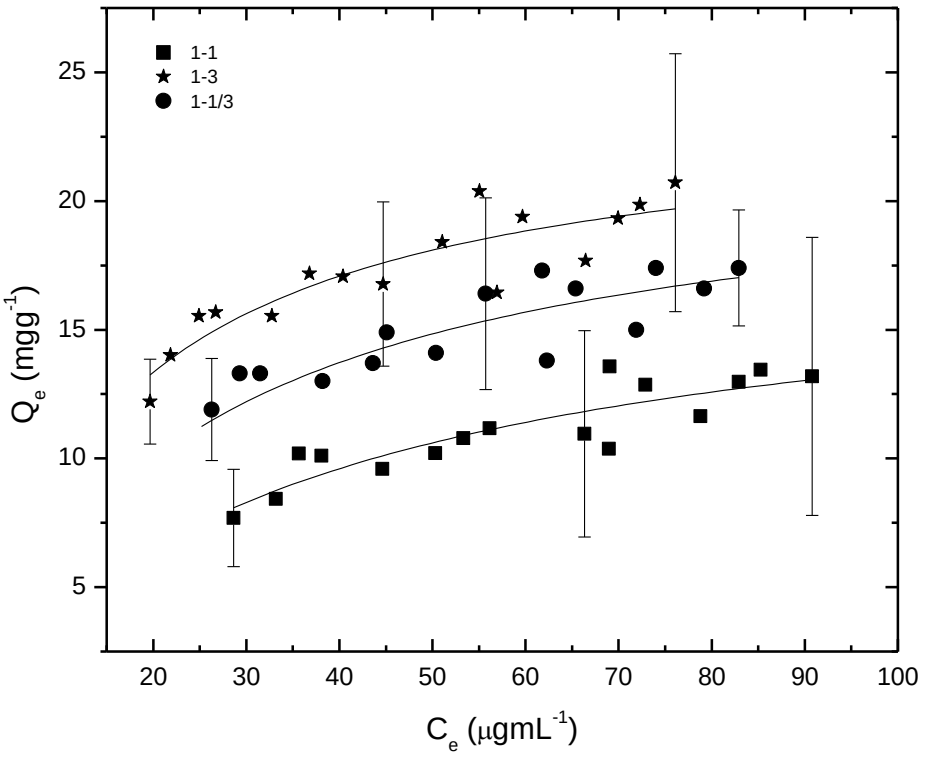

Figure 4.12. The sorption isotherm of fixed amounts (~20 mg) of three-component biopolymers of HMWCH-βCD:Glu biopolymers with $HAsO_4^{2-}$ at various concentrations at pH 8.5 and 295 K. The solid line represents the best-fit according to the Sips restricted isotherm when n_s=1.

Table 4.22. Sorption parameters for $HAsO_4^{2-}$ in aqueous solution with three-component biopolymers of HMWCH-βCD:Glu at 295 K and pH 8.5 (unbuffered)* obtained using the Sips isotherm model.

Sorbent	Q_m (mg g^{-1})	K_S (mL μg^{-1})	n_s	SSE	R^2
1-3	23.0	0.0668	1.09	1.23	0.811
1-1	41.3	0.00278	0.546	0.758	0.792
1-1/3	45.4	0.00362	0.423	1.12	0.716

*Solutions were unbuffered and pH did not need to be adjusted.

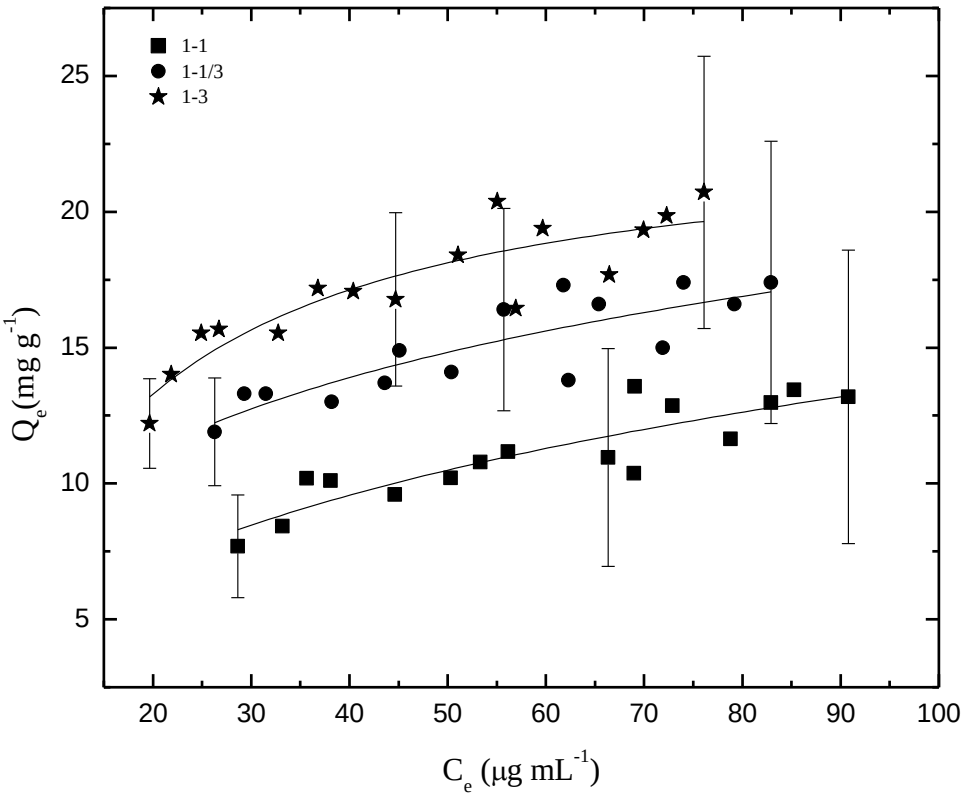

Figure 4.13. The sorption isotherm of fixed amounts (~20 mg) of three-component biopolymers of HMWCH-βCD:Glu biopolymers with $HAsO_4^{2-}$ at various concentrations at pH 8.5 and 295 K. The solid line represents the best-fit according to the Sips isotherm.

4.3 Commercial Biosorbents (Chitosan and Activated Carbon) for Arsenate(V) Oxoanion Equilibrium Sorption

The commercially available sorbents, low molecular weight (powder) and high molecular weight (flake) chitosan, and activated carbon, were used for the comparison of arsenate(V) oxoanion equilibrium sorption. The results were compared with two- and three-component chitosan-based biopolymers. Figure 4.14 summarizes the $\varepsilon_R\%$ ~ 0% for all three commercial sorbents. Chitosan cross linked biosorbent materials exhibit superior sorption properties for sorption-based applications such as arsenic cation species and arsenate oxoanions.

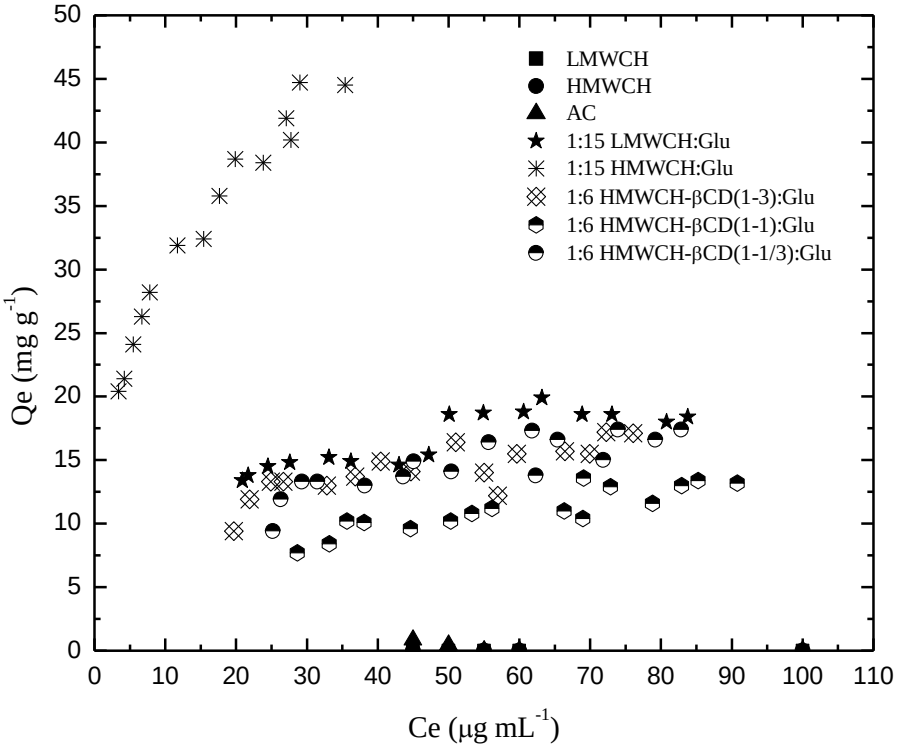

Figure 4.14 The equilibrium sorption of fixed amounts (~20 mg) of commercial sorbents and chitosan based two- and three-component biosorbent materials with various concentrations of $HAsO_4^{2-}$ at pH 8.5 and 295 K.

Chapter 5

5.0 Summary

Many researchers utilize sorption since it represents a "green strategy" for the separation and sequestration of target compounds from aqueous solution and chemical mixtures. Sorption is a relatively simple, inexpensive and a low energy intensive technology for various chemical sorption and processing, including the remediation of contaminated aquatic environments. The development of novel sorbent materials in conjunction with an improved understanding of the mechanism of sorption will facilitate the development of tunable materials for specific chemical targets by exploiting the principles of supramolecular chemistry.

Two- and three-component chitosan-based biosorbent materials were successfully synthesized through a Schiff base reaction under acidic conditions. These materials were characterized using FT-IR, TGA, and EA. The sorption properties were studied at pH 8.5 with two very different adsorbates: the arsenate oxoanion species ($HAsO_4^{2-}$) and the phenoxide anion of PNP. The synthetically derived sorbent materials each contained chitosan in their frameworks and displayed variable sorption with each type of adsorbate species.

The characterization data also showed that there are differences amongst the types of cross linked chitosan-based biosorbent materials. The TGA showed two thermal decomposition events where the two-component biopolymers, LMWCH:Glu and HMWCH:Glu, exhibit thermal events centered on ~215°C and ~420°C, glutaraldehyde and chitosan mass loss, respectively. The three-component biopolymer (HMWCH-βCD:Glu) exhibits thermal events centered on ~250°C and ~420°C. A complex transition between 390°C and 475°C arises from the three-component biopolymer. The FT-IR spectra show two new bands appearing at ~1560cm^{-1} (C=C)

and ~1655cm-1 (C=N), and their appearance of these bands confirms that cross linking occurs between the amine groups on CH and the aldehyde groups of Glu.

For the two-component biopolymers, LMWCH:Glu showed a decrease in sorption as the co-monomer mole ratio increased and displayed attenuated binding with PNP; whereas, stronger binding affinity to the $HAsO_4^{2-}$ species was observed. The 1:15 LMWCH:Glu sorbed the highest amount of deprotonated phenoxide anion of PNP and the $HAsO_4^{2-}$ sorbate. In contrast to the LMWCH:Glu, the HMWCH:Glu showed a increase in sorption as the co-monomer mole ratio increased. The 1:35 HMWCH:Glu sorbed the highest amount of PNP and performed similarly to the 1:25 HMWCH:Glu for the highest amount of $HAsO_4^{2-}$. The three-component biopolymer system, HMWCH-βCD:Glu showed graphically the 1-1/3 chitosan-βCD mass ratio had the highest PNP sorption and the 1-3 mass ratio had the highest $HAsO_4^{2-}$ sorption.

It was important to compare the HMWCH and LMWCH based materials because they had variable sorption properties based on the Glu co-monomer mole ratios and/or the presence of β-CD. The differences are attributed to a number of factors: the variation in crosslink density affects the SA and pore structure properties of copolymer materials.[4] Variable co-monomer mole ratios affects the swelling, hydration properties and the relative accessibility of sorption sites for such microporous materials. The occurrence of cross linking with glutaraldehyde at the OH *vs.* NH sites of chitosan will also affect the surface chemistry and the types of intermolecular interactions of such sorbent materials. It was also imperative to compare the chitosan-based biosorbent cross linked materials to the commercially available sorbents (LMWCH, HMWCH and AC) to illustrate the phenomenal changes in the sorption capacities and removal efficiencies of these biopolymer sorbent materials. It has been reiterated over and over again in the literature that the "free amine group" on chitosan acts as effective metal chelators (*i.e.* M^{n+} species).

However, a comparison of chitosan in its powder or flake form with the cross linked chitosan biopolymers reveals significant differences in sorption properties toward arsenate and phenolate anion species. In order to effectively capture heavy metals in aqueous environments, biosorbent materials should behave similarly to a sponge, i.e. swellability and surface area are favourable properties observed in cross linked biosorbent materials. The tunability of the biopolymers, through varying the co-monomer mole ratios (1:15, 1:25 and 1:35) and mass ratios (*i.e.* 1-1, 1-3 and 1-1/3) enable tuning of the binding affinity and selectivity of anions in aqueous solutions.

5.1 Future Research

- To examine the charge effects (*i.e.* singly vs. multiply charged states) of the oxoanion (1^-, 2^-, 3^- anions) of adsorbate species, it is necessary to examine the pH and ionic strength dependence of sorption.
- To examine the neutral (uncharged species) in relation to the deprotonated species of PNP and H_3AsO_4.
- A further understanding of the thermodynamic mechanism of sorption of the PNP and H_3AsO_4 species through a temperature dependent sorption study which would yield enthalpic and entropic parameters that would help elucidate the importance of H-bonding and van der Waal interactions between sorbate and sorbent.
- Design a binary system of H_3AsO_4 with another heavy metal species to examine metal-metal interactions by investigating sorption capacities and selectivity.
- To obtain the surface area of the anhydrous chitosan based biopolymers in powder form through N_2 porosimetry.

- Investigate the swellability of chitosan:Glu and chitosan-βCD:Glu biosorbents materials by determining the surface areas of chitosan-based biopolymers. The higher the swellability the greater the surface area which relates to an increased sorption capacity.
- To understand the nature of the sorption sites in chitosan cross linked glutaraldehyde biopolymers through a Raman/IR spectroscopic study by identifying which functional groups participate on the sorbent and sorbate (i.e. C=O, OH or NH groups).
- For quantitative analysis of adsorbate species, TGA-based thermal events may provide some understanding of the sorption phenomena described herein. This can be done by TGA-MS, DSC-IR and ICP-MS.
- To understand the binding interactions such as hydrophobic effects occurring between solvent, sorbate and sorbent. Measuring the heat released and/or absorbed from the mixing of two or more components will aid in the investigation of the enthalphic and entropic entities by utilizing an ITC in water, D_2O and mixed H_2O/D_2O systems.
- To obtain structural information as to the binding sites of the adsorbates by the sorbent, it is necessary to investigate the sorption mechanisms utilizing EXAFS. This method identifies chemical bonding such as nearest atomic neighbouring shells, average bond lengths, atomic coordination, chemical identification of atoms in the shells, and the degree of ordering/strength of bond. PXRD provides structural information (long range), XANES analyses the oxidation states of adsorbate speciation existing in aqueous solutions, XPS identifies sorption sites and species sorbed.
- Establish all reaction mechanisms to confirm all products by determining the connectivity of the framework by using ^{13}C solid state NMR spectroscopy.

- Establish the reusability of chitosan:Glu and chitosan-βCD:Glu biosorbents materials (*i.e* # of cycles) that the sorbent can be used to adsorb $HAsO_4^{2-}$ or PNP^-.
- Optimize all criteria such as pH, temperature and ionic strength to improve the sorption capacities of the chitosan based sorbent in aqueous solution.
- To study the nature of the cross linker monomer by comparing a $HAsO_4^{2-}$ sorption study using βCD:EP and βCD:Glu copolymers compared to the sorption results obtained in this thesis.
- To investigate the relative inclusion site accessibility of β-CD of the three-component polymer materials through the phenolphthalein sorption study.[76]
- To examine the $(A\text{-}B)_n$ *vs.* $A_n\text{-}B_n$ type biopolymer by studying these types of polymers through molecular imprinting of the polymer with guests of interest to see if the use of molecular imprinting polymers will improve the sorption properties of such sorbents.[80] Also, the drop-wise addition *vs.* fast addition of cross linker to control the rate of gelation and the type of biopolymer.

References

1. Guanghui Wang, Jinsheng Liu, Xuegnag Wang, Zhiying Xie, Nansheng Deng, Adsorption of uranium (VI) from aqueous solution onto cross-linked chitosan, J. Haz. Mat., **2009**, 168, 1053-1058
2. Pratap Chutia, Shigeru Kato, Toshinori Kojima, Shigeo Satokawa, Arsenic adsorption from aqueous solution on synthetic zeolites, J. Haz. Mat., **2009**, 162, 440-447
3. Derivation of a General Adsorption Isotherm Model, J. Environ. Eng., October 2005
4. Pratt, D.Y.,Wilson; L.D., Kozinski, J.A., Morhart, A., Preparation and Sorption Studies of Carbohydrate Polymers", J. App. Polym. Sci., **2010**, 116, 2982-2989.
5. Oyrton A.C., Monteiro Jr., Claudio Airoldi, Some studies of crosslinking chitosan-glutaraldehyde interaction in a homogenous system, Int. J. Biol. Macromol., **1999**, 26, 119-128
6. El-Tahlawy, Khaled, Venditti, Richard A., Pawlak, Joel J., Aspects of the preparation of starch microcellular foam particles crosslinked with glutaraldehyde using a solvent exchange technique, Carbohyd. Polym., **2007**, 67, 319-331
7. Koopmans, C., Ritter, H., Formation of Physical Hydrogels via Host-Guest Interactions of β-cyclodextrin Polymers and Copolymers Bearing Adamantyl Groups, Macromol., **2008**, 41, 7148-7422
8. Wei Liang X., Ji Dong L., Yan Ping S., Preparation of cyclomaltoheptaose (β-cyclodextrin) cross-linked chitosan derivative via glyoxal or glutaraldehyde, Chin. Chem. Lett., **2003**, 14, 7, 767-770
9. Badal, K.M., Kazuo, T.S., Arsenic round the world: a review, Talanta **2002**, 58, 201-235
10. Denesh M., Charles U.P. Jr., Arsenic removal from water/wastewater using adsorbents-A critical review, J. Haz. Mat., **2007**, 142, 1-53
11. Mondal, P., Majumder, C.B., Mohanty, B., Laboratory based approaches for arsenic remediation from contaminated water: Recent developments, J. Haz. Mat., **2006**, B137, 464-479
12. Waniepee, W., Weiss, D.J., Sephton, M.A., Coles, B.J., Unsworth, C., Court, R., The effect of crude oil on arsenate adsorption on goethite, Water Res., **2010**, 44, 19, 5673-5683
13. Treehugger, science and technology (water) retrieved **August 4, 2010** available at http://www.treehugger.com/files/2010/07/oil-spill-could-mean-toxic-arsenic-build-up-in-gulf.php
14. Babel, S., Kurmoawam, T.A., Low-cost adsorbents for heavy metals uptake from contaminated water: a review, J. Haz. Mat., **2003** B97, 219-249
15. Kulshreshtha, S. N., A Global Outlook for Water Resources to the Year 2025, Water Res. Manag., **1998**, 12, 167-184
16. Guibal, E., Interactions of metal ions with chitosan-based sorbents: a review, Sep. Purif. Technol., **2004**, 38, 43-74

17. Kurita, K., Chemistry and application of chitin and chitosan, Polym. Degrad. Stabil., **1998**, 59, 117-120
18. Majeto N.V. Ravi Kumar, A review of chitin and chitosan applications, React. Func. Polym., **2000**, 46, 1-27
19. Rinaudo, M., Chitin and chitosan: Properties and applications, Prog. Polym. Sci., **2006**, 31, 603-632
20. Pillai, C.K.S., Paul, W., Sharma, C.P., Chitin and chitosan polymers: Chemistry, solubility and fiber formation, Prog. Polym. Sci., **2009**, 34, 641-678
21. Trimukhe, K.D., Varma, A.J., Complexation of heavy metal by crosslinked chitin and its deacetylated derivatives, Carbohyd. Polym., **2008**, 71, 66-73
22. Kwon, J. Soprtion studies of surface modified activated carbon with b-Cyclodextrin, University of Saskatchewan, MSc. Thesis, 2007, Saskatoon, SK., and references cited therein.
23. Li, M-J., Meng, X-G., Hu, C-W., Du, J., Adsorption of phenol, p-chlorophenol and p-nitrophenol onto functional chitosan, Bioresour. Technol., **2009**, 100, 1168-1173
24. Wilson, L.D., Mohamed, M.H., Headley, J.V., Surface Area and Pore Structure Properties of Urethane-Based Copolymer Containing β-Cyclodextrin, J. Colloid Interf. Sci., **2011**, 357, 1, 215-222
25. Langmuir, I., The Constitution and Fundamental Properties of Solids and Liquids Part I Solids, J. Amer. Chem. Soc., **1916**, 2221-2295
26. Langmuir, I., The Constitution and Fundamental Properties of Solids and Liquids Part II Liquids, J. Amer. Chem. Soc., **1917**, 1848-1906
27. Miretzky, P., Cirelli, A.F., Hg(II) removal from water by chitosan and chitosan derivatives: A review, J. Haz. Mat., **2009**, 167, 10-23
28. Sailaja, A.K., Amareshwar, P., Chakravarty, P., Chitosan nanoparticles as a drug delivery system, Res. J. Pharm. Biol. Chem. Sci., **2010**, 1, 3, 474
29. Chielewski, A.G., Chitosan and radiation chemistry, Radiat. Phys. Chem., **2010**, 79, 272-275
30. Niu, C.H., Volesky, B., Cleiman, D., Biosorption of arsenic (V) with acid-washed crab shells, Water Res., **2007**, 41, 2473-2478
31. Dambies, L., Existing and Prospective Sorption Technologies for the Removal of Arsenic in Water Sep. Sci. Technol., **2004** 39 (3) 603-627
32. Niu, C.H., McGill University, Ph.D. Thesis, 2002, Montreal, QB., and references citied therein.
33. Roberts, G.A.F., Chitin Chemistry **1992**, MacMillan: London, UK,
34. Cutler, J.N., Chen, N., Jiang, D.T., Demopoulos, G.P., Jia, Y., Rowson, J.W., The Nature of Arsenic in Uranium Mill Tailings, J. Phys. IV, **2003**, 107, 337
35. IUPAC. Compendium of Chemical Terminology, 2nd ed. (the "Gold Book"). Compiled by A. D. McNaught and A. Wilkinson. Blackwell Scientific Publications, Oxford (1997). XML on-line corrected version: http://goldbook.iupac.org (2006-) created by M. Nic, J.

Jirat, B. Kosata; updates compiled by A. Jenkins. ISBN 0-9678550-9-8. doi:10.1351/goldbook.
36. Morgan, G.T., Drew, H.D.K., CLXII. - Researches on residual affinity and co-ordination. Part II. Acetylacetones of selenium and tellurium, J. Chem. Soc. Trans., **1920**, 117, 1456-1465
37. Koch, I., Mace, J. V., Reimer, K. J., Arsenic speciation in terrestrial birds from Yellowknife, Northwest territories, Canada: The unexpected finding of arsenobetaine. Environ. Toxicol. Chem., **2005**, 24(6), 1468-1477
38. Moldovan, B. J., Jiang, D. T., Hendry, M. J., Minerological characterization of arsenic in uranium mine tailings precipitated from iron-rich hydrometallurgical solutions. Environ. Sci. Technol., **2003**, 37, 873-879
39. Jaworska, J.S., Schowanek, D., Feijtel, T.C.J., Environmental Risk Assessment for Trisodium [S,S]-Ethylene Diamine Disuccinate , A Biodegradable Chelator used in Detergent Application, Chemosphere, **1999**, 38(15), 3597-3625
40. Brusseau, M.L., Wang, X., Wang, W-Z., Simultaneous Elution of Heavy Metals and Organic Compounds from Soil by Cyclodextrin, Environ. Sci. Technol., **1997**, 31, 1087-1092
41. Dambies, L., Guimon, C., Yiacoumi, S., Guibal, E., Characterization of metal ion interactions with chitosan by X-ray photoelectron spectroscopy, Colloids Surf. A, 2001, 177(2-3), 203-214
42. Bushee, D.S., Krull, I.S., Demko, P.R., Smith, S.B., Trace Analysis and speciation for arsenic anions by HPLC-Hydride generation inductively coupled plasma emission spectroscopy, J. Liq Chromatogr., **1984**, 7(5), 861-876
43. Steed, J.W., Astwood, J.L., Supramolecular Chemistry 2nd Edition, Wiley, **2009**, Chichester, West Sussex, U.K.
44. Bambo, M.F., Synthesis, Characterisation and Application of Nanoporous Cyclodextrin Polymers Dissertation, University of Johannesburg, **2007**
45. Pearson, R.G., Hard and Soft Acids and Bases, J. Amer. Chem. Soc., **1963**, 85(22), 3533-3539
46. Peterson ,H., Pratt, R., Neapetung R., Steinhauer A., Development of Effective Drinking Water Treatment Processes for small Communities with Extremely Poor , West Water on the Canadian Prairie, Can. Soc. Environ. Biol., 64, 1, 28-35
47. Tro, N.J., Chemistry A Molecular Approach **2008**, Pearson Prentice Hall, ISBN: 0-13-100065-9
48. Mohamed, M. H., Wilson, L. D., Headley, J. V., Peru, K. M., Sequestration of Naphthenic Acids from Aqueous Solution using β-Cyclodextrin-based Polyurethanes, Phys. Chem. Chem. Phys., **2010**, 12, 1112-1122
49. Health Canada, Report on Human Biomonitoring of Environmental Chemical in Canada, 2010, retrieved January 27, 2011 available at http://www.hc-sc.gc.ca/ewh-semt/pubs/contaminants/chms-ecms/section8-eng.php?n8_1

50. Health Canada. (2006). Guidelines for Canadian Drinking Water Quality: Guideline Technical Document - Arsenic. Ottawa: Water Quality and Health Bureau, Healthy Environments and Consumer Safety Branch, Health Canada, retrieved January 27, 2011, from www.hc-sc.gc.ca/ewh-semt/alt_formats/hecs-sesc/pdf/pubs/water-eau/arsenic/arsenic-eng.pdf
51. Bharadwaj, L., Drinking water contaminants and human health, In Velma I Grover (Ed), Water: Global Common and Global Problems, **2006**, 169-189, Enfield, NH, USA: Science Publisher
52. Li, Z., Beachner, R., McManama, Z., Hanlie, H., Sorption of Arsenic by Surfactant-Modified Zeolites and Kaolinite, Micropor. Mesopor. Mat., **2007**, 105(3), 291-297
53. Yolcubal, I., Akyol, N. H., Adsorption and Transport of Arsenate in Carbonate-Rich Soils: Coupled Effects of Nonlinear and Rate-Limited Sorption, Chemosphere, **2008**, 73(8), 1300-1307
54. Cornejo, L., Lienqueo, H., Arenas, M., Acarapi, J., Contreras, D., Yanez, J., Mansilla, H.D., In field arsenic removal from natural water by zero-valent iron assisted by solar radiation, Environ. Pollut., **2008**, 156(3), 827-831
55. An, J-H., Dultz, S., Adsorption of Cr(VI) and As(V) on chitosan-montmorillonite: selectivity and pH dependence, Clays Clay Miner., **2008**, 56(5), 549-557
56. Mohamed, H.M., Soprtion of Naphthenic Acids using β-Cyclodextrin-based Polyurethanes, University of Saskatchewan, PhD. Thesis **2010**, Saskatoon, SK., and references cited therein.
57. Vikhoreva, G.A., Shablyukova, E.A., Kil'deeva, N.R., Modification of Chitosan Films With Glutaraldehyde To Regulate Their Solubility and Swelling, Fibre Chem., **2001** 33(3), 38-42
58. Jamali, M.K., Kazi, T.G., Arain, M.B., Afridi, H.I., Jalbani, N. and Adil, R.S., The correlation of total and extractable heavy metals from soil and domestic sewage sludge and their transfer to maize (Zea mays L.) plants, Toxicol. Environ. Chem., **2006**, 88(4), 619-632
59. Domard, A., A perspective on 30 years research on chitin and chitosan, Carbohyd. Polym., **2011**, 84, 696-703
60. Szejtli, J., Utilization of cyclodextrins in industrial products and processes, J. Mat. Chem., **1997**, 7(4), 575-587
61. di Cagno, M., Stein, P.C., Skalko-Basnet, N., Brandl, M., Bauer-Brandl, A., Solubilization of ibuprofen with β-cyclodextrin derivatives:energetic and structural studies, J. Pharm. Biomed. Anal., **2011**, 55(3), 446-451
62. Wen-Wu, L., Claridge, D.W., Quihong, L., Wormald, M., Davis, B.G., Bayley, H., Tuning the Cavity of Cyclodextrins: Altered Sugar Adaptors in Protein Pores, J. Amer. Chem. Soc. **2011**, 133, 1987-2001

63. Lopez-de-Dicastillo, C., Gallur, M., Catala, R., Gavara, R., Hernandez-Munoz, P., Immobilization of β-cyclodextrin in ethylene-vinyl alcohol copolymer for active food packaging applications, J. Membrane Sci., **2010**, 353(1-2), 184-191
64. Cravotto, G., Binello, A., Baranelli, E., Carraro, P., Trotta, F., Cyclodextrins as Food Additives and in Food Processing, Curr. Nutr. Food Sci., **2006**, 2(4), 343-350
65. Knaul. J., Hudson, S.M., Creber, K.A.M., Crosslinking of Chitosan Fibers with Dialdehydes: Proposal of a New Reaction Mechanism, J. Polym. Sci. Pol. Phys., 1999, 37(11), 1079-1094
66. Silverstein, R.M., Webster, F.X., Kiemle, D.J., Spectrometric Identification of Organic Compounds 7th Edition, John Wiley & Sons Inc., **2005**
67. Hong, P-Z., Li, S-D., Ou, C-Y., Li, C-P., Yang, L., Zhang, C-H., Thermogravimetric Analysis of Chitosan, J. Appl. Polym. Sci., **2007**, 105(2), 547-551
68. Li, N., Mei, Z., Ding, S., 2.4-Dichlorophenol sorption on cyclodextrin polymers, J. Inclusion Phenom. Macrocyclic Chem., **2010**, 68, 123-129
69. El-Hefian, E., Elgannoudi, E.S., Mainal, A., Yahaya, A.H., Characterization of Chitosan in Acetic Acid: Rheological and Thermal Studies, Turk. J. Chem., **2010**, 34, 47-56
70. Uzqueda, M., Zornoza, A., Isasi, J.R., Martin, C., Sanchez, M., Velaz, I., Interactions of terbinafine with β-cyclodextrin polymers: sorption and release studies, J. Inclusion Phenom. Macrocyclic Chem., **2011**, 69, 469-474
71. Kurkov, S.V., Ukhatskaya, E.Y., Loftsson, T., Drug/cyclodextrin: beyond inclusion complexation, J. Incl. Phenom. Macro., **2011**, 69, 297-301
72. World Health Organization, retrieved on May 12, 2011 available at: http://www.who.int/ipcs/publications/cicad/en/cicad20.pdf.
73. Crini, G., Recent developments in polysaccharide-based materials used as adsorbents in wastewater treatment, Prog. Polym. Sci., **2005**, 30, 38-70
74. Kwon, J.H., Wilson, L. D., Activated carbon surface-modified with β-cyclodextrin – Part I. Synthesis and Characterization, J. Environ. Sci. Health A Tox. Hazard Subst. Environ. Eng., **2010,** 45(13), 1775-1792.
75. Kwon, J.H., Wilson, L. D., Activated carbon surface-modified with β-cyclodextrin – Part II. Sorption properties, J. Environ. Sci. Health A Tox. Hazard Subst. Environ Eng., **2010**, 45(13), 1793-1803.
76. Mohamed, M.H., Wilson, L.D., Headley, J. V., Estimation of the Surface Accessible Inclusion Sites of β-Cyclodextrin Based Copolymer Materials, Carbohyd. Polym., **2010**, 8091), 186-196.
77. Gregg, S.J., Sing, K.S., "Adsorption, Surface Area and Porosity", 2nd Ed., Academic Press, New York, **1982**, p. 4
78. Brauner, S., Deming, L.S., Deming, E., Teller, E., J. Amer. Chem. Soc., **1940**, 62, 1723-1732
79. Singleton, J.H., Halsey, G.D., Symposium on Problems Relating to the Adsorption of Gases by Solids, **1954**, Sep., 10-11, Kinston, Ontario

80. Zhang, J., Shen, X., Chen, Q., Separation Processes in the Presence of Cyclodextrins Using Molecular Imprinting Technology and Ionic Liquid Cooperating Approach, **2011**, Curr. Org. Chem., 15(12), 1, 74-85
81. Hininger, I., Waters, R., Osman, M., Garrel, C., Fernholz, K., Roussel, A.M., Anderson, R.A., Acute prooxidant effects of vitamin C in EDTA chelation therapy and long-term antioxidant benefits of therapy, Free Radical Bio. Med., **2005**, 38, 1565-1570.